Driver Behavior in Car Following – The Implications for Forward Collision Avoidance

Rong Chen

Dissertation submitted to the faculty of the Virginia Polytechnic Institute and State University in partial fulfillment of the requirement for the degree of

Doctor of Philosophy
In
Biomedical Engineering

Hampton C. Gabler, Chair
Stefan M. Duma
Andrew R. Kemper
Francis S. Gayzik
Miguel A. Perez

June 1, 2016

Blacksburg, Virginia

Keywords: driver behavior, car following, naturalistic driving data, forward collision avoidance system, active safety, autonomous vehicle

Driver Behavior in Car Following – The Implications for Forward Collision Avoidance

Rong Chen

Abstract

Forward Collision Avoidance Systems (FCAS) are a type of active safety system which have great potential for rear-end collision avoidance. These systems use either radar, lidar, or cameras to track objects in front of the vehicle. In the event of an imminent collision, the system will warn the driver, and, in some cases, can autonomously brake to avoid a crash. However, driver acceptance of the systems is paramount to the effectiveness of a FCAS system. Ideally, FCAS should only deliver an alert or intervene at the last possible moment to avoid nuisance alarms, and potentially have drivers disable the system. A better understanding of normal driving behavior can help designers predict when drivers would normally take avoidance action in different situations, and customize the timing of FCAS interventions accordingly. The overall research object of this dissertation was to characterize normal driver behavior in car following events based on naturalistic driving data.

The dissertation analyzed normal driver behavior in car-following during both braking and lane change maneuvers. This study was based on the analysis of data collected in the Virginia Tech Transportation Institute 100-Car Naturalistic Driving Study which involved over 100 drivers operating instrumented vehicles in over 43,000 trips and 1.1 million miles of driving. Time to Collision in both braking and lane change were quantified as a function of vehicle speed and driver characteristics. In general, drivers were found to brake and change lanes more cautiously with increasing vehicle speed. Driver age and gender were found to have significant influence on both time to collision and maximum deceleration during braking. Drivers age 31-50 had a mean braking deceleration approximately 0.03 g greater than that of novice drivers (age 18-20), and female drivers had a marginal increase in mean braking deceleration as compared to male drivers. Lane change maneuvers were less frequent than braking maneuvers. Driver-specific models of TTC at braking and lane change were found to be well characterized by the Generalized Extreme Value distribution. Lastly, driver's intent to change lanes can be predicted using a bivariate normal distribution, characterizing the vehicle's distance to lane boundary and the lateral velocity of the vehicle.

This dissertation presents the first large scale study of its kind, based on naturalistic driving data to report driver behavior during various car-following events. The overall goal of this dissertation is to provide a better understanding of driver behavior in normal driving conditions, which can benefit automakers who seek to improve FCAS effectiveness, as well as regulatory agencies seeking to improve FCAS vehicle tests.

Acknowledgement

Toyota Motor Corporation is gratefully acknowledged for providing the funding for this dissertation.

This work is dedicated to my mother. Thank you for being my biggest fan and for always believing in me. To all my family members, thank you all for supporting my decision to seek higher education and the continuing encouragement to always do my best.

I would also like to thank my advisor Dr. Clay Gabler. Thank you for being the role model and mentor who always encouraged and inspired me to do better than I think I can.

Thank you to my committee members, Dr. Stefan Duma and Dr. Andrew Kemper, Dr. F. Scott Gayzik, and Dr. Miguel Perez, for your advice and inspiration throughout my PhD career.

To my Virginia Tech Center for Injury Biomechanics lab mates: Dr. Vanessa Alphonse, Zachary Bailey, Dr. Stephanie Beeman, Dr. Bryan Cobb, Danielle Cristino, Dr. Allison Daniello, Dr. Evon Ereifej, Dr. Liz Fievisohn, Tom Gorman, Dr. Carolyn Hampton, Nora Hlavac, Brad Hubbard, Dr. Nicholas Johnson, Taylor Johnson, Dr. Kristofer Kusano, Anna MacAlister, Dr. Sujit Sajja, John Scanlon, Whitney Tatem, Dr. Ada Tsoi, and Tyler Young. Thank you all for the helping hands that you've lend me as well as brighten the lab with smiles each and every day.

Finally, to everyone that I have had the pleasure of meeting here at Virginia Tech. Thank you for being a part of the community that brought me memories that I will cherish for the rest of my life. You all have taught me the value of community and what it truly means to be a Hokie and live out our motto of "Ut Prosim".

TABLE OF CONTENTS

1 Introduction 1
1.1 The Inherent Limitation of Passive Safety Technology 1
1.2 Rear-end Collisions: Incidence and Consequences 2
1.3 Active Safety Systems: Forward Collision Avoidance 3
1.3.1 Forward Collision Warning 3
1.3.2 Dynamic Brake Support 3
1.3.3 Autonomous Emergency Braking 4
1.3.4 Adaptive Cruise Control 4
1.3.5 Autonomous Vehicle 5
1.4 The Need to Understand Driver Behavior 5
1.5 Driver Behavior Data Sources 7
1.5.1 Crash Databases 7
1.5.2 Test Track Experiments and Virtual Driving Simulator 8
1.5.3 Event Data Recorders 9
1.5.4 Naturalistic Driving Studies 10
1.6 Research Objective 10
2 Data Sources and Overall Approach 12
2.1 Data Source 12
2.2 Overview of the 100-Car Naturalistic Driving Study 12
2.3 Driver Selection 13
2.4 Driver Demographic Weighting Factor 15

2.5 Automated Lead Vehicle Identification Algorithm 15
2.5.1 Calculation of Position of Radar Objects 16
2.5.2 Search Trips for Car-following 17
2.5.3 Validation of Automated Search Algorithm 21
2.6 Driver Risk Perception Index 23
2.6.1 Performance Index for Approach and Alienation 23
2.6.2 Perceptual Risk Estimate 23
2.6.3 Required Deceleration Parameter 24
2.6.4 Time to Collision 24
2.6.5 Enhanced Time to Collision 24
2.7 Conclusion 25
3 Driver Behavior During Braking in Car-Following 27
3.1 Comparison of TTC and ETTC during Normal Braking Events 27
3.1.1 Introduction 27
3.1.2 Methods 27
3.1.3 Results 29
3.1.4 Conclusion and Discussion 43
3.2 Age and Gender Differences in Brake Pulse during Car Following 44
3.2.1 Introduction 44
3.2.2 Method 45
3.2.3 Results 49
3.2.3.1 Dataset Composition 49

3.2.4 Conclusion and Discussion 61

3.3 Effect of Percent Overlap on Car-Following Behavior 63

3.3.1 Introduction 63

3.3.2 Method 63

3.3.3 Results 70

3.3.4 Conclusion and Discussion 74

4 Driver Behavior during Overtaking Maneuvers in Car Following 77
4.1 Introduction 77

4.2 Method 77

4.2.1 Identification of Lane Change Events 78

4.2.2 Determine Lead Vehicle Search Window 80

4.3 Results 82

4.3.1 Lane Change Detection Algorithm Validation 82

4.3.2 Lead Vehicle Identification Validation in Lane Change Events 84

4.3.3 Dataset Summery 85

4.3.4 Population Distribution of TTC at Lane Change 85

4.4 Conclusion and Discussion 88

5 Comparison of TTC at Braking with TTC at Overtaking 91
5.1 Introduction 91

5.2 Method 91

5.3 Theory/calculation 92

5.3.1 Time to Collision 92

5.3.2 Relative Frequency 92
5.3.3 Probability Density Function 93
5.3.4 Model Selection Criterion 93
5.4 Results 94
5.4.1 Dataset Summary 94
5.4.2 Automated Search Algorithm Results 95
5.4.3 Lane Change and Braking Frequency 95
5.4.4 Comparison of TTC at Braking and Lane Change 96
5.4.5 Ranking of Driver TTC 98
5.4.6 Driver Specific Probability Distribution of TTC in Lane Change and Braking 100
5.5 Conclusion and Discussion 102
6 Distribution of TTC and ETTC at Start of Steering during Overtaking 105
6.1 Introduction 105
6.2 Methods 106
6.2.1 Overall Approach 106
6.2.2 Bivariate Normal Distribution 107
6.2.3 Steering Maneuver Detection Algorithm 108
6.2.4 Data Signal Processing 110
6.2.5 Algorithm Validation 111
6.2.6 Results 112
6.3 Conclusion and Discussion 125
7 Conclusions 129

7.1 Key Points 129
7.1.1 Comparison of TTC and ETTC 129
7.1.2 Age and Gender Differences in Brake Pulse in Car Following 131
7.1.3 Effect of Percent Overlap on Car-following Behavior 132
7.1.4 Driver Behavior during Overtaking Maneuvers in Car-following 132
7.1.5 Comparison of TTC at Braking with TTC at Overtaking 133
7.1.6 Distributing of TTC and ETTC at Start of Steering during Overtaking 133
7.2 Comparison of TTC and ETTC during Normal Driving 133
7.3 Age and Gender Difference in Braking Behavior during Car Following 135
7.4 Effect of Percent Overlap on Car-Following Behavior 136
7.5 Driver Behavior during Overtaking Maneuvers in Car Following 138
7.6 Comparison of TTC at Braking with TTC at Overtaking 140
7.7 Distribution of TTC and ETTC at Start of Steering during Overtaking 142
7.8 Publication Summary 143
8 References 144
9 Appendix 154
9.1 Appendix A – Driver Ranking of 10th Percentile TTC at Braking and Lane Change 154
9.2 Appendix B – Driver Max Probability TTC at Braking and Lane Change Events 162

List of Figures

Figure 1. Combined Video Views from the 100-Car Naturalistic Study [98]. 13

Figure 2. Proportions of Distance Traveled and Trips with Valid Sensor Data. 14

Figure 3. Summary of Processing of Radar and Vehicle Instrumentation Data to Determine TTC of Lead Vehicles. Signals in blue were recorded by the vehicle instrumentation and green and red signals were computed using the formulae to the right. 16

Figure 4. Schematic of Transformation of Radar Position to Path Position. 17

Figure 5: Process for Determining Lead Vehicle in Car Following from Radar Data to Generate Time to Collision (TTC) Distribution. 18

Figure 6. Visual Representation of Car Following Scenarios. The arrow indicates the vehicle the algorithm identified as the lead vehicle. In scenarios (a) and (b) the algorithm and visual inspection agreed. In scenarios (c), (d), and (e) the algorithm and visual inspection disagreed. 22

Figure 7. Automated Search Algorithm Validation Results (n = 7,135 braking events) 22

Figure 8. 10th Percentile ETTC for Each Driver in Speed Ranges from 3-80+ mph (n = 876,619 braking events) 30

Figure 9. 10th Percentile TTC for Each Driver in Speed Ranges from 3-80+ mph (n = 985,259 braking events) 31

Figure 10. Cumulative Distribution of Relative Acceleration for Braking Events with a Closing Lead Vehicle 32

Figure 11. 10th Percentile ETTC with ETTC of Crash and Near-Crash Braking Events 34

Figure 12. 10th Percentile TTC with TTC of Crash and Near-Crash Braking Events 35

Figure 13. Histogram of ETTC at Brake Application with General Extreme Value Probability Distribution fit ($k = 0.640$, $\sigma = 3.981$, $\mu = 5.536$) 38

Figure 14. Histogram of TTC at Brake Application with General Extreme Value Probability Distribution fit ($k = 0.674$, $\sigma = 8.053$, $\mu = 9.706$) 38

Figure 15. Cumulative Distribution Function of ETTC GEV Model Fit and Braking Event Sample 39
Figure 16. General Extreme Value Probability Distribution fit of ETTC for Each 3-80+ Speed Bins..41
Figure 17. General Extreme Value Probability Distribution fit of TTC for Each 3-80+ Speed Bins.....41
Figure 18. Sample Brake pulse Characteristics.....46
Figure 19. Sample Brake Pulses.....48
Figure 20. Distribution of Braking Duration.....50
Figure 21. Distribution of Maximum Braking Deceleration.....51
Figure 22. Distribution of Vehicle deltaV.....52
Figure 23. Braking Duration and Vehicle deltaV.....52
Figure 24. Distribution of t_c/t_m.....53
Figure 25. TTC at Braking and t_c/t_m.....54
Figure 26. Distribution of Maximum/Average Braking.....55
Figure 27. Idealized Example of Mid Load Brake Pulses.....55
Figure 28. Front Load Brake Pulse Corridor.....56
Figure 29. Mid Load Brake Pulse Corridor.....57
Figure 30. Rear Load Brake Pulse Corridor.....57
Figure 31. LS Mean Estimate of Maximum Braking Deceleration by Travel Speed and Age Group....61
Figure 32. LS Mean Estimate of t_c/t_m by Travel Speed and Age Group.....61
Figure 33. Calculation of Percent (%) Overlap.....63
Figure 34. Identify Lead Vehicle Position Using Radar Range and Azimuth.....64
Figure 35. Vehicle Path Reconstruction to Improve Overlap Percentage Estimate.....65
Figure 36. Reconstruction of Vehicle Path.....66
Figure 37. Flow chart for vehicle trajectory reconstruction.....66
Figure 38. Calculation of Overlap Distance.....68
Figure 39. LS Mean Estimates of Minimum TTC by Travel Speed and Overlap Categories.....74

Figure 40. Road Scout Lane Change Signal Trigger Diagram 78
Figure 41. Definition of Lane Change Duration 79
Figure 42. Distribution of Lane Change Duration in Sample of Manually Reviewed Trips 80
Figure 43. Multiple Lead Vehicles in Lane Change Scenario 81
Figure 44. Lead Vehicle Search Window 81
Figure 45. Optimize Lead Vehicle Search Window 82
Figure 46: True Positive and False Negative Matrix 83
Figure 47: Lead Vehicle Detection Scenarios 84
Figure 48. Weighted Distribution of Lane Changes with Closing Lead Vehicle and TTC (90,639 total lane changes) 87
Figure 49. Weighted Distribution of Minimum TTC for Each Driver by Travel Speed Bin (n =90,639 lane changes) 88
Figure 50. Lane Change and Braking Frequency Ratio. 96
Figure 51. 10th Percentile TTC at Braking and Lane Change. 97
Figure 52. Driver Ranking of 10th Percentile TTC at Braking and Lane Change Events 99
Figure 53. Probability Distribution of Brake Application by TTC for Driver 1002 101
Figure 54. Probability Distribution of Lane Change Initiation by TTC for Driver 1002 102
Figure 55. Improved Method of Determining Start of Lane Change Event 105
Figure 56. Vehicle Kinematic Parameters Used to Estimate Start of Lane Change 106
Figure 57. Lateral Velocity and Distance to Lane Boundary (DTLB) Distribution from Fujishiro and Takahashi [88] (Reproduced with Permission from Authors) 107
Figure 58. Steering Maneuver Detection Algorithm Procedure 110
Figure 59. Algorithm Validation with Manual Video Review 112
Figure 60. Cumulative Distribution of Lead Time 113
Figure 61. Definition of Lead Time 113

Figure 62. Sensitivity Analysis of Confidence Interval 114
Figure 63. Sample Validation Result 115
Figure 64. Sample Event Distance Past Edge 116
Figure 65. Sample Event Lateral Velocity 116
Figure 66. Cumulative Distribution of Lead Time 118
Figure 67. Distribution of 10th Percentile ETTC at Start of Steering Maneuver 119
Figure 68. Distribution of 10th Percentile TTC at Start of Steering Maneuver 120
Figure 69. Distribution of Relative Velocity and ETTC at Start of Steering in 10th Percentile ETTC Lane Change Events 121
Figure 70. Distribution of Relative Velocity and Distance at Start of Steering in 10th Percentile ETTC Lane Change Events 122
Figure 71. GEV Distribution of ETTC at Start of Steering Maneuver 123
Figure 72. GEV Distribution of TTC at Start of Steering Maneuver 123
Figure 73. Comparison Modes of GEV Distributions for ETTC in Lane Change 124
Figure 74. Comparison Modes of GEV Distributions for TTC in Lane Change 125

List of Tables

Table 1. Post Stratification Weights 15

Table 2. Driver Selection with Valid Sensor Data 29

Table 3. Model Fit Criterion Summary for All Braking ETTC with Closing Lead Vehicle (n = 876,619 braking events) 36

Table 4. Model Fit Criterion Summary for All Braking TTC with Closing Lead Vehicle (n = 985,259 braking events) 36

Table 5. ETTC Probability Distribution Model Parameters 40

Table 6. TTC Probability Distribution Model Parameters 40

Table 7. ETTC GEV Probability Model Characteristics 42

Table 8. TTC GEV Probability Model Characteristics 42

Table 9. Dataset Composition 49

Table 10. LS Mean Maximum Braking Deceleration 58

Table 11. LS Mean t_c/t_m 58

Table 12. Analysis of Variance for Linear Mixed Effect Model 59

Table 13. Analysis of Variance for Linear Mixed Effect Model 60

Table 14. Dataset Summery - Overlap Analysis 70

Table 15. Driving Context Distribution - Overlap Analysis 71

Table 16. Analysis of Variance for Linear Mixed Effects Model for Minimum TTC 72

Table 17. Least Squared (LS) Mean Estimates of Minimum TTC by Main Effect Levels 73

Table 18. Comparison Results of Video and Lane Tracking Indicated Lane Changes 84

Table 19. Driver Selection with Valid Sensor Data 85

Table 20. Lane Change Scenario Distribution 86

Table 21. List of Common Probability Density Distributions 94

Table 22. Driver Selection with Valid Sensor Data 94

Table 23. Brake Events with Lead Vehicle 95
Table 24. 10th Percentile TTC at Braking and Lane Change 98
Table 25. Driver 1002 Max Probability TTC Summary 102
Table 26. Dataset Composition 117
Table 27. Summary of Relevant Publications 143
Table 27. Driver Max Probability TTC at Braking Events 162
Table 28. Driver Max Probability TTC at Lane Change Events 163

1 INTRODUCTION

1.1 THE INHERENT LIMITATION OF PASSIVE SAFETY TECHNOLOGY

In occupant protection, passive safety technology refers to vehicle safety technologies which limit occupant injury in the event of a crash. National Highway Traffic Safety Administration (NHTSA) began to issue Federal Motor Vehicle Safety Standards (FMVSS) in the 1960's to enforce the adoption of passive safety technology, in an effort to improve vehicle fleet crashworthiness. Passive safety technologies, such as the 3-point seat belts, frontal airbags, side and curtain airbags, seat belt pre-tensioners, and load limiters have all become standard equipment in modern vehicles due to the implementation of "FMVSS 208 – Frontal Crash Protection" [1], "FMVSS 214 – Side Crash Protection" [2], and other FMVSS over the years. NHTSA estimates that between the years 1960-2012, over 600,000 lives have been saved by these safety technologies [3].

However, as the name suggests, these passive safety technologies are only capable of preventing injuries in the event of a crash. Therefore, there exists an inherent limitation in passive vehicle safety. Despite the implementation of advanced passive safety technologies, passenger vehicle and light truck occupant fatalities still totaled over 29,000 in 2014 [4]. In severe crashes, occupants are still exposed to traumatic and fatal injuries despite the advancement of passive safety technologies [5]–[10]. Vulnerable road-users, such as pedestrians and motorcyclists, are offered even less protection in vehicle crashes [11]–[16]. In order for a vehicle to withstand crashes of increasing severity, automakers have the option of incorporating less comfortable safety devices, such as the 5-point seat belts or steel roll cages. Changes to infrastructures, such as road side barriers, have also been proposed [17]–[21], however, these implementations are costly and require long time period to install.

One alternative to break through the plateau of vehicle crashworthiness is active safety technology. Active safety technologies refer to crash avoidance methods in which the system is able to predict an imminent crash and either issue a warning or intervene to prevent the crash. These

active safety technologies operates under the mantra "the best accident is the ones that never happens". Examples of active safety system include forward collision avoidance, lane departure avoidance, lane departure warning/prevention, and pedestrian/animal detection.

1.2 Rear-end Collisions: Incidence and Consequences

One of the primary goals of forward collision avoidance systems is to reduce the incidence of rear-end collisions. Rear-end collisions are vehicle-to-vehicle crash events in which the front of the striking vehicle collides with the rear of the struck vehicle. Rear-end collisions are the most frequent crash mode on the roadway. NHTSA reported that approximately 1.9 million rear-end crashes occurred in the United States in 2014, accounting for approximately 32% of all crashes in 2014 [4]. Although rear-end collisions are often low speed, low severity crashes, the high frequency of occurrence can nevertheless result in substantial number of injuries and even fatalities. In 2014, approximately 32% of all injured occupants and 7% of occupant fatalities in the U.S. were associated with rear-end collisions [4].

There are injury consequences for occupants of both the striking and the struck vehicle. In the struck vehicle, low severity rear-end impact account for more long term injuries than any other crash mode [22]. Occupant neck injuries contribute to a significant portion of injuries sustained in low speed rear-end collisions [23]. The rear-end impact causes the struck vehicle occupant to experience sudden flexion and/or extension of the cervical spine, which can result in soft tissue injuries, commonly known as whiplash-associated disorders (WAD) [24]. Injury consequences of WAD range from pain and discomfort, to reduced range of motion and neurological loss, and even quadriplegia in severe events [25], [26].

Occupants of the striking vehicle of the rear-end collision experience a frontal collision with equal or more severe injury consequences. Numerous advanced passive safety systems, such as seat belts, pre-tensioners, load limiters, and advanced airbags have been implemented to protect

occupants in a frontal impact. However, in high severity frontal collisions, the occupants may still suffer serious injuries despite the latest passive safety technology [5], [27], [28].

1.3 Active Safety Systems: Forward Collision Avoidance

Forward Collision Avoidance Systems (FCAS) are a family of active safety technologies which aim to prevent forward vehicle collisions, such as rear-end crashes. FCAS typically utilize one or more range sensors, such as radar, infrared laser, ultrasonic, or machine vision, to track objects in front of the vehicle. In addition to analyzing the vehicle's surrounding, FCAS also considers host vehicle states, such as speed, yaw, acceleration, brake pedal, and turn signals, in order to evaluate collision potential. The on-board FCAS algorithm then processes this information to predict a potential collision. In the event of an imminent collision, the system warns the driver, or autonomously controls other systems such as vehicle throttle, steering angle modulator, and braking to avoid a crash. The following subsection describes five different types of FCAS.

1.3.1 Forward Collision Warning

Forward collision warning (FCW) systems have great potential to reduce rear end collisions on the roadway. These systems use radar scanning technology to track objects in front of the vehicle, and warn the driver through visual, audio, and/or tactile feedback in the event of an impending collision [29]–[31]. Studies have estimated that FCW can reduce the number of fatally injured drivers by as much as 29% [32]. The current U.S. New Car Assessment Program (NCAP) includes a confirmation test to check if the vehicle is equipped with FCW, and lists the feature as a part of the "Recommended Advanced Safety Technology" [33].

1.3.2 Dynamic Brake Support

Dynamic Brake Support (DBS) systems aim to mitigate forward collisions on the roadway. DBS is typically triggered when the system recognizes an emergency braking event, and amplifies

driver braking to avoid or decrease the severity of a collision. In a vehicle equipped with multiple component FCAS, DBS can be coupled with FCW to first warn the driver and then apply supplementary braking [29], [34]. For a system which includes both FCW and DBS, Kusano et al. estimates that the reduction in moderately to fatal injuries can be as much as 39% [32].

1.3.3 Autonomous Emergency Braking

Similar to DBS, Autonomous Emergency Braking (AEB) aims to prevent collisions by braking. AEB can be viewed as the last resort for the FCAS, and is only activated if the driver does not respond to the FCW and brake or steer to avoid the crash. If the vehicle recognizes that a collision is imminent and the driver will not be able to respond in time, AEB automatically applies full braking in order to avoid a crash. Previous studies has shown that a AEB system coupled with FCW has the potential of reducing rates of rear-end striking crash involvement with injures by 42% [35]. For a system which includes FCW, DBS, and AEB, the reduction in moderately to fatal injuries is estimated to be as much as 50% [32].

1.3.4 Adaptive Cruise Control

Each of the systems presented in the previous sub-sections illustrate the potential that, with increasing vehicle autonomy, the benefits in injury and fatality reduction can also increase. Adaptive Cruise Control (ACC) is another autonomous system which helps to prevent collisions. ACC is typically classified as an Advanced Driver Assistance System (ADAS), however ACC still has benefits in forward collision avoidance. ACC is initiated with the vehicle cruise control, and uses the vehicle forward radar to maintain following distance with the vehicle in front [30]. In certain systems, ACC can automatically slow the vehicle to a stop in the event that the lead vehicles comes to a stop.

1.3.5 AUTONOMOUS VEHICLE

Autonomous vehicles represent the ultimate version of vehicle automation. These vehicles are currently being tested on public road ways and have shown initial success. Arguably the most well-known autonomous vehicle project at this date is the Google Self-Driving Car Project. In their latest report, published in July 2015, the Google Self-Driving Cars had completed 1,101,171 miles of driving. The Google Self-Driving Cars had been involved in 15 minor traffic accidents, none of which was caused by the self-driving car [36]. In a recent study, published by the Virginia Tech Transportation Institute, the Google Self-Driving Car was found to have lower crash rate per million miles of traveled in all crash severities as compared to traditional vehicles[37]. In additional to Google, vehicle manufactures, such as Audi, BMW, Nissan, Volvo, have all announced plans for self-driving cars in the near future [38]–[41].

Autonomous vehicles, such as the Google Self-Driving Car, utilize Light Detection and Ranging (LiDAR) to collect information about the vehicle's surrounding. An algorithm then analyzes the LiDAR input to safely navigate through traffic in the roadway. In one of the scenario encountered by the Google Self-Driving Car, the autonomous vehicle was in the left turning lane prepare to make a left turn, the vehicle to the right of the self-driving car is attempting to pass the self-driving car and merge onto the left turning lane. The self-driving car recognize the intent of other drivers and proceeds to respond as if a human driver was operating the vehicle, and slows down to let the adjacent vehicle merge into the lane [36].

1.4 THE NEED TO UNDERSTAND DRIVER BEHAVIOR

As previous studies suggest, vehicles with increasing levels of automation have the potential to decrease the incidence and injuries associated with motor vehicle collisions. However, these active safety systems are only beneficial if the drivers do not turn off the system.

Despite the crash avoidance potential exhibited by FCAS systems, driver acceptance of the systems is paramount to their effectiveness [42]–[45]. If a FCW system delivers the warning too early, or if an autonomous braking system brakes unnecessarily or too early, it may distract the driver or annoy the driver and cause him/her to turn the system off [31], [46]–[48]. The question of when to deliver alarm is complex, as human perception of risk is not well understood, and may change with both the driver and the driving situation [49]. A better understanding of normal driving behavior can help designers predict when drivers take action in different situations [50]–[56]. If this were better understood, system would then only deliver alarm or intervene at the last possible moment to avoid nuisance alarms.

One approach to designing an ideal autonomous vehicle is to have a system which is human-centered [57], [58]. In the context of forward collision avoidance and vehicle automation, "human-centered" refers to a system which behaves like a human driver would. Such a system would be able to correctly deliver the warning during an imminent forward collision and, if needed, initiate an evasive maneuver, such as braking, both in magnitude and pulse shape, similar to a human driver. A better understanding of driver braking behavior can assist active safety system designers to better tailor the vehicle braking pattern to the driver and driving context.

In addition to improving active safety system effectiveness, a large dataset of normative driving behavior can serve as the scientific foundation for better mathematical models of driver behavior. One example of driver models are safety benefit estimate models, which are useful in estimating the potential benefits of prototype active safety systems. These driver models utilize driver response in normal behavior, such as steering reaction time and magnitude, or braking reaction time and magnitude, to simulate crash events when an active safety system would have been beneficial in avoiding or reducing the severity of the crash [32], [54], [59]–[62].

Therefore, an increase understanding of driver behavior can provide several benefits to future vehicle safety research. First, better understanding of driver behavior leads to improved

activation threshold for active safety systems and improved the effectiveness of these safety systems. Secondly, we also want future autonomous vehicles to apply braking similar to a human, therefore improving driver comfort. Lastly, the knowledge of driver behavior can help improve future driver models.

1.5 Driver Behavior Data Sources

Several data sources are available to study and characterize driver behavior. The following sub-sections describe several methods of estimating driver behavior.

1.5.1 Crash Databases

Crash databases provide detailed records of real world crashes, including the vehicle, environment, and occupant injuries. These databases can provide valuable insight into driver behavior which contributed to a crash, and in some datasets, driver actions taken in attempt to avoid a crash.

One of the largest real world crash databases is the National Automotive Sampling System (NASS), maintained by NHTSA. NASS includes two separate databases, first is the Crashworthiness Data System (NASS/CDS), which provides exhaustive detail on occupant injuries associated with each of the 4000-5000 in-depth crash investigations collected each year at 24 sites nationally. The second NASS database is the General Estimation System (NASS/GES), a database of approximately 60,000 U.S. police reported crashes per year, sampled from 60 representative regions across the United States.

Based on a review of 74 NASS/CDS cases, Knipling et al. found that the most common causes of rear-end crashes was identified to be driver inattention and following too closely [63]. Similarly, Wang et al. analyzed a subset of lane change crashes in NASS/GES and FARS, and found that the majority of lane change crash events (77%) occurred in daylight, and most lane change crash events involve two vehicles traveling at approximately the same speed [64]. More recent studies by Kusano

et al. simulated the subset of rear-end in NASS/CDS as if the vehicles were equipped with FCAS, to estimate the potential effectiveness of different FCAS systems [32].

Although real world crashes can provide a large database of accident information [65], pre-crash information of real world crash databases are estimated based on vehicle damage, scene investigation, and witness records. Therefore, one major drawback of crash databases is the fact that details regarding vehicle kinematics and driver reaction to pre-crash events are limited.

1.5.2 TEST TRACK EXPERIMENTS AND VIRTUAL DRIVING SIMULATOR

Another method of collecting detailed pre-crash vehicle kinematics and driver reactions is through test track experiments and virtual driving simulators. Test tracks provide a closed, controlled environment for researchers to monitor subject drivers. The test vehicles can be instrumented to capture additional information, such as driver video to monitor distraction, foot-pedal video to analyze reaction time, and different inertial monitors to capture vehicle kinematics.

Smith et al. evaluated several test track car following events, where the subject experienced several different crash imminent scenarios caused by the lead vehicle braking at different speeds and severities. The study found that, in the context of crash avoidance maneuvers, drivers generally initiate braking at longer distances than steering maneuvers in order to avoid a lead vehicle ahead in their lane of travel [66].

Similar to test tracks, virtual driving simulators can provide a controlled and flexible environment to create various pre-crash conditions. In addition, the major advantage of virtual simulators over test tracks is the relatively low cost. Bella et al. developed a new collision warning algorithm based on the analysis of driver reactions in a driving simulator. Drivers were exposed to four different driving conditions, and the result was used to assess the safety distances and risk perception of the drivers [67]. McGehee et al. compared data collected from test track experiments

and a high fidelity simulator on driver reaction time in crash avoidance, and found that driver performance in the two settings were statistically equivalent [68].

1.5.3 EVENT DATA RECORDERS

Although test track and simulator experiments provide detailed vehicle kinematics and driver reaction data, they do not fully describe driver behavior in an actual crash. One data source which has the potential to provide both detailed vehicle kinematics and driver reaction data is Event Data Recorders (EDR) [69]. EDR modules are installed in most new cars and light trucks, and are similar to the "black-boxes" used in the aviation industry. In the event of a crash, these EDR modules are able to record pre-crash data (e.g. brake and throttle input, vehicle speed), event severity, and restraint performance (e.g. seatbelt status, and airbag deployment status). EDR's have shown to be a useful tool to estimate crash severity [70]–[75], estimate occupant injury risk [76]–[80], and evaluation of passive safety system performance, such as airbag deployment [81], [82]. Furthermore EDRs have been validated by previous studies to be very accurate in both frontal and side crashes [83]–[85], and the data recorded by EDR's have been shown to be reliable even after extreme crash conditions, such as fire, immersion, and crush [86], [87].

Previous EDR studies by Kusano et al. have successfully extracted vehicle dynamics from advanced EDR to estimate pre-crash movement, such as vehicle speed, throttle and brake application, vehicle yaw, and steering input, for select real world lane departure crashes [88] [89].

Although data gathered from EDRs has been shown to be useful in characterizing driver behavior [90]–[93], one major limitation of the EDR data is that it only includes short durations of pre-crash information. Federal standard Part 563 only requires EDR modules to record a minimum of 5 seconds of pre-crash vehicle speed, engine throttle, and brake application [94]. In addition, EDR data only provides pre-crash data and is only triggered to record for crashes over a certain severity

threshold. In order to fully characterize driver behavior, normal driving information is also an essential component to the equation.

1.5.4 NATURALISTIC DRIVING STUDIES

Naturalistic Driving Studies (NDS) involve instrumenting drivers' personal vehicles and recording all normal driving for a period of months or years. NDS combine the detailed time-series information provided by test track, simulator, and EDRs, and real world crash environment that drivers experience. In addition to characterizing crash causation[95], NDS have become a valuable data source to characterize driver behavior to design and evaluate active safety systems [96], [97]. Large scale NDS can result in thousands to millions of vehicle miles of instrumented driving. Participants are in a "naturalistic driving environment", meaning they are not given any particular instructions and researchers are not present to monitor during the course of the study. Therefore, NDS provides objective data on driver behavior under normal conditions. Two of the largest NDS studies to date are the 100-Car Naturalistic Driving Study [98] and the Second Strategic Highway Research Project [99].

The instrumentation on-board a NDS vehicle includes cameras, typically of the vehicle interior and exterior, and vehicle sensors, such as acceleration, velocity, and GPS position. These large, high-resolution, continuously recorded data provide a high level of detail to study driver behavior in crashes, near-crashes, and normal driving conditions.

1.6 RESEARCH OBJECTIVE

The overall research object of this dissertation was to characterize normal driver behavior in car following events. The dissertation presents the first large scale study of its kind, based on naturalistic driving data to report driver behavior during various car-following events. The overall goal of this dissertation was to provide a better understanding of driver behavior in normal car-

following driving conditions, which can benefit automakers who seek to improve FCAS effectiveness in rear impact avoidance, as well as regulatory agencies seeking to improve FCAS vehicle tests.

2 DATA SOURCES AND OVERALL APPROACH

2.1 DATA SOURCE

The research in this dissertation was based primarily on the analysis of naturalistic driving study (NDS) data. Several large-scale NDS are currently available. Examples include the Integrated Vehicle-Based Safety Systems (IVBSS) program, conducted by the University of Michigan Transportation Research Institute (UMTRI) [100], and the 100-Car NDS, conducted by the Virginia Tech Transportation Institute (VTTI) [98]. The most recent and the largest NDS collection effort to date is the Second Strategic Highway Research Program (SHRP-2), which instrumented 3,362 private vehicles over 3 years [99]. In comparison, the 100-Car NDS includes the largest set of naturalistic data currently available, in terms of number of vehicles and drivers, and miles of vehicle travel, and was the main data source in the following dissertation.

2.2 OVERVIEW OF THE 100-CAR NATURALISTIC DRIVING STUDY

The 100-Car study was a landmark large-scale NDS conducted by the Virginia Tech Transportation Institute (VTTI) from 2001 to 2004 [98]. Drivers were recruited from the Washington D.C. metropolitan area. Few restrictions were used to select subjects, e.g. excluding those with traffic violations. Younger drivers, i.e. under 25 years, and self-reported high mileage drivers were sought and oversampled, however.

Vehicles were instrumented with cameras and inertial measurement devices and equipped with a PC-based computer to collect and store the data. The data collection box housed a yaw rate sensor, dual axis accelerometers, and a GPS navigation unit. In addition, radar sensors were mounted on the front and rear of the vehicle that were able to track other vehicles. The data collection box was usually installed on the roof of the trunk of the vehicle in order to be unobtrusive. . In addition to the on-board instrumentation, vehicle data, such as vehicle speed and brake pedal switch, was collected from the vehicle CAN bus. All data were sampled at a rate of 10 samples per second. Some of the

sensors had lower sample rates. These data were still sampled at 10 samples per second but would have multiple samples with equal magnitude.

There were five (5) cameras that offered continuous views in and around the vehicle, as shown in Figure 1. The upper left frame shows a view of the driver's face and upper body, blurred to protect the identity of the driver in Figure 1. The lower left pane is an over-the-shoulder view of the driver, the upper right pane is a forward view out the front of the vehicle, and the lower right pane is split between a view out the passenger side of the vehicles and out the rear of the vehicle.

Figure 1. Combined Video Views from the 100-Car Naturalistic Study [98]**.**

2.3 DRIVER SELECTION

A total of 108 primary drivers and 299 secondary drivers were included in the 100-Car study period in which all driving in an instrumented vehicle was recorded [101]. Primary drivers were the primary owners or leasers of the instrumented vehicles. Secondary drivers occasionally drove the vehicles. Primary drivers accounted for 89% of all miles driven during the study period. The entire 100-Car database contains approximately 1.2 million miles of driving. A total of 1,119,202 miles of which were driven by primary drivers in 139,367 trips [101].

Some primary drivers drove in multiple vehicles. For the current study only trips where a primary driver was driving in the vehicle that he or she most frequently drove during the study, i.e.

their primary vehicle, were selected. Two drivers were excluded because they were enrolled in the study for a very short period of time resulting in few trips. One driver was enrolled for 11 days and the other was enrolled for 7 days, resulting in a total of 70 and 7 trips, respectively. These two drivers were excluded leaving 106 primary drivers.

Prior to the analysis, the status of all time-series data was inspected. Instrumentation data, such as the front facing radar, vehicle speed, brake switch status, yaw rate signals, and lane tracking signal, were checked for missing or invalid data. Studies in the following dissertation only included vehicles which had valid data in at least 60% of all trips and 60% of all distance traveled. The 60% threshold was determined by a distribution of distance traveled and trips with valid sensor data, as shown in Figure 2. Each point in the figure represents one driver and the color and size of the point represents the total number of miles traveled by the participant in the study. First, there were 10 drivers that had no trips with valid data. For most other drivers, the proportion of distance and trips traveled with valid data were proportional. The drivers along the upper left edge of Figure 2 were drivers that had very few trips with valid vehicle speed data, which was used to compute distance traveled.

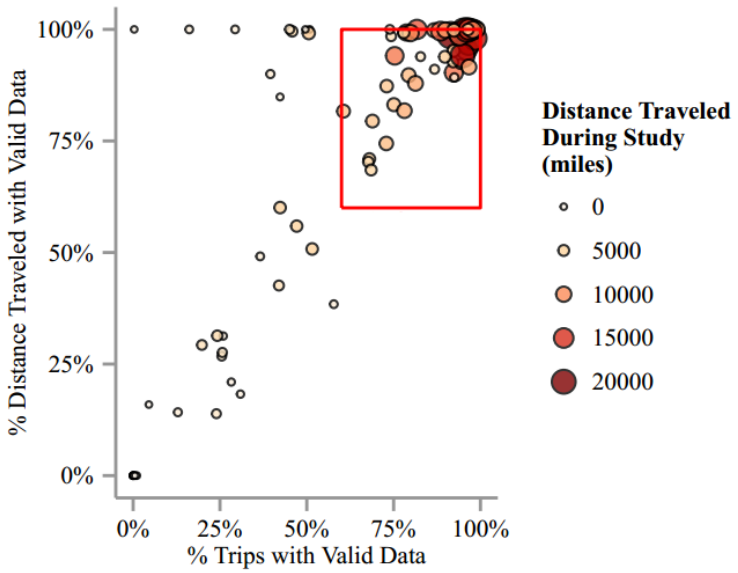

Figure 2. Proportions of Distance Traveled and Trips with Valid Sensor Data.

2.4 DRIVER DEMOGRAPHIC WEIGHTING FACTOR

The 100-Car NDS oversampled younger drivers by design. The following dissertation employed a weighting factor to adjust for the oversampled young drivers in the dataset. The weighting factor was calculated based on a post stratification strategy, in which we compared the distribution of age and gender between licensed drivers nationwide in 2012, the most recent year available from Federal Highway Administration [102], and the current sample of drivers from the 100-Car NDS. Each driver was assigned a weight, w, as shown in Equation 1,

$$w = \frac{p_{reg}}{p_{sample}} \qquad \textbf{Equation 1}$$

where p_{reg} represents the proportion of registered drivers, and p_{sample} represents the proportion of drivers in the sample. The complete tabulation of weighting factors for age and gender is shown in Table 1. In general, younger drivers had lower weights than the other age groups because they were oversampled.

Table 1. Post Stratification Weights

Age Group (years), Gender	% Drivers	% Sample	Weight
Novice (18-20), Female	2.8%	9.4%	0.30
Novice (18-20), Male	2.9%	9.4%	0.31
Young (21-30), Female	7.7%	7.8%	0.98
Young (21-30), Male	7.7%	23.4%	0.33
Middle (31-50), Female	17.7%	4.7%	3.78
Middle (31-50), Male	17.6%	21.9%	0.8
Mature (51+), Female	22.3%	10.9%	2.03
Mature (51+), Male	21.4%	12.5%	1.71

2.5 AUTOMATED LEAD VEHICLE IDENTIFICATION ALGORITHM

In order to efficiently analyze a large number of events in the 100-Car NDS, an automated algorithm was developed by Kusano et al. to identify car-following events [103]. The following section summarizes the overall development of the algorithm.

2.5.1 *Calculation of Position of Radar Objects*

The first step in identifying car following situations was to use the radar and vehicle data to determine the position of radar objects with respect to the equipped vehicle. Figure 3 summarizes how the radar (range, range rate, and azimuth) and vehicle (yaw rate and speed) data were used to compute the distance along (s) and from (d) the vehicle's path to a potential lead vehicle. Distance from the vehicle's path (d) was used to identify lead vehicles. Distance along the vehicle's path (s) was used to compute the headway (H) of the lead vehicle.

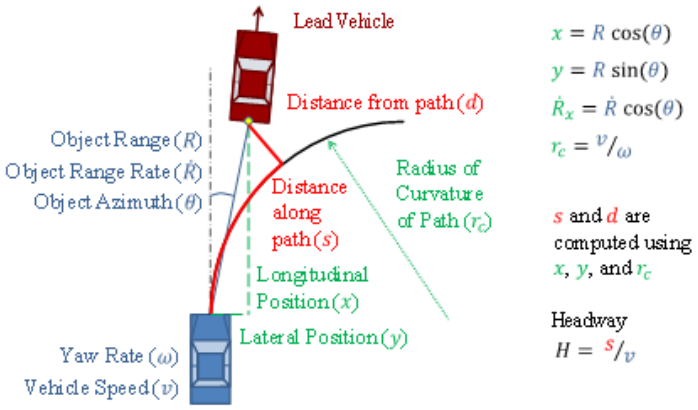

Figure 3. Summary of Processing of Radar and Vehicle Instrumentation Data to Determine TTC of Lead Vehicles. Signals in blue were recorded by the vehicle instrumentation and green and red signals were computed using the formulae to the right.

Distance along the vehicle path (s) and distance from the vehicle path (d) were calculated from the radar position (x, y) and radius of path curvature (r_c), as shown in Figure 4. The calculation to transform the radar position was done in order to better track objects in front of the equipped vehicle while it was traveling around curved road sections.

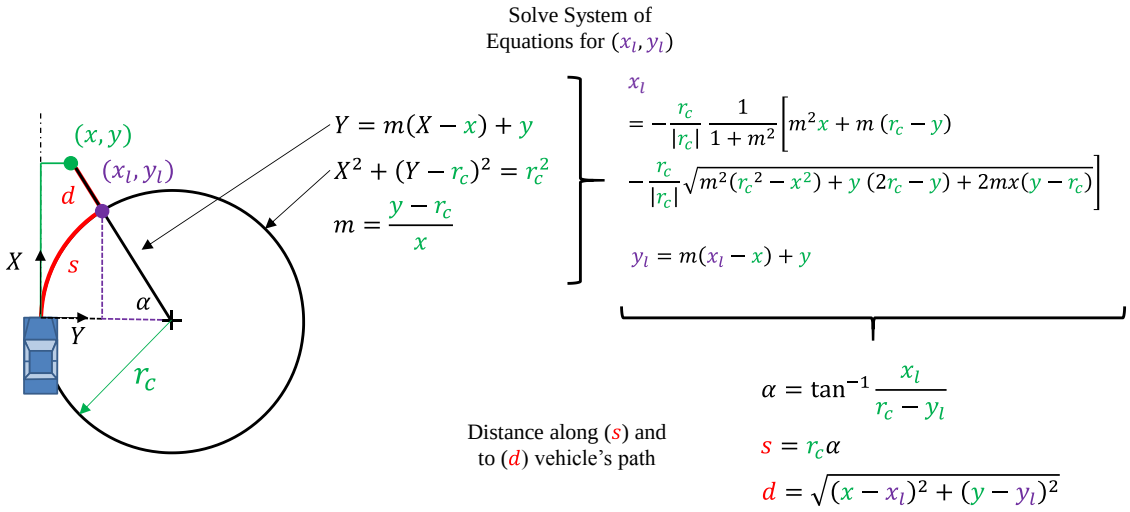

Figure 4. Schematic of Transformation of Radar Position to Path Position.

Subsequently, time headway (H) was calculated from vehicle speed (v) and distance along the vehicle path (s) as:

$$H = s/v\,. \qquad \textbf{Equation 2}$$

In this algorithm, a time headway less than 3 seconds was used to define a car-following event as suggested in the American Association for State Highway Transportation Officials (AASHTO) Highway Capacity Manual [104].

Two additional radar signals were used to determine if a vehicle was a lead vehicle: object ground speed, v_t, and the change in the azimuth angle $d\theta/dt$. The object ground speed was computed using the radar relative speed and vehicle speed:

$$v_t = \dot{R}_x + v \qquad \textbf{Equation 3}$$

A positive value for v_t describes an object that has velocity in the same direction as the equipped vehicle. The change in azimuth angle is simply the time derivative of the radar azimuth angle.

2.5.2 *Search Trips for Car-following*

The overall objective of the automated search algorithm was to take each individual trip data file and identify which object tracked by the forward-facing radar was the lead vehicle, or the vehicle

directly in front of the subject vehicle, during each brake application. A process diagram of the search for lead vehicles is shown in Figure 5. Each of the 5 main processes are explained in detail below.

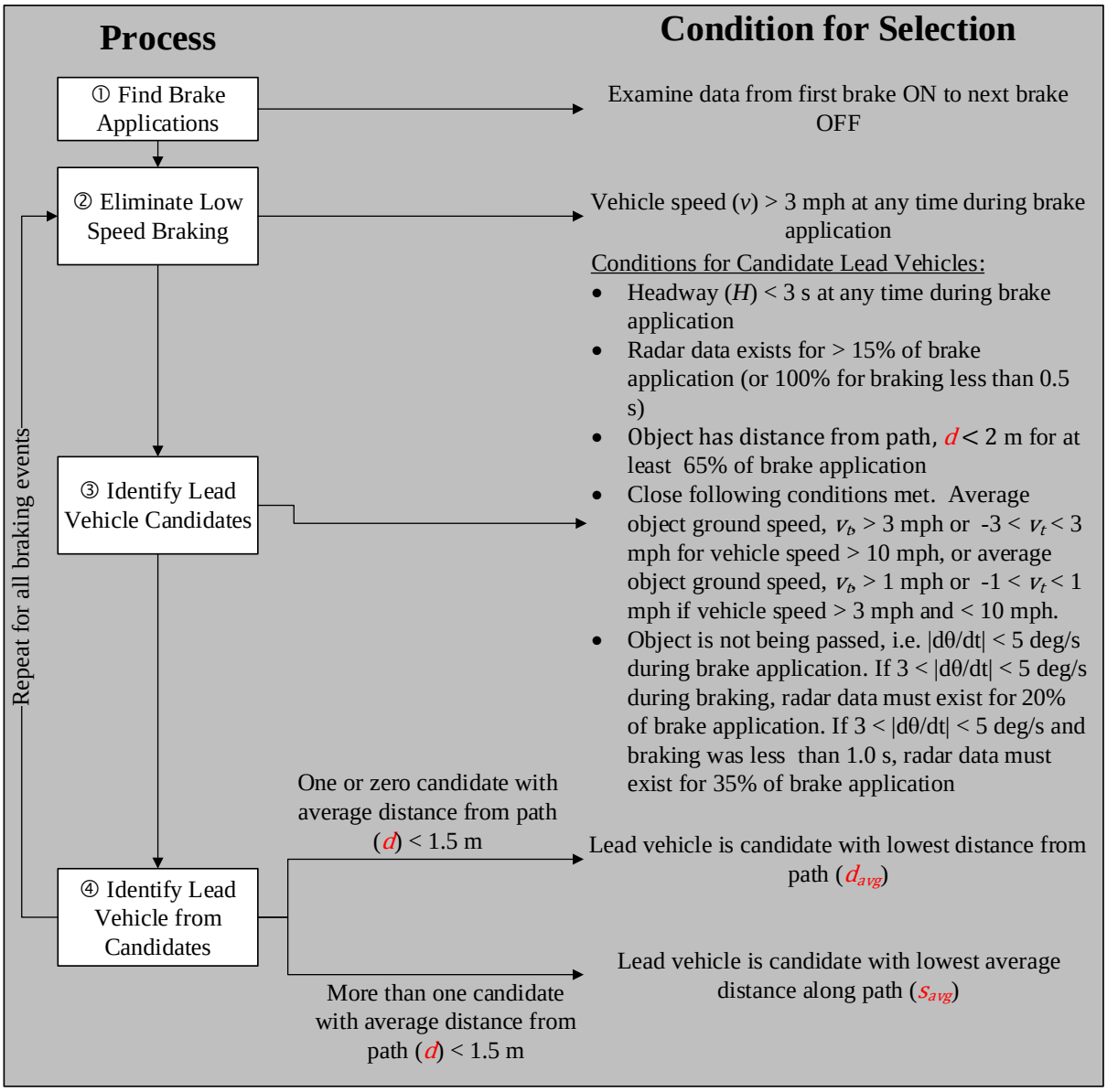

Figure 5: Process for Determining Lead Vehicle in Car Following from Radar Data to Generate Time to Collision (TTC) Distribution.

① Find Brake Applications

Brake applications were defined as when the recorded brake switch status was first in the ON state to the time when the brake switch status was next OFF. Brake applications less than two data points (~0.2 seconds) apart were combined into one braking event. For each

braking event, the unique radar tracking ID number of each tracked object was identified and extracted. Braking events without any occurrence of tracked objects were discarded as events having no lead vehicle.

② Eliminate Low Speed Braking

Any brake applications where the vehicle speed was never above 3 mph were eliminated because low speed braking is not of interest to the current FCW design.

③ Identify Lead Vehicle Candidates

- Time headway (H) less than 3 seconds was used to define a car-following event as suggested in the American Association for State Highway Transportation Officials (AASHTO) Highway Capacity Manual [104]. Time headway was calculated using Equation 2.
- Tracked radar objects where considered in front of the equipped vehicle if two conditions were met:
    1. Radar data was present for 15% of brake application (tracking percent condition)
    2. The distance from the vehicle's path (d) was < 2 m for 65% of brake application (In-lane percent condition)
- To eliminate fixed objects and objects that were being passed in adjacent lanes, two additional conditions must have been satisfied in order to be labeled a candidate lead vehicle:
    1. The object ground speed, v_t, was > 3 mph. If the object had an average ground speed between -3 mph and 3 mph and the minimum distance along the vehicle's path, s, was less than 6 m or the minimum speed of the equipped vehicle was less than 30 mph, the object could qualify as a candidate lead vehicle. These close following conditions were added to

include stopped vehicles and exclude vehicles traveling in the opposite direction or fixed roadside objects.

2. The magnitude of the change in azimuth angle, $|d\theta/dt|$, was < 5 deg/s during brake application. If $3 < |d\theta/dt| < 5$ deg/s, the tracking percent must have been at least 20% to be considered a candidate lead vehicle. If $3 < |d\theta/dt| < 5$ deg/s and the brake application was less than 1.0 s the tracking percent must have been at least 35%. These conditions were added to exclude objects that were in adjacent lanes that were being passed quickly by the equipped vehicle. This adjacent vehicle condition also eliminated some fixed roadside objects that exhibited the same behavior.

For cases where the braking event exceeded 150 frames (15 seconds) tracking percentage was calculated as the percentage of the first 50 frames of the braking event where the radar identified and tracked the object. This allowed the search algorithm to account for very long braking events during which the subject vehicle or lead vehicle may have changed lanes or situations where radar lost tracking when both vehicles were at a complete stop.

In-lane percentage was calculated as the percentage of tracked points during the braking event where the object's distance from the vehicle path (d) was less than 2 meters. A parametric study varying the in-lane distance between 1.0 m and 3.0 m found that the lowest error in identifying the correct lead vehicle was 2 meters. A standard lane width in the U.S. is approximately 3 to 3.5 m, so 2 meters is slightly larger than half of a lane width. A length slightly greater than half a lane width allowed for flexibility in identifying leading vehicles while not greatly increasing the number of vehicles that were actually in adjacent lanes identified as the lead vehicle.

④ Identify Lead Vehicle from Candidates

More than one candidate lead vehicle could be identified in step ③. If more than 1 candidate was found, a refined search was performed. The refined search was determined if the average distance from the vehicle's path, d_{avg}, was less than 1.5 m during braking for each candidate.

- If one or zero candidates met $d_{avg} < 1.5$ m: Lead vehicle is the candidate with minimum d_{avg}
- If more than one candidate met $d_{avg} < 1.5$ m: Lead vehicle is candidate with minimum average distance along path, s_{avg}

After repeating steps ②-④ for all brake applications for all drivers, brake applications with valid lead vehicle were selected based on the following criteria:

1. A radar object was identified as lead vehicle during brake application
2. Radar data was available at the start of braking (time of first brake ON)
3. The equipped vehicle was getting closer to lead vehicle, i.e. closing

2.5.3 Validation of Automated Search Algorithm

In order to assess the accuracy of the automated lead vehicle identification algorithm, undergraduate interns in our lab group compared results from manual video inspection to the result reported by the algorithm. The following section presents the method of the algorithm validation for braking events, similar validation process was done for lane change events and will be presented in later chapters of the dissertation.

2.5.3.1 Lead Vehicle Identification Validation in Braking Events

For the validation of lead vehicle identification during braking events, undergraduate interns in our lab group manually examined video footages from 323 trips containing 3,765 miles of travel and 115 hours of data. For each braking event, the results of the automated search algorithm were

compared to the results of the manual video review. This comparison was classified into one of the scenarios depicted in Figure 6. The arrow indicates the object identified by the search algorithm as the lead vehicle. Scenario (a) and (b) show successful algorithm identification scenarios while scenarios (c), (d) and (e) show unsuccessful scenarios where the algorithm differed from the visual inspection.

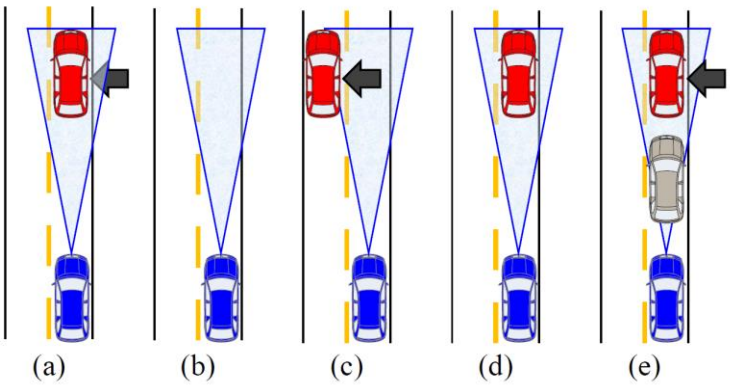

Figure 6. Visual Representation of Car Following Scenarios. The arrow indicates the vehicle the algorithm identified as the lead vehicle. In scenarios (a) and (b) the algorithm and visual inspection agreed. In scenarios (c), (d), and (e) the algorithm and visual inspection disagreed.

Figure 7 shows the result of the automated search algorithm validation. The validation was based on the comparison of the automated search algorithm against 7,135 manually inspected braking events. The result of the validation shows that the automated search algorithm correctly identified 90.7% of the car following situations.

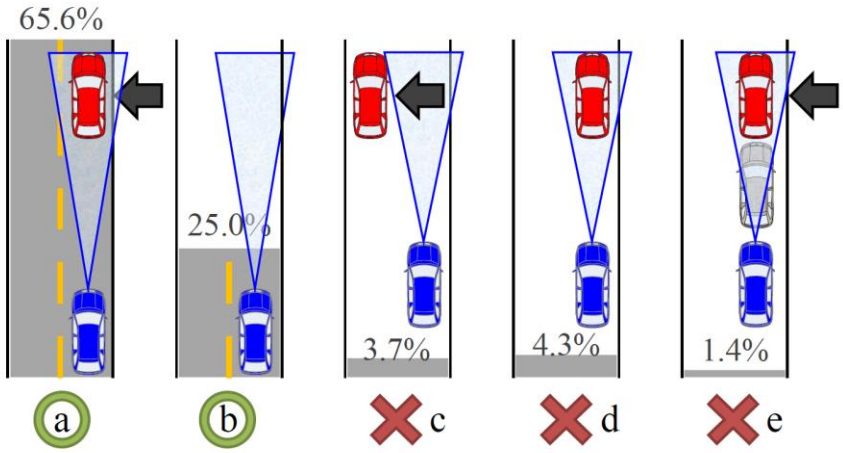

Figure 7. Automated Search Algorithm Validation Results (n = 7,135 braking events)

2.6 DRIVER RISK PERCEPTION INDEX

Several metrics have been developed in an effort to quantify driver risk perception in car-following situations, distinguish normal car-following behavior and distracted and crash imminent driver behavior, and improve forward collision avoidance system activation. A selected number of published metrics are described below.

2.6.1 PERFORMANCE INDEX FOR APPROACH AND ALIENATION

Performance Index for Approach and Alienation is a driver risk perception index developed by Wada et al. [105]. This particular index is unique in that it is based on the changes of area of the preceding vehicle on the driver's retina to evaluate the driver alert status. Equation 4 shows the relationship between driver visual input and vehicle kinematic, where the variable KdB describes the change of the preceding vehicle's area on driver's retina, Vr is the relative velocity between the vehicles, and D is the distance between the vehicles.

$$KdB = 10\log_{10}(|\, 4x10^{7}\, x\frac{Vr}{D^{3}}\,|)sign(-Vr) \qquad \textbf{Equation 4}$$

2.6.2 PERCEPTUAL RISK ESTIMATE

Perceptual Risk Estimate (PRE) is a driver risk perception index developed by Aoki et al. [106]. PRE was developed based on the hypothesis that drivers' decision to brake is based on two different perceptions: kinematic perception, which refers to events when drivers approach a slow moving or stopped vehicle, and dynamic perception, which refers to events when the lead vehicle decelerates. The relationship between the two components of driver perception can be described as follows:

$$PRE = \frac{V_r + \alpha V_s + RT(Ap + Af)}{D^n} \qquad \textbf{Equation 5}$$

where V_r is the relative velocity, α is the driver sensitivity to subject vehicle speed (used to adjust driver's perception error in subject vehicle speed), RT is the driver reaction time between

throttle release and brake application, Ap is the actual deceleration of the lead vehicle, Af is the foreseen deceleration of the lead vehicle (i.e. driver estimated deceleration), and D is the distance between the vehicles, adjusted by the perceptual scaling of distance, n.

2.6.3 REQUIRED DECELERATION PARAMETER

Required Deceleration Parameter (RDP) is another metric which measures the theoretical deceleration necessary to bring the vehicle to a stop. The equation for RDP is shown in Equation 6, and was derived based on traditional kinematics equations for constant acceleration. RDP is a popular metric to characterize drivers through intersections to aid in the development of intersection assist systems and pedestrian detection systems [107], [108].

$$RDP = \frac{V^2}{2 * WD} \qquad \textbf{Equation 6}$$

2.6.4 TIME TO COLLISION

One of the most widely used metrics of characterizing car-following events is using time to collision (TTC). TTC is a measure of time required for two vehicles to collide if both vehicles continue at their present speed and current path, and is calculated as the ratio of the range (D) between vehicles and the rate of change of range (V_r), as shown in Equation 7. Studies have shown that TTC is correlated to drivers' risk perception [109], where lower TTC indicates close following distance and higher risk of collision in car following situations.

$$TTC = \frac{D}{V_r} \qquad \textbf{Equation 7}$$

2.6.5 ENHANCED TIME TO COLLISION

TTC is of course not accurate if a driver either accelerates or brakes (decelerate) to avoid a lead vehicle. As an improvement to TTC, other metrics have been proposed to evaluate driver perceived risk and as a basis for a warning triggering threshold. Enhanced Time to Collision, or ETTC,

is similar to TTC and measures the time that it will take a subject vehicle to collide with the target vehicle. However, ETTC takes into account vehicle acceleration and assumes the relative acceleration between the vehicles remains constant.

The equation for ETTC is derived based on the equations of motion, in which the distance between two point masses is calculated as shown in Equation 8.

$$D = D_o + \frac{1}{2} * A_r * t^2 + V_r * t \qquad \textbf{Equation 8}$$

Where D is the distance between two objects at time t, D_0 is the distance between the two objects, A_r is the relative acceleration of the objects with respect to time t, and V_r is the relative speed of the two objects with respect to time.

For each braking event, we can compute the ETTC by solving for the time (t) when the distance between the two vehicles (d) equals to zero. The quadratic formula was used to transform the equations of motion in Equation 8 to solve for the time, as shown in Equation 9.

$$ETTC = \frac{-V_r - \sqrt{V_r^{\,2} - 2 * A_r * D}}{A_r} \qquad \textbf{Equation 9}$$

Where V_r is the relative speed between the two vehicles, A_r is the relative acceleration between the vehicles, and D is the distance between the two vehicles. Because ETTC accounts for relative acceleration, ETTC has the potentially to be a more accurate metric of collision time and perceived risk. NHTSA's current FCW confirmation test requires the system to deliver a warning within a specified ETTC threshold when approaching a stopped, decelerating, and constant speed vehicles [33].

2.7 CONCLUSION

The following dissertation used data from the 100-Car Naturalistic Driving Study to characterize driver behavior, both braking and lane change maneuvers, in normal car-following events.

In order to efficiently aggregate a large sample of car-following events, an automated search algorithm has been developed to automatically identify lead vehicles in car-following events. A comparison of the algorithm and manual video inspection shows that the algorithm is ~91% accurate in identifying lead vehicles in car-following events.

Lastly, this chapter presented a sample of existing metrics to quantify driver behavior. Although several metrics are currently available, due to the ease of use and availability of instrumentation data, the following dissertation uses TTC and ETTC to characterize driver behavior in car-following.

3 DRIVER BEHAVIOR DURING BRAKING IN CAR-FOLLOWING

3.1 COMPARISON OF TTC AND ETTC DURING NORMAL BRAKING EVENTS

3.1.1 INTRODUCTION

A major challenge in the design of Forward Collision Warning (FCW) systems is to increase driver acceptance of the systems. As described in the introduction, drivers can become annoyed and may disable the system if they feel they are receiving unnecessary warnings. One strategy to reduce these so-called nuisance alarms is to design a FCW with several different user settings, for example "near" or "far" warning settings. These settings can change when the FCW system will warn the driver. In a "near" setting, warnings would only be delivered at the last second for drivers to avoid a collision. In a "far" warning setting, the system would warn the driver earlier but at the cost of delivering more frequent alarms.

In order to design a FCW with multiple use settings, the designer needs a distribution of braking characteristics of the general population. The objectives of this chapter was to determine the distribution of TTC and ETTC at brake onset in car-following situations using the 100-Car Naturalistic Driving Study (NDS). In addition, the study presents probability distributions of ETTC and TTC values across various vehicle speeds. The result from the following study provides active safety designers a better understanding of driver braking behavior, and aids in the design of FCW warning threshold

3.1.2 METHODS

3.1.2.1 ETTC Calculation

In this study, we computed ETTC at the start of the brake application according to the equations described in Chapter 2.6.5. The distance and relative speed was recorded by the

instrumented radar in each vehicle of the 100-Car NDS. The relative acceleration was computed as the rate of change of the range rate.

3.1.2.2 Probability Density Function

Probability density functions characterize the probability of occurrence for a set of continuous random variables, such as TTC and ETTC. The following study investigates braking behavior over all normal driving in 100-Car NDS, and finds the best probability distribution which describes the ETTC and TTC values.

3.1.2.3 Model Selection Criterion

The approach to finding the distribution which best fit the calculated TTC and ETTC was to compare a number of common probability density distributions. Model selection was determined based on two statistical criteria, the Akaike's information criterion (AIC) [110], and the Bayesian information criterion (BIC) [111]. If a model is constructed based on a sample of training data, AIC and BIC provides an estimate of the model performance on a similar sample of testing data. In order to avoid the addition of parameters which will overfit the model to the training data, both AIC and BIC controls for the number of parameters in a model using a penalty term, as seen in Equation 10 and Equation 11.

$$AIC = -2 * \ln(likelihood) + 2 * k \qquad \textbf{Equation 10}$$

$$BIC = -2 * \ln(likelihood) + k * \ln(n) \qquad \textbf{Equation 11}$$

Where n is the number of observations, and k is the number of parameters in the model. The *likelihood* term in both equations denotes the likelihood function, which measures the agreement between the model and the observed data.

3.1.3 RESULTS

3.1.3.1 Dataset Summary

Table 2 summarizes the number of trips and miles traveled by all primary drivers in their primary vehicles, as well as drivers with valid sensor data. A total of 72,380 trips from 64 drivers was used in this study.

Table 2. Driver Selection with Valid Sensor Data

Group	Drivers	Number of Trips	Miles
All Trips (Primary Drivers/Vehicles)	106	132,721	1,118,905
Drivers with >60% Valid Sensor Data	64	81,696	747,282
Trips with Valid Data	64	72,380	609,620

3.1.3.2 10th Percentile ETTC Distribution

An ideal FCW system must deliver timely warnings while eliminating nuisance alarms. Therefore, it is important to understand drivers' perception of the lowest acceptable ETTC or TTC values in normal braking events. The following section presents the distribution of the 10th percentile ETTC and TTC in braking for each driver. Unlike minimum values, the 10th percentile provides the valuable lower end threshold and eliminate extreme values which may be captured by calculating the minimum.

Figure 8 shows the distribution of 10th percentile ETTC for each drivers. The speed shown on the horizontal axis corresponds to the vehicle speed at the start of the braking event, and is organized into 9 bins by vehicle speeds ranging from 3 to 10 mph, and 10 to 80+ mph in 10 mph increments. The vertical axis shows ETTC value at the start of the braking event. Each data point represents the 10th percentile ETTC for all braking events within each speed bin for one driver. The count on top of the figure, i.e. n = 64, represents the number of drivers included in each speed bin. The number of drivers are less than 64 in higher vehicle speed bins due to the fact that not all drivers performed braking maneuvers in all speed bins. The black solid and dotted lines represent the

median and 10th percentile for the entire driver population. Similarly, Figure 9 shows the distribution of 10th percentile TTC for each driver in each speed bins.

As shown in the figures, both the distribution of TTC and ETTC generally increase with respect to vehicle speed. In addition, the variance between drivers are shown to increase with vehicle speed. One major difference between the two distributions is the median and 10 percentile for all drivers. The median (50th percentile) and 10th percentile is significantly lower for the distribution of ETTC than the distribution of TTC. One hypothesis for the difference is the addition of relative acceleration in the ETTC calculation. Braking events with a closing relative speed may have a much lower time to collision if the relative acceleration indicates that the relative speed is increasing.

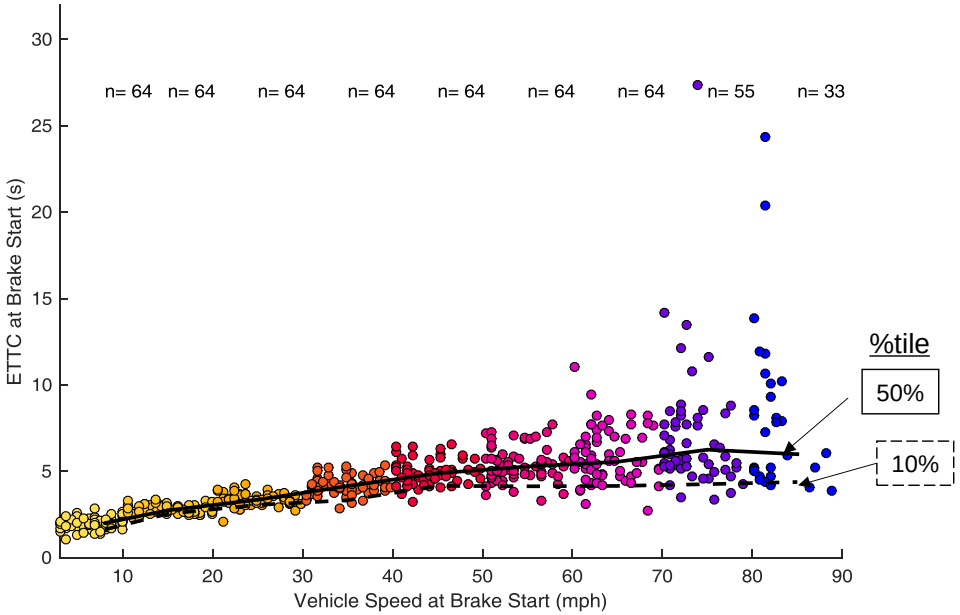

Figure 8. 10th Percentile ETTC for Each Driver in Speed Ranges from 3-80+ mph (n = 876,619 braking events)

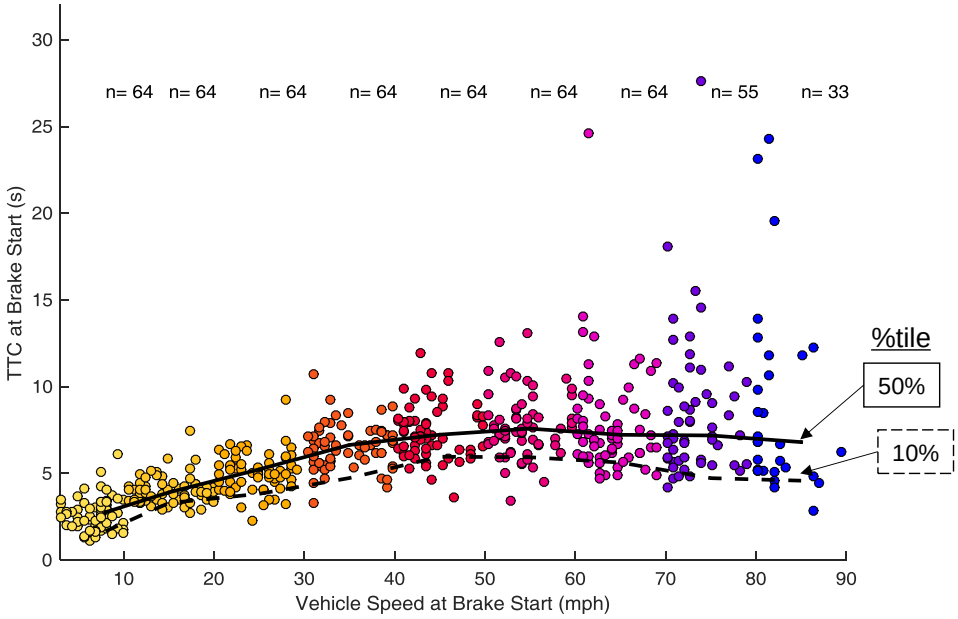

Figure 9. 10th Percentile TTC for Each Driver in Speed Ranges from 3-80+ mph (n = 985,259 braking events)

In order to evaluate the effect of relative acceleration in closing braking events, Figure 10 shows a cumulative distribution of relative acceleration in closing braking events. The relative acceleration was calculated based on the time difference of vehicle relative speed at the start of the braking event, i.e. within the first 0.1 second of driver brake application. Positive relative acceleration indicate that the vehicle is accelerating at the start of the braking event, and negative value indicate deceleration. As shown by the figure, the median relative acceleration at the start of closing braking events was 0.3 m/s^2, indicating that in most closing braking events, the vehicle is still accelerating towards the lead vehicle at the onset of brake application. An example scenario would be when the instrumented vehicle and the lead vehicle are traveling down the road at the same speed and the lead vehicle suddenly applies the brake, causing the relative acceleration to increase, and leads to the instrumented vehicle driver applying the brake. In addition, Figure 10 shows that the relative acceleration was zero in only 1/3 of the braking events. Therefore in only 1/3 of the braking

events TTC and ETTC are the same. The result shown in the figure suggests that ETTC can provide an improved measure of time remaining until collision by considering relative acceleration.

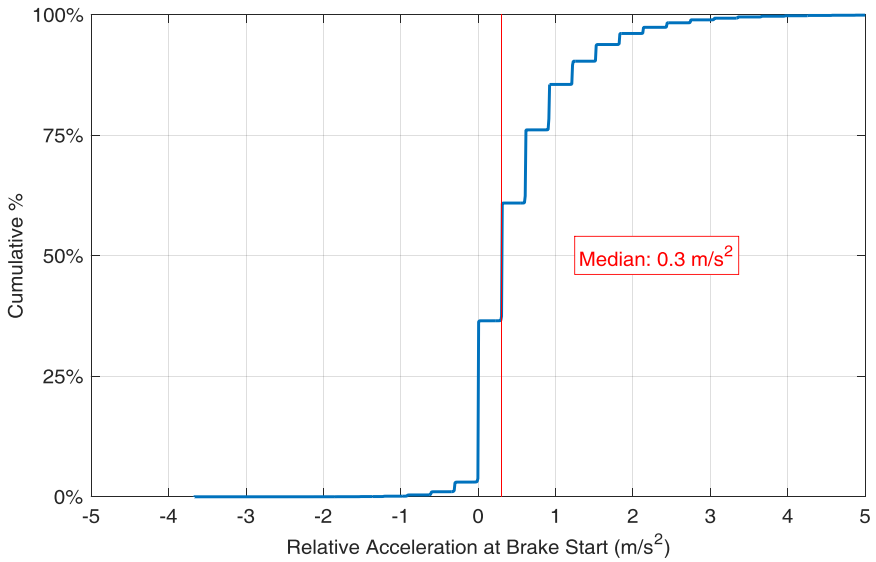

Figure 10. Cumulative Distribution of Relative Acceleration for Braking Events with a Closing Lead Vehicle

3.1.3.3 Near-Crash and Crash Events

VTTI has identified a total of 66 crash events and 738 near-crash events in a previous data reduction effort. The data for these crash and near-crash events are publically available through the VTTI Data Warehouse (http://forums.vtti.vt.edu/index.php?/files/category/3-100-car-data/).

In addition to calculating the 10th percentile TTC and ETTC, we used the publically available data to identify any braking events in the current study which were associated with the previously identified crash and near-crash event, and the 10th percentile TTC and ETTC associated with these braking events.

In order to identify the crash and near-crash events that were relevant to the current study, the events were restricted to ones which involved brake applications, and where the vehicle was driven by a primary driver with sufficient valid data (>60% of trips or distance driven). These filters produced 13 crash events and 219 near-crash events which were associated with braking events in this study.

Figure 11 shows the plot of 10th percentile ETTC distribution, similar to Figure 8, overlaid with ETTC associated with crash and near-crash braking events. Individual data points associated with driver 10th percentile values have been removed to increase clarity. The green diamonds represent the crash events while the yellow squares represent the near-crash events. The figure only includes crash and near-crash events which included a closing braking event as defined by the ETTC value at the start of the braking event. In addition, the figure only includes crash and near-crash events which were identified as relevant to car-following. Event identification was done manually using the event narrative compiled by VTTI reductionist. An example of a car-following near-crash event is when the subject brakes to avoid rear-ending a stopped lead vehicle. Events in which the subject vehicle brakes to avoid rear-ending a merging vehicle have been excluded from this comparison, since our current automated lead vehicle identification algorithm is not yet able to identify conflict vehicles which merge into the path of the subject vehicle. After the manual review, the sample of crash and near-crash events included a total of 3 crash events which involved a closing braking event as defined by ETTC, and a total of 57 near-crash events involved a closing braking event as defined by ETTC.

Lastly, we can compare the ETTC at the start of braking from the 3 crash events and 57 near-crash braking with the respective driver's 10th percentile ETTC. In other words, if we use the driver's 10th percentile ETTC from the relevant vehicle speed range as a threshold, how many of the driver's crash and near-crash events had braking ETTC lower than the 10th percentile threshold? The result of the comparison shows that, if driver's 10th percentile ETTC at braking was used as the threshold, 35 of 57 near-crash events (61.4%) had braking ETTC below the threshold, and all 3 crash events (100%) had braking ETTC below the threshold.

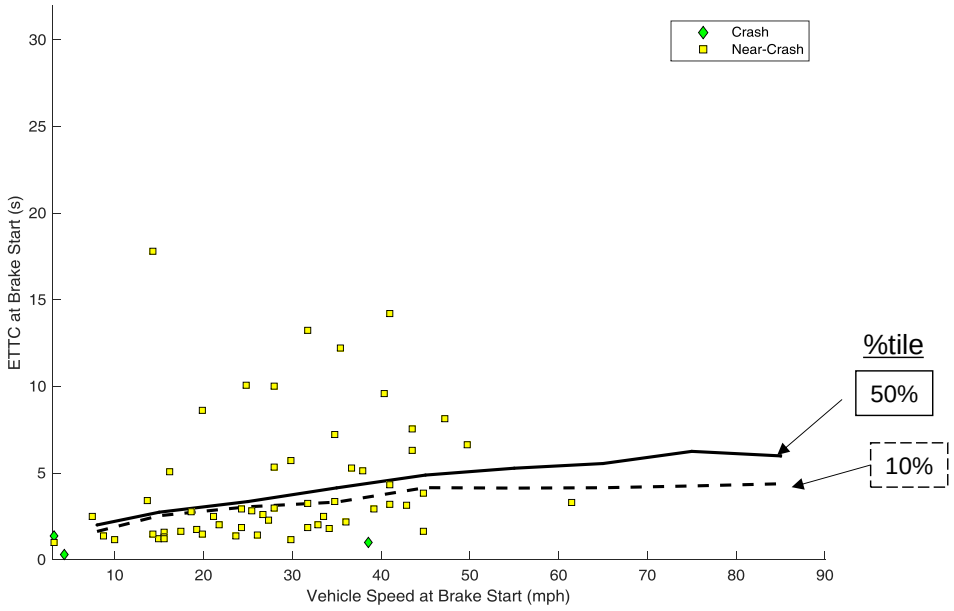

Figure 11. 10th Percentile ETTC with ETTC of Crash and Near-Crash Braking Events

Figure 12 shows a similar plot representing the 10th percentile TTC distribution. Once again, the figure only includes crash and near-crash car-following events, and only included closing braking events as defined by the TTC value at the start of the braking event. A total of 3 crash events involved a closing braking event as defined by TTC, and similarly, a total of 61 near-crash events involved a closing braking event as defined by TTC.

We can also compare the driver's 10th percentile braking TTC values to the braking events associated with the crash and near-crash events. Based on the result of the comparison, if driver's 10th percentile TTC at braking was used as the threshold, 32 of 61 near-crash events (52.5%) had braking TTC below the threshold, and 2 of 3 crash events (66.6%) had braking TTC below the threshold.

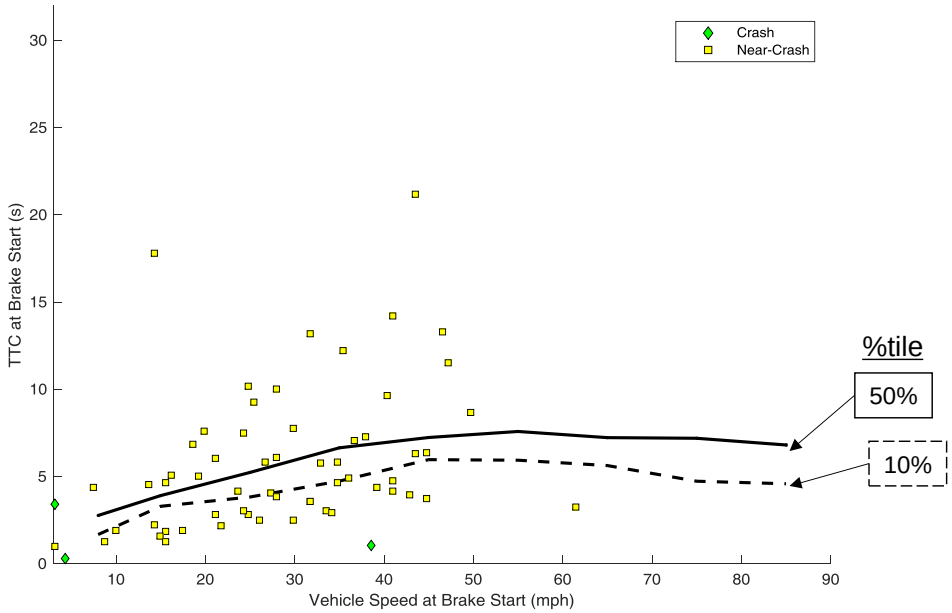

Figure 12. 10th Percentile TTC with TTC of Crash and Near-Crash Braking Events

3.1.3.4 Model Selection

The next objective was to fit a probability distribution to the closing braking events. Table 3 shows the summary of BIC and AIC, in ascending order, for all models included in the model selection process. All braking events with a valid lead vehicle and a closing ETTC were selected to fit to each of the distributions. Based on both the BIC and AIC values, the generalized extreme value distribution was selected as the model with the best fit for the sample of braking event. Similarly, Table 17 shows a summary of the model selection fit criteria for the distribution of TTC. The generalized extreme value model was also selected as the best fit model for the TTC distribution.

Table 3. Model Fit Criterion Summary for All Braking ETTC with Closing Lead Vehicle (n = 876,619 braking events)

Distribution Name	BIC	AIC
Generalized Extreme Value	5,694,230	5,694,195
Log-logistic	5,778,070	5,778,046
Log-normal	5,830,949	5,830,925
Inverse Gaussian	5,832,440	5,832,417
Birnbaum-Saunders	5,959,761	5,959,737
Generalized Pareto	6,067,434	6,067,399
t Location-Scale	6,113,622	6,113,587
Weibull	6,249,533	6,249,510
Gamma	6,293,641	6,293,618
Exponential	6,294,071	6,294,059
Nakagami	6,843,938	6,843,915
Logistic	7,264,496	7,264,472
Normal	8,302,907	8,302,884
Rayleigh	9,054,429	9,054,418
Rician	9,054,445	9,054,421
Extreme Value	9,787,732	9,787,708

Table 4. Model Fit Criterion Summary for All Braking TTC with Closing Lead Vehicle (n = 985,259 braking events)

Distribution Name	BIC	AIC
Generalized Extreme Value	7,948,454	7,948,418
Log-logistic	7,995,026	7,995,003
Inverse Gaussian	8,003,511	8,003,487
Lognormal	8,012,455	8,012,431
Birnbaum-Saunders	8,094,492	8,094,468
Generalized Pareto	8,207,647	8,207,612
Weibull	8,354,062	8,354,038
Gamma	8,389,399	8,389,375
Exponential	8,390,649	8,390,637
t Location-Scale	8,468,701	8,468,666
Nakagami	8,843,905	8,843,881
Logistic	9,472,258	9,472,234
Normal	10,283,094	10,283,071
Rayleigh	10,929,883	10,929,871
Rician	10,929,898	10,929,874
Extreme Value	11,592,834	11,592,811

Generalized extreme value distribution (GEV) is a family of probabilistic models based on the extreme value theory (EVT), and models the frequency distribution of the smallest or largest member of a random distribution [112], [113]. GEV probability density function for any random variable x is

shown in Equation 12, where the variables k, μ, σ represent the shape, location, and scale parameters of the function. Additionally, the cumulative distribution function for a GEV is shown in Equation 13.

$$f(x \mid k, \mu, \sigma) = (\frac{1}{\sigma}) * \exp(-(1 + k * \frac{(x-\mu)}{\sigma})^{-\frac{1}{k}}) * (1 + k\frac{(x-\mu)}{\sigma})^{-1-\frac{1}{k}} \quad \textbf{Equation 12}$$

$$F(x \mid k, \mu, \sigma) = \exp(-(1 + k * \frac{(x-\mu)}{\sigma})^{-\frac{1}{k}}) \quad \textbf{Equation 13}$$

GEV has commonly been used in extreme event distribution in fields such as meteorology [114], hydrology [115], and financial crisis prediction [116]. Recent studies have shown GEV to be a useful tool in modeling traffic collision frequency [117], [118]. In this study, GEV models the most frequent TTC or ETTC values in the sample.

Figure 13 shows the histogram and fit distribution of ETTC for all braking events with a closing lead vehicle. The parameters estimates k, σ, and μ were computed using the *gevfit* function in MATLAB. Similarly, Figure 14 shows the histogram and fit distribution of TTC for all braking event with a closing lead vehicle.

Both distribution fits in Figure 13 and Figure 14 show close correlation with their corresponding histograms. The probability density distribution of ETTC shows a peak probability (mode) of 21% for ETTC ~4 s. In contrast, the probability density distribution of TTC shows a peak probability (mode) of 11% for TTC of ~6 s.

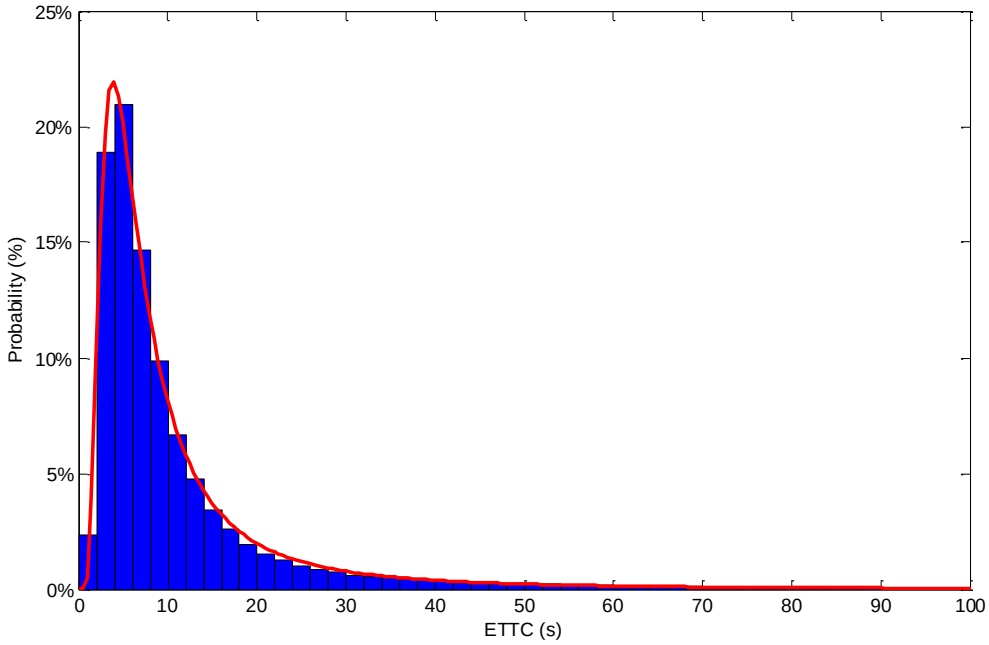

Figure 13. Histogram of ETTC at Brake Application with General Extreme Value Probability Distribution fit (k = 0.640, σ = 3.981, μ = 5.536)

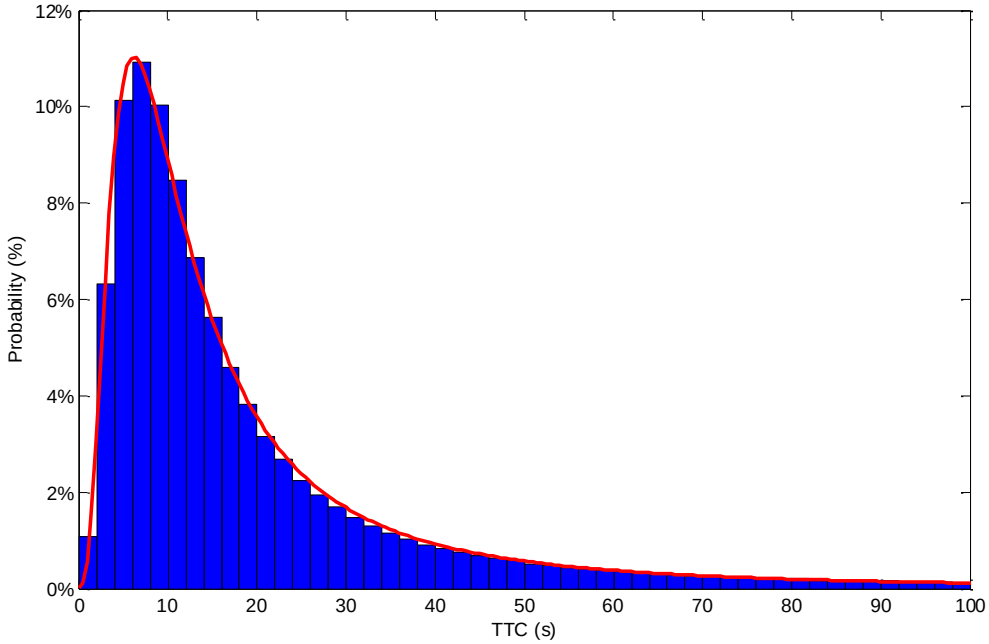

Figure 14. Histogram of TTC at Brake Application with General Extreme Value Probability Distribution fit (k = 0.674, σ = 8.053, μ = 9.706)

To further verify the fit of the GEV probability distribution to the sample of braking events from the 100-Car NDS, Figure 15 shows the cumulative distribution function fit based on the GEV model fit and the sample of braking events with a lead vehicle. As shown in the figure, the two cumulative distribution plots are nearly identical.

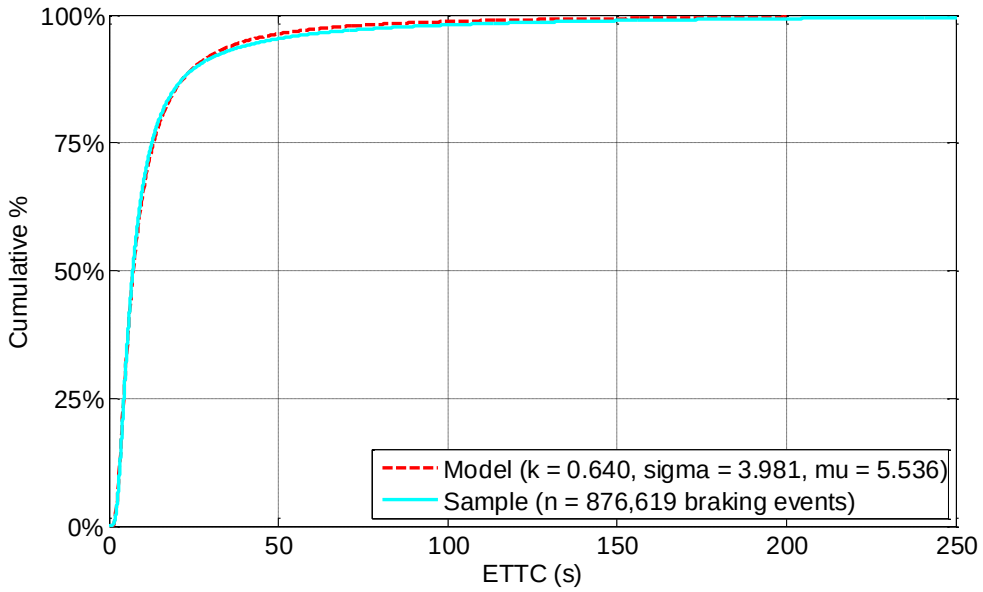

Figure 15. Cumulative Distribution Function of ETTC GEV Model Fit and Braking Event Sample

3.1.3.5 Probability Density Distribution by Speed Bin

As shown in Figure 8 and Figure 9, the distributions of ETTC and TTC are both affected by vehicle travel speed. In order to generate an appropriate probability density distribution function for all speed ranges, we separated all braking events by travel speed and fit the list of probability distribution to each group of braking events, similar to the methodology described in previous sections in this chapter, Table 5 and Table 6 shows that the best probability distribution fit for both ETTC and TTC values was GEV for all speed ranges. The tables include the parameter estimates for the GEV distribution for all speed bins.

Table 5. ETTC Probability Distribution Model Parameters

Speed Range (mph)	Distribution Name	Parameter Estimates		
		k	σ	μ
3-10	GEV	0.522	1.953	3.135
10-20	GEV	0.597	2.337	4.224
20-30	GEV	0.592	3.147	5.261
30-40	GEV	0.604	4.322	6.824
40-50	GEV	0.596	5.213	8.066
40-60	GEV	0.603	6.124	9.108
60-70	GEV	0.625	6.961	9.873
70-80	GEV	0.631	7.394	10.330
80+	GEV	0.514	7.134	10.277

Table 6. TTC Probability Distribution Model Parameters

Speed Range (mph)	Distribution Name	Parameter Estimates		
		k	σ	μ
3-10	GEV	0.607	3.934	5.009
10-20	GEV	0.666	5.177	7.345
20-30	GEV	0.649	7.298	9.582
30-40	GEV	0.654	9.244	12.221
40-50	GEV	0.658	9.993	13.338
40-60	GEV	0.666	10.824	14.167
60-70	GEV	0.699	11.637	14.500
70-80	GEV	0.724	11.381	13.684
80+	GEV	0.569	9.533	12.558

Using the parameter estimates tabulated in Table 5 and Table 6, we constructed probability distribution fits for each speed range, as shown in Figure 16 and Figure 17. The probability of occurrence for any ETTC or TTC can be calculated by substituting the parameter estimates into Equation 12.

As shown by the figures, the peak probability for both the ETTC and TTC distributions decreased with increasing vehicle speed. The distributions also widen, showing that the variance increases with increasing vehicle speed. The increase in variance is similar to the distribution of 10th percentile ETTC and TTC, shown in Figure 8 and Figure 9.

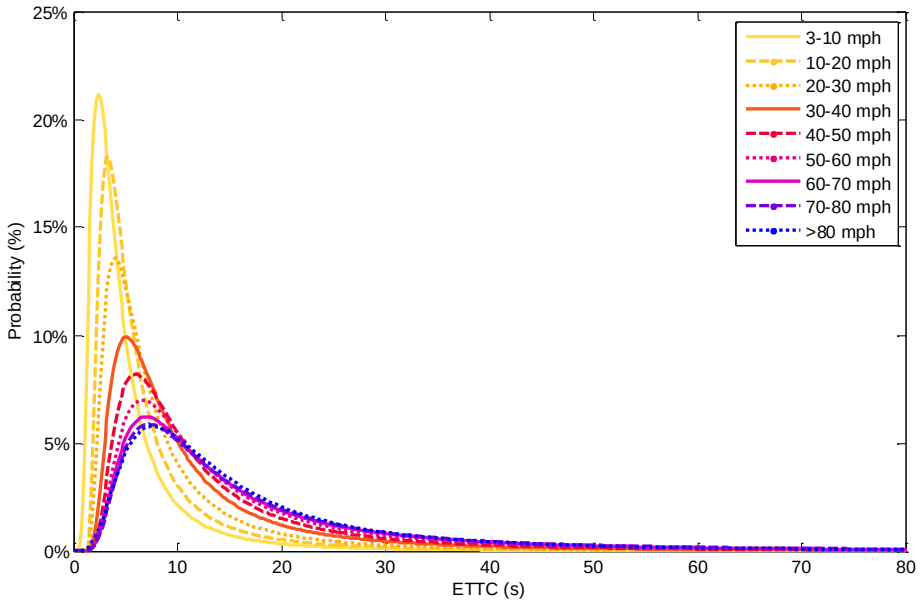

Figure 16. General Extreme Value Probability Distribution fit of ETTC for Each 3-80+ Speed Bins

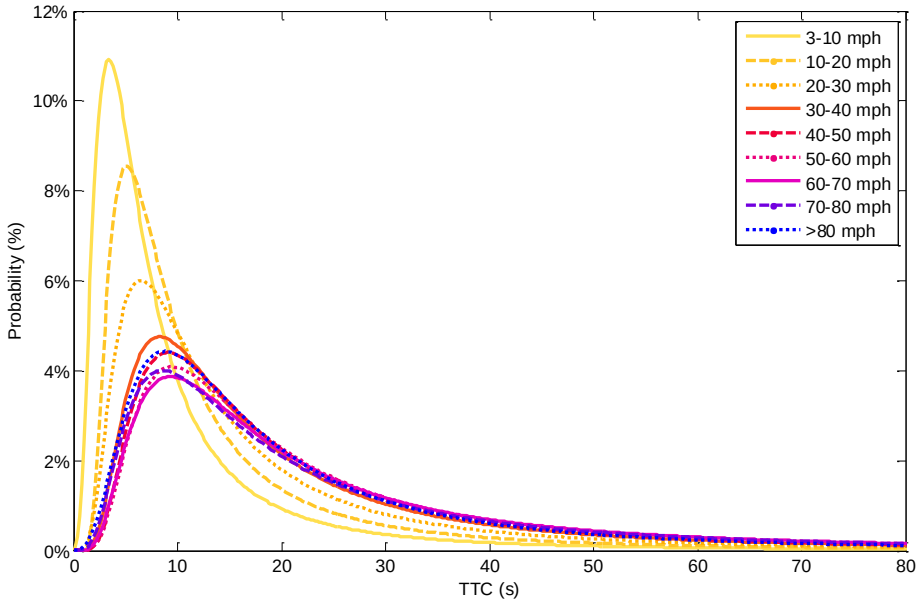

Figure 17. General Extreme Value Probability Distribution fit of TTC for Each 3-80+ Speed Bins

Table 7 and Table 8 present selected characteristics of each of the GEV probability distribution fit models shown in Figure 16 and Figure 17. The Mode of the distribution represents the highest probability of occurrence for each speed range. The Max ETTC/TTC refers to the ETTC/ETTC value corresponding to the Mode in each speed range. As expected, the 10th, 50th, and 90th percentile ETTC and TTC values all increase with respect to vehicle speed. In addition, for the same speed range, ETTC consistently shows greater mode as compare to TTC, indicating that ETTC distributions have lower variance across all speed ranges.

Table 7. ETTC GEV Probability Model Characteristics

Speed Range (mph)	Mode (%)	Max ETTC (s)	10 %tile (s)	50 %tile (s)	90 %tile (s)
3-10	21.2	2.402	1.982	3.666	12.647
10-20	18.3	3.203	2.779	4.984	16.380
20-30	13.6	4.004	3.331	6.265	20.936
30-40	9.9	5.005	4.161	8.225	29.478
40-50	8.2	6.006	4.824	9.754	35.400
50-60	8.0	6.607	5.305	11.06	42.358
60-70	6.2	7.007	5.546	12.18	49.055
70-80	5.9	7.207	5.629	12.96	51.403
80+	5.8	7.608	5.621	12.56	43.213

Table 8. TTC GEV Probability Model Characteristics

Speed Range (mph)	Mode (%)	Max TTC (s)	10 %tile (s)	50 %tile (s)	90 %tile (s)
3-10	10.9	3.403	2.503	6.543	24.167
10-20	8.5	5.205	4.002	9.472	34.762
20-30	6.0	6.406	4.990	12.317	49.000
30-40	4.8	8.208	6.464	15.599	63.583
40-50	4.4	9.009	7.080	17.018	69.532
50-60	4.1	4.409	7.332	18.317	76.087
60-70	3.9	9.409	7.087	19.421	80.429
70-80	4.0	8.609	6.278	18.968	78.879
80+	4.4	8.809	6.171	16.340	58.664

3.1.4 CONCLUSION AND DISCUSSION

The overall objective of the current study was to calculate the ETTC for all braking events with a lead vehicle in the 100-Car NDS. In addition, we determined the probability distribution functions which best fit both samples of ETTC and TTC. The model selection criterion was based upon AIC and BIC. The study used an automated search algorithm, developed in previous studies [103], [119], to identify lead vehicles in all braking events in 100-Car.

This study only included drivers with at least 60% valid sensor data. A total of number of 64 drivers had sufficient valid sensor data to be included, resulting in a total of 72,380 trips with 609,620 miles of travel in the study. A total of 1,682,093 braking events with a valid lead vehicle were identified using the automated search algorithm. Using TTC as a metric, 985,259 of the braking events were identified as having a closing lead vehicle. Using ETTC as a metric, a total of 876,619 of the braking events were identifed as having a closing lead vehicle.

The braking events with a closing lead vehicle identified by ETTC and TTC were used to compute the 10^{th} percentile ETTC and TTC values for each driver. In genenral, the ETTC and TTC, as shown in Figure 8 and Figure 9, both increased with vehicle speed. The variance of both distributions also increased with vehicle speed. However, the median and 10^{th} percentile across all drivers was higher for TTC values than ETTC values. In addition, the variance for drivers within each speed range was also higher for TTC values than ETTC values.

The result of the relative acceleration distribution shows that only 1/3 of the braking events had zero relative acceleration. Approximately 65% of the braking events contained postive relative acceleration, indicating increasing closing speed and resulting in lower time remaining until collision than considering relative velocity alone. The effect of positive relative acceleration is also illustrated in the distribution of 10^{th} percentile ETTC and TTC, shown in Figure 8 and Figure 9, where the distribution of ETTC had lower median and 10^{th} percentile as comapred with the distribution of TTC.

The result shows that the addition of relative acceleration in the ETTC calculation provides a more accurate measurement of time remaining until collision.

The generalized extreme value model was found to be the best fit distribution for both ETTC and TTC values based on AIC and BIC score. The distribution fits, shown in Figure 13 and Figure 14, showed close correlation with the underlying data. Probability density distribution of ETTC showed a higher peak probability, or mode, as compared to TTC. The higher mode is also evident across all speed ranges, as shown in Table 7 and Table 8.

In summary, this study has chararacterized TTC and ETTC distributions in braking events in car-following. Futhremore, we compared ETTC and TTC as metrics for characterizing driver braking behavior in car following. ETTC possesses an advantage over TTC by incorporating relative acceleration in calculating the time to collision. The results of this study shows that ETTC distributions have lower variance between drivers across all vehicle speed ranges. In addition, we found that both distributions of ETTC and TTC can be represented by a GEV distribution. The distributions provide the probability of occurrence across a range of continuous ETTC and TTC values. The results from this study provide a better understanding of driver behavior in car following events, and can be used to improve various driver models, such as normal braking time threshold, and driver perception of risk in car following events.

3.2 Age and Gender Differences in Brake Pulse during Car Following

3.2.1 Introduction

Autonomous braking is an integral component of active safety systems such as Dynamic Brake Support (DBS) and Autonomous Emergency Braking (AEB). These systems are designed to reduce the incidence and severity of collisions by automatically apply the brake in situations where the driver cannot apply sufficient brake force or were not able to brake in time. As vehicles are introduced into the fleet with increasing levels of automation, emerging Advanced Driver Assistance

System (ADAS), may rely on autonomous braking systems to maintain following distance or navigate through "stop-and-go" traffic.

One of the challenges in designing an ideal autonomous braking system is to achieve automation which is human-centered [57], [58]. An ideal autonomous braking system would be able to apply braking, both in magnitude and pulse shape, similar to a human driver to achieve a comfortable driving experience. A better understanding of driver brake pulse can assist active safety system and ADAS designers to better tailor the vehicle braking pattern to the driver and driving context. Previous studies have characterized driver braking behavior in crash avoidance scenarios, using test track and/or simulator [120]–[122]. Other studies have modeled car following behavior using traffic flow data [123], or by numerical simulations [124]. Currently, no large scale study has been conducted on driver braking behavior in normal driving scenario.

One of the factors which may influence driver braking force and brake pulse is driver age. Studies have suggested that muscle mass declines at approximately 1% per year after the age of 30 [125]. The effect of this age related muscle mass loss, or sarcopenia, is directly correlated with loss of strength. In addition, differences in strength also exists across gender [126]. Both age and gender differences can contribute to driver braking capacity and influence autonomous braking activation time. The objective of this study was to characterize braking pattern in normal driving, and analyze the potential differences in brake pulse, both magnitude and shape, between drivers of different age group and gender.

3.2.2 METHOD

3.2.2.1 Data Source

This study was based on data extracted from the 100-Car NDS. Drivers in the 100-Car NDS were divided into male and female, and the following four age categories: Novice (age 18-20), Young (ages 21-30), Middle (ages 31-50), and Mature (ages 51-61+).

3.2.2.2 Brake Pulse Characteristics

Several metrics were selected to characterize driver brake pulses. Figure 18 shows a sample brake pulse, illustrated with the list of metrics which were characterized in this study. These metrics include: 1) Braking Duration, computed as the length of the braking event in seconds, 2) Maximum Braking Deceleration, computed as the largest change in longitudinal acceleration during the braking event, and 3) the centroid, or the center of mass, used to characterize the center of the peak of the brake pulse. Calculations of these metrics will be detailed in the following subsection.

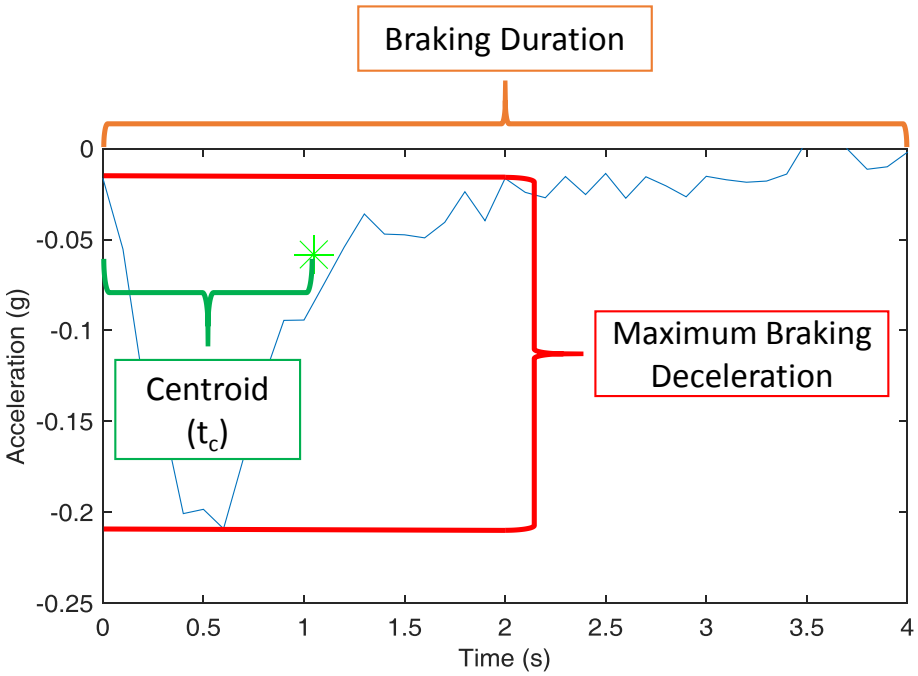

Figure 18. Sample Brake pulse Characteristics

3.2.2.2.1 Maximum Braking Deceleration

Maximum braking deceleration was determined based on the longitudinal acceleration recorded from the on-board instrumentation. The acceleration data was normalized by subtracting the acceleration at the start of the braking event from the remaining data. This was done in order to reduce the effect of existing acceleration caused by road slope. A five point moving average was

performed on each acceleration trace prior to extracting the maximum to reduce the noise. No moving average was performed for braking events less than five data points (0.5 seconds)

3.2.2.2.2 Brake Pulse Centroid

For each braking event, the shape of the driver brake pulse was characterized based on the time centroid of the acceleration vs. time curve, as shown in Equation 14, where t is the time duration and a(t) is the acceleration with respect to time. The integrals shown in Equation 14 were performed with trapezoidal integration. As a quality control, the integral of a(t) for each event was compared against the change in velocity as reported by the vehicle CAN bus.

$$t_c = \frac{\int ta(t)dt}{\int a(t)dt} \qquad \textbf{Equation 14}$$

In order to compare the centroid, t_c, of each event with the population of all events, we have normalized the centroid using the length of the braking event, t_m, as show in Equation 15.

$$Normalized\ Centroid = \frac{t_c}{t_m} \qquad \textbf{Equation 15}$$

In this study, we classify brake pulses as "Front Load", "Mid Load", and "Rear Load" based on the normalized centroid for each brake pulse. A t_c/t_m of 0.2 indicates that the driver "front loaded" the brakes in this event, where the peak braking deceleration occurred near the beginning of the braking event. On the other hand, t_c/t_m = 0.8 indicates the driver "back loaded" the brakes in the event, and the peak braking deceleration occurred near the end of the braking event. Figure 19 shows examples of brake pulse for "front load", "mid load", and "rear load" events. The blue solid line shows the raw acceleration trace, the dashed red line shows the acceleration trace after the five point moving average filter, and the green star shows the location of the centroid.

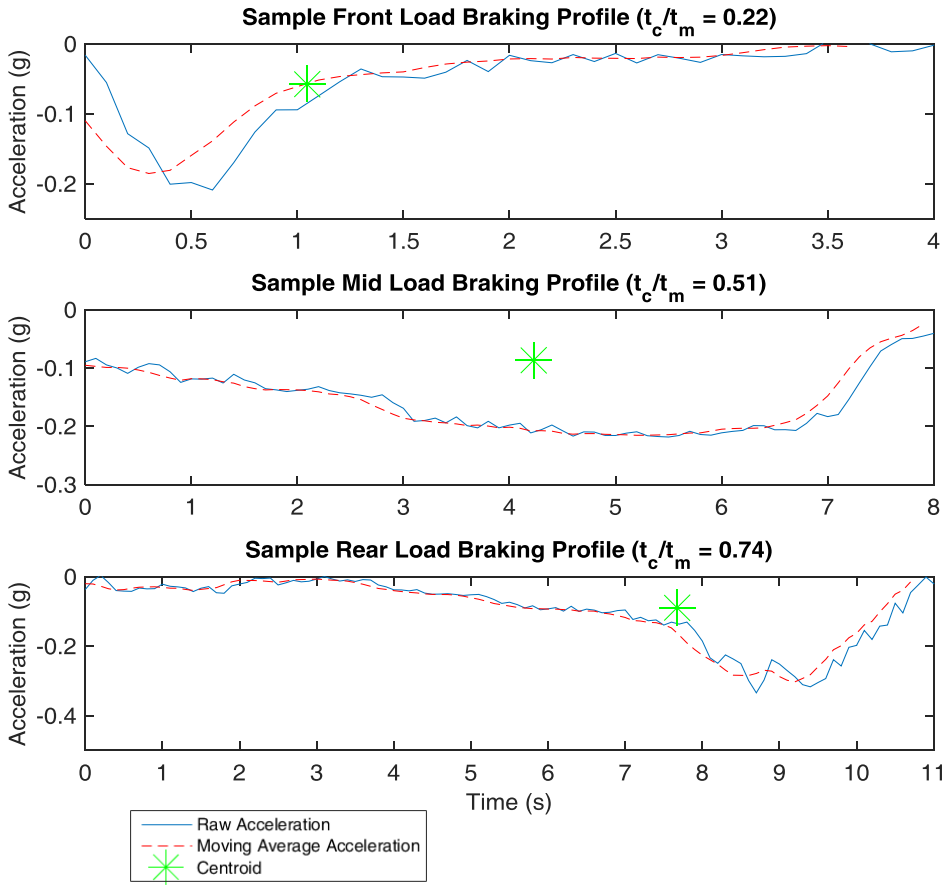

Figure 19. Sample Brake Pulses

3.2.2.3 Brake Pulse Corridor

Brake pulse corridors were generated to further characterize the three different types of brake pulses (front load, mid load, and rear load).

Each brake pulse was normalized in two methods in order to generalize a large series of different brake pulses. We first normalized the duration of the braking event by dividing the each time point within the event by the duration, therefore the duration of the braking event spans from 0 to 1. While each brake pulses now all span from 0 to 1, due to their different duration, each acceleration are now reported at different time points from 0 to 1. The second step of the

normalization procedure was to sample each brake pulse at the same time point. Linear interpolation was performed to estimate the value of each brake pulse at 100 equally spaced time points from 0 to 1 to further normalize each brake pulse.

Brake pulses were then separated into three groups based on their t_c/t_m value. "Front load" brake pulses included brake pulses with $t_c/t_m < 0.33$, "Mid load" brake pulses included brake pulses with $t_c/t_m >= 0.33$ and < 0.66, and "Rear load" brake pulses included brake pulses with $t_c/t_m >= 0.66$. There threshold were arbitrary selected however, they equally separated the three characteristic brake pulses. For each braking pulse group, we compute the mean and standard deviation at each of the 100 time point. The brake pulse corridors were then generated by taking the mean ± standard deviation.

3.2.3 RESULTS

3.2.3.1 *DATASET COMPOSITION*

Table 9 shows the data composition in the analysis. A total of 58,611 trips with valid data, driven by 64 different drivers were extracted from the 100-Car NDS. A total of 889,268 braking events with closing lead vehicles were found in these trips, totaling over 16,000 hours of data.

Table 9. Dataset Composition

Group	Count
Number of Trips	58,611
Number of Drivers	64
Number of Braking Events	889,268
Hours of Data	16,319

3.2.3.2 Braking Duration

Figure 20 shows the braking duration in all braking events with a closing lead vehicle. The median braking duration was approximately 2.6 seconds. Approximately 20% of the braking events were found to be less than 1 second, and 90% of the braking events lasted less than 11 seconds.

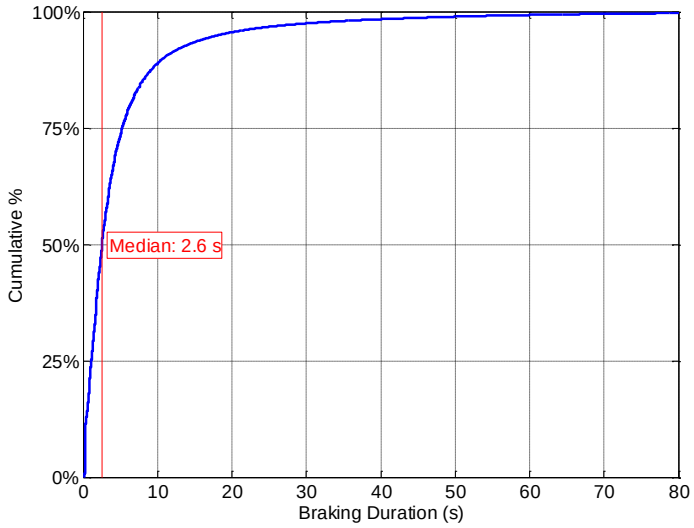

Figure 20. Distribution of Braking Duration

3.2.3.3 Braking Deceleration

Figure 21 shows the distribution of maximum braking deceleration for all braking events with closing lead vehicle. The median braking deceleration was approximately 0.08 g. In 90% of the braking events, the maximum braking deceleration was less than 0.2 g.

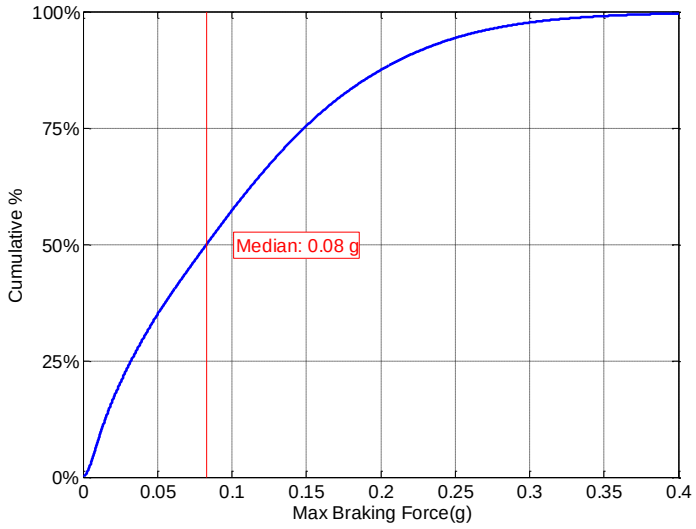

Figure 21. Distribution of Maximum Braking Deceleration

3.2.3.4 Vehicle Change in Velocity

Figure 22 shows the vehicle change in velocity, or deltaV, in mph. For each braking event, the deltaV was computed by trapezoidal integration of the acceleration data. As shown in the figure, the median change in vehicle velocity was approximately 4 mph. As shown in Figure 20, approximately 20% of braking events in the sample had a change in vehicle speed of less than 1 mph. These low change in velocity braking events are tied to the short duration events, since it is unlikely to have made a significant change in vehicle speed in this short braking duration. Figure 23 shows a scatter plot of braking duration and vehicle deltaV. As shown by the figure, braking durations less than 1 s were generally associated with deltaV lower than 1 mph.

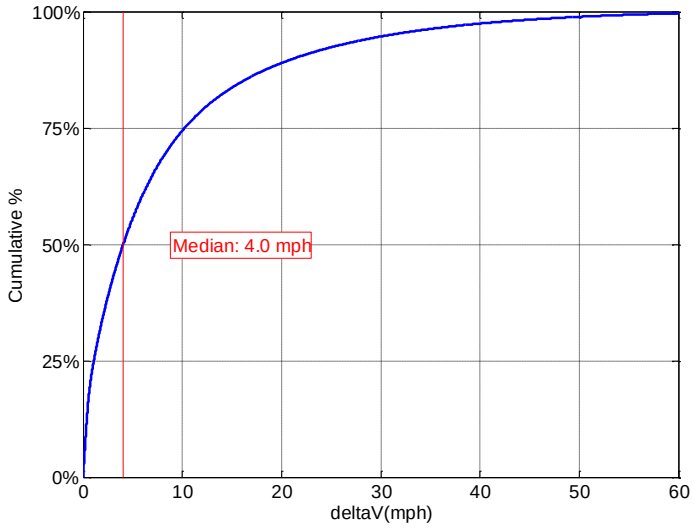

Figure 22. Distribution of Vehicle deltaV

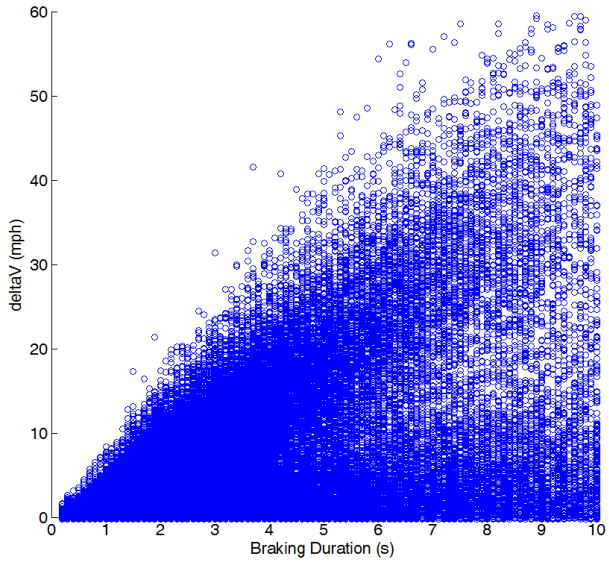

Figure 23. Braking Duration and Vehicle deltaV

3.2.3.5 Brake Pulse Shape

Figure 24 shows the distribution of t_c/t_m. As shown by the figure, the median t_c/t_m is approximately 0.5. In other words, the median brake pulse is one which the peak occurred near the middle of the event, or a brake pulse with uniform distribution and no discernable peak.

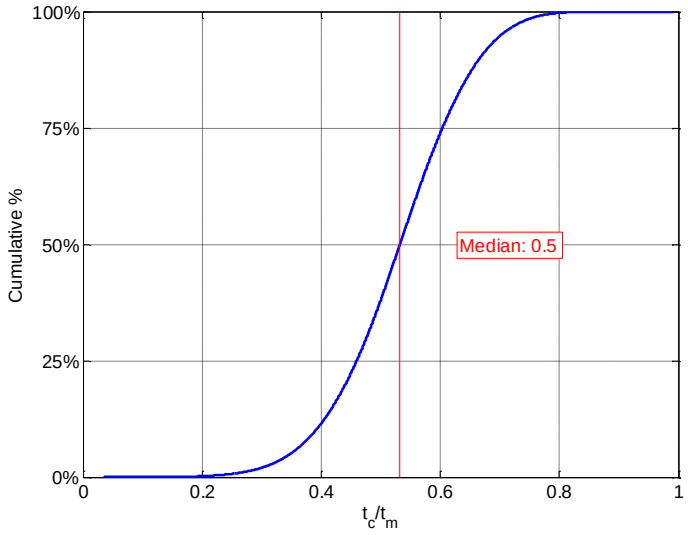

Figure 24. Distribution of t_c/t_m

Figure 25 shows a scatter plot of normalized t_c/t_m and TTC at the start of the braking event for all braking events in the sample. The figure also includes a "heat map" to indicate the density of braking events. Where red areas indicate more frequent occurrences, and blue areas indicate less frequent occurrences.

The relationship between TTC and t_c/t_m reveals several interesting characteristics about braking behavior. First, very few braking events were reported with t_c/t_m less than 0.25. This suggests that it is uncommon for drivers to "front load" brakes, or apply peak braking deceleration early, in normal driving situations. The figure also shows that, the most frequent normal braking events have TTC's lower than 10 seconds and a t_c/t_m ranging from 0.4 to 0.6.

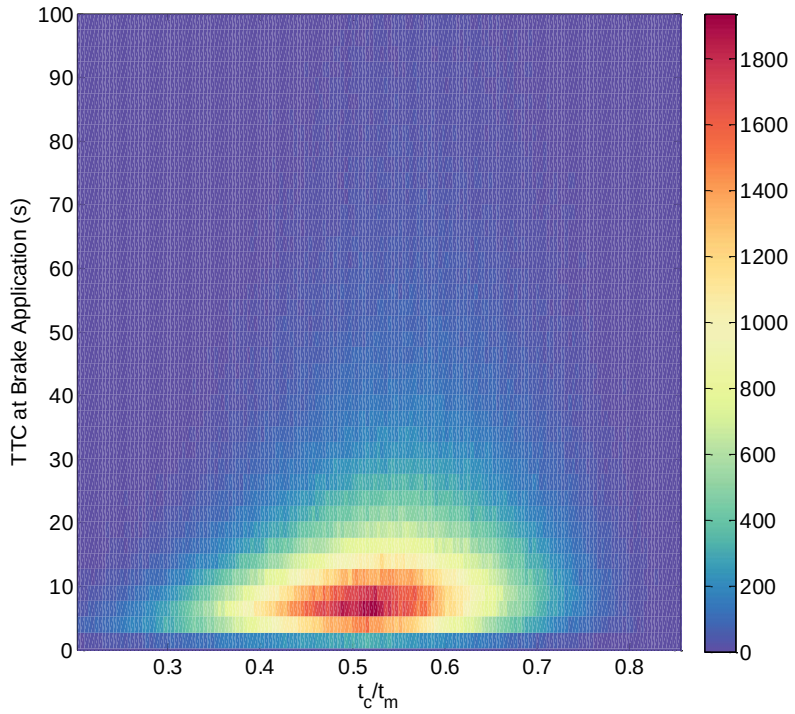

Figure 25. TTC at Braking and t_c/t_m

In order to further characterize these frequent braking events which have t_c/t_m ranging from 0.4 to 0.6, we calculated the ratio of average braking deceleration and peak braking deceleration, as shown in Figure 26. An average/peak braking ratio of 1 indicate that the braking deceleration is uniformly distributed with no obvious peak, similar to the left profile in Figure 27. On the other hand, a ratio greater than 1 would indicate that a sharp peak exist in the brake pulse, similar to the right profile in Figure 27.

The distribution shown in Figure 26 shows that only a small percentage of mid loaded brake pulses have a braking deceleration ratio of 1, suggesting that the majority of mid loaded braking included noticeable peaks near the middle of the braking pulse.

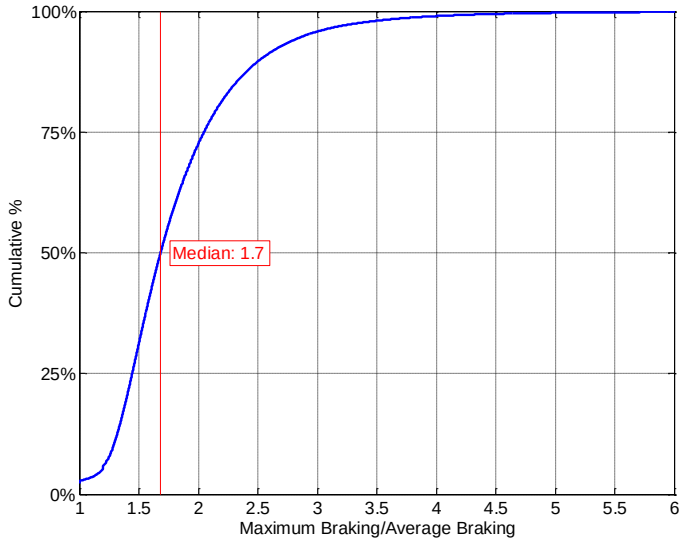

Figure 26. Distribution of Maximum/Average Braking.

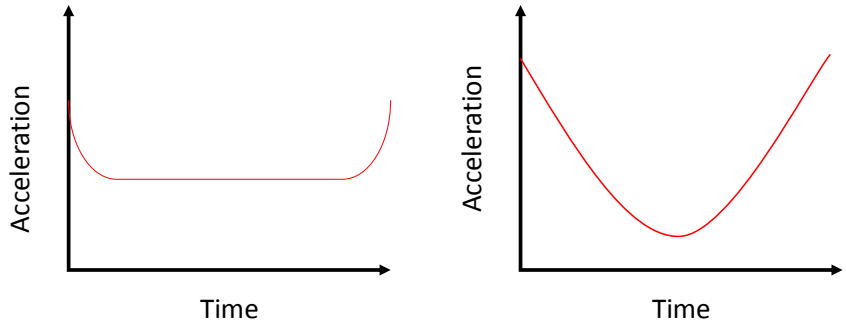

Figure 27. Idealized Example of Mid Load Brake Pulses

3.2.3.6 Brake Pulse Corridors

Figure 28, Figure 29, and Figure 30 show the brake pulse corridor for the front load, mid load, and rear load braking pulses. The blue line the middle of each figure shows the "average" braking pulse, and the light blue shading shows the corridor constructed using the mean and standard deviation of each group's braking pulses.

In each brake pulse corridor, larger areas shows areas of wide variability, while the smaller areas shows smaller variability between brake pulses. In the front loaded scenario, shown in Figure 28, drives are shown to quickly decelerate and resume near zero acceleration quickly, suggesting that

these are short braking events followed by a period of standing still, likely in congested traffic or at a stop light or intersection.

Similarly, in the mid load braking pulse corridor, shown in Figure 29, drivers are shown to more likely to evenly decelerate and then reduce the magnitude of the braking force in the remaining braking duration. Compared to the front loaded braking pulses, these mid load braking events show very short or no zero deceleration period, suggesting that drivers never completely stop the vehicle and only slow down to increase following distance or react to braking of lead vehicle.

The rear load brake pulse corridor, shown in Figure 30, shows a gradual decrease in braking and then the driver reach near zero deceleration. Similar to the mid load profile, these rear load brake pulses show very short or no zero deceleration period, suggesting that drivers are more likely to be traveling in traffic during these events.

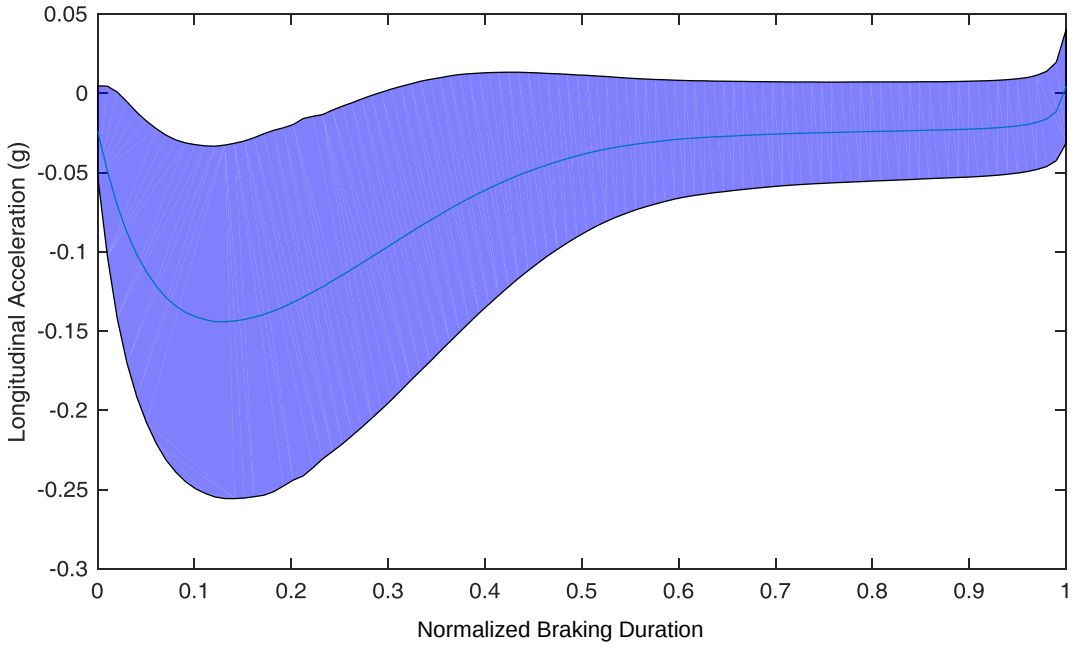

Figure 28. Front Load Brake Pulse Corridor

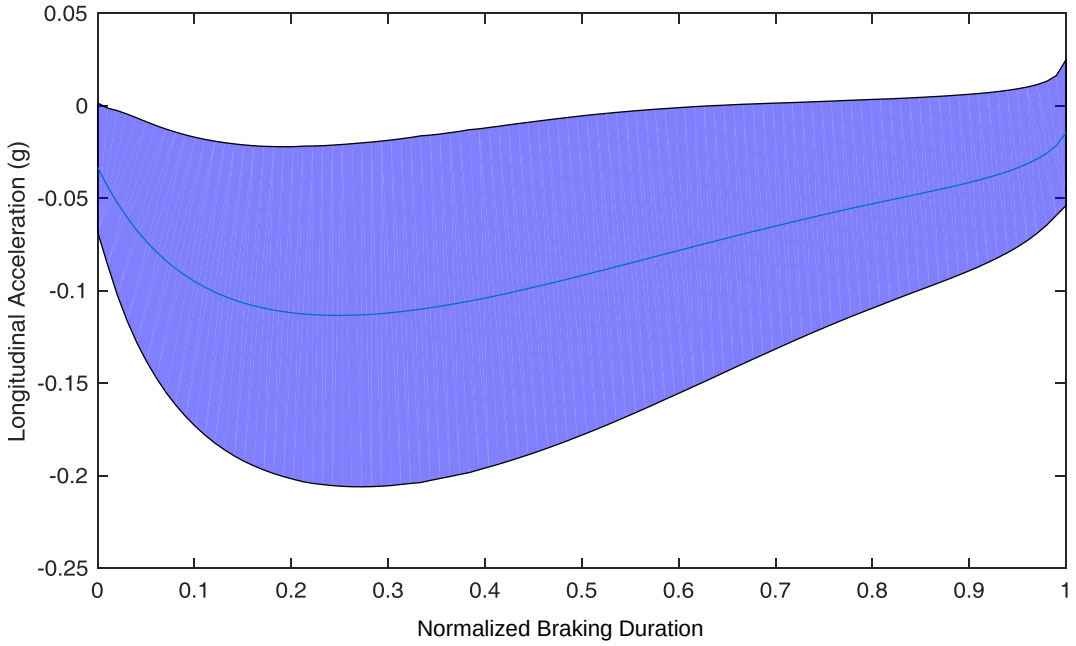

Figure 29. Mid Load Brake Pulse Corridor

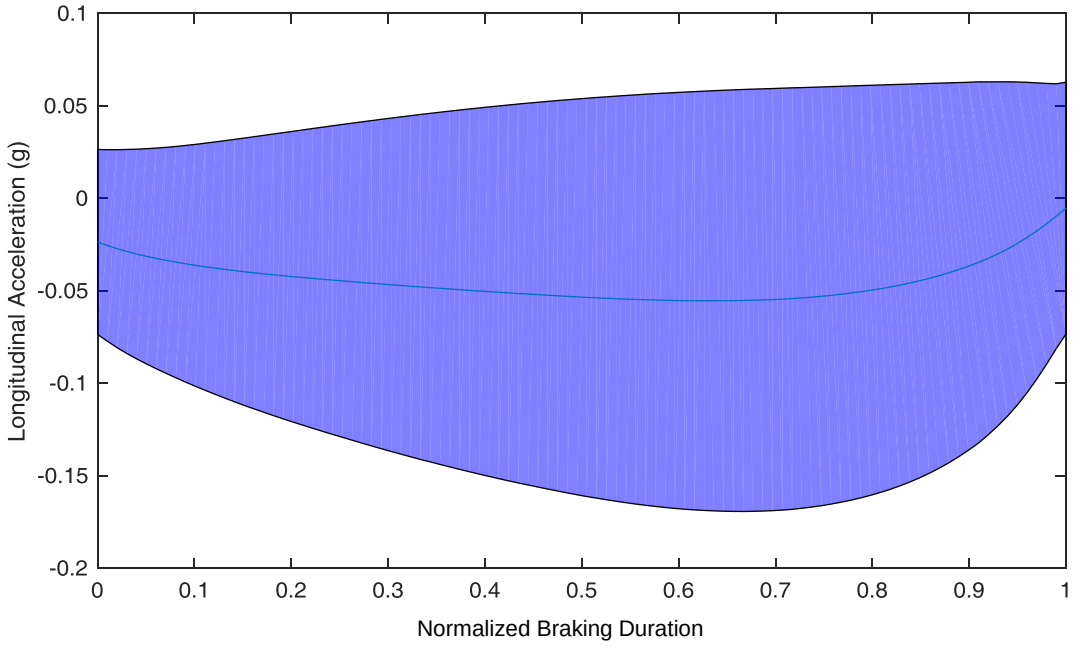

Figure 30. Rear Load Brake Pulse Corridor

3.2.3.7 Group Mean and Analysis of Variance

Our hypothesis was that braking magnitude may vary by driver age and gender. Table 10 shows the least square mean (LS mean) maximum braking deceleration for each group. As shown, maximum braking deceleration increases with increasing driver age. Middle age drivers (31-50) had the highest LS mean maximum braking deceleration. Female drivers also had slightly higher mean braking deceleration than male.

The deceleration magnitudes shown in Table 10 are similar to values reported by previous studies. Wada et al. used test track data to model driver deceleration in car following scenarios and reported maximum decelerations ranging from 0.08g to 0.13g, for following distances of 50 m to 25 m, respectively [120]. The numerical model by Hiroaoka et al., using minimum-jerk theory, reported a maximum deceleration of approximately 0.15g [124]. Similarly, the Gazis model, using traffic flow data, reported a maximum deceleration of approximately 0.2g [123].

Table 10. LS Mean Maximum Braking Deceleration

Groups	LS Mean Braking Force (g)
Novice (18-20)	0.084
Young (21-30)	0.093
Middle (31-50)	0.115
Mature (51+)	0.107
Male	0.093
Female	0.107

Similarly, Table 11 shows LS means of the t_c/t_m. The centroid locations for all age and gender groups were near the middle of the braking events.

Table 11. LS Mean t_c/t_m

Groups	t_c/t_m
Novice(18-20)	0.542
Young (21-30)	0.529
Middle (31-50)	0.518
Mature (51+)	0.526
Male	0.538
Female	0.519

A linear mixed effects model was constructed in order to detect any potential significant difference in braking deceleration between the driver demographic groups. "Age Group" and "Gender" was included in a linear regression model as categorical variables to control for driver characteristics, and vehicle speed and TTC was included as continuous variables in the model to control for traffic context. The driver was treated as a random intercept. Table 12 shows the result of the Analysis of Variance for the linear mixed effect model. As shown by the figure, all main effect and interaction variables were statistically significant in influencing driver brake deceleration at α level of 0.05.

Table 12. Analysis of Variance for Linear Mixed Effect Model (Response = Braking Deceleration)

Parameter	DF	F Value	Pr(>F)	
Age Group	3	344.16	P < 0.0001	***
Gender	1	192.83	P < 0.0001	***
Vehicle Speed	1	7093.72	P < 0.0001	***
TTC	1	2984.36	P < 0.0001	***
(Age Group)*(Gender)	3	892.39	P < 0.0001	***
(Age Group)*(Vehicle Speed)	3	2075.87	P < 0.0001	***
(Age Group)*(TTC)	3	43.92	P < 0.0001	***
(Gender)*(Vehicle Speed)	1	313.89	P < 0.0001	***
(Gender)*(TTC)	1	31.53	P < 0.0001	***
(Vehicle Speed)*(TTC)	1	742.7	P < 0.0001	***

******* = P < 0.0001, ** = P < 0.05

Similarly, Table 13 shows the result of the ANOVA using centroid location, t_c/t_m, as the response. The only factor which was not statistically significant at alpha = 0.05 was the interaction between gender and TTC. All other factors were statistically significant at effecting t_c/t_m.

Table 13. Analysis of Variance for Linear Mixed Effect Model (Response = t_c/t_m)

Parameter	DF	F Value	Pr(>F)	
Age Group	3	326.31	P < 0.0001	***
Gender	1	2276.72	P < 0.0001	***
Vehicle Speed	1	13185.8	P < 0.0001	***
TTC	1	3722.76	P < 0.0001	***
(Age Group)*(Gender)	3	2364.18	P < 0.0001	***
(Age Group)*(Vehicle Speed)	3	118.88	P < 0.0001	***
(Age Group)*(TTC)	3	3.01	0.0288	**
(Gender)*(Vehicle Speed)	1	272.04	P < 0.0001	***
(Gender)*(TTC)	1	0.12	0.7251	
(Vehicle Speed)*(TTC)	1	1590.07	P < 0.0001	***

******* = P < 0.0001, ** = P < 0.05

Figure 31 shows the least square means estimates of maximum braking deceleration with respect to vehicle speeds and age groups. Each '*' over top of the bars indicates that the groups were statistically different at alpha = 0.05. As shown in Figure 31, maximum braking deceleration generally decreases with increasing vehicle speed. The change in braking deceleration over different vehicle speed categories was more prominent for novice and young drivers. Middle age drivers (age 31-50) had statistically higher maximum braking deceleration compared to all other age groups in almost all speed ranges.

Similarly, Figure 32 shows the least square means estimate of t_c/t_m with respect to vehicle speed and age groups. In general, t_c/t_m was approximately 0.5 for all age groups. We can see a slight increase in t_c/t_m with increasing speed for all age groups, suggesting that brake pulse begins to "rear load" as vehicle speed increases. Contrary to other age groups, mature age group drivers (51+) tends to "front load" braking as vehicle speed increases. While the difference was significant across most age groups in each speed bin, we chose to only highlight the practical differences in Figure 32, i.e. the difference between the Mature age group in 60+ mph vehicle speeds. This was largely due to the large sample size used in the study, which magnifies the statistical significance of small differences.

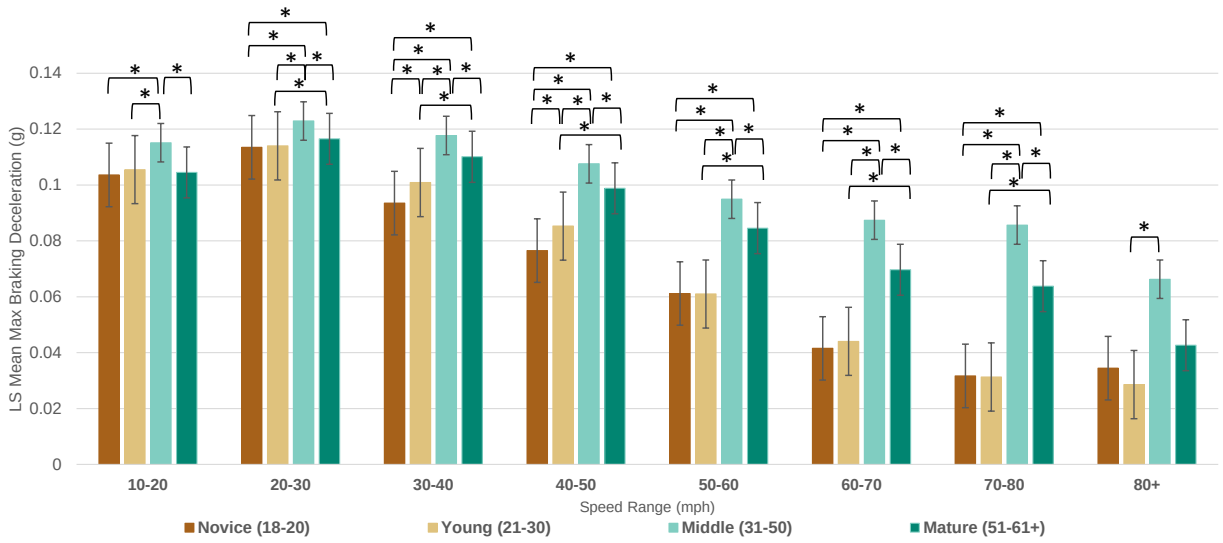

Figure 31. LS Mean Estimate of Maximum Braking Deceleration by Travel Speed and Age Group

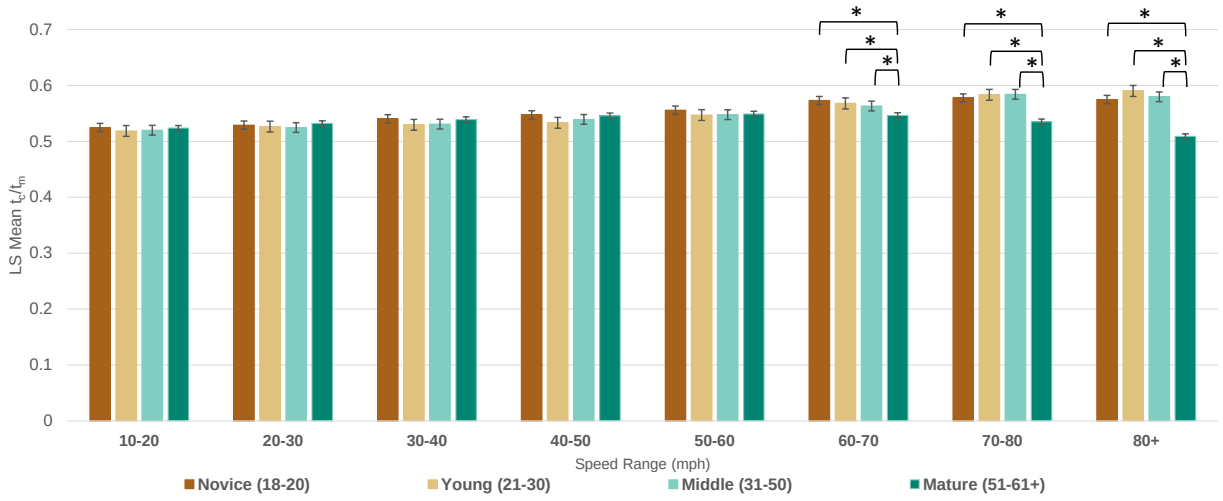

Figure 32. LS Mean Estimate of t_c/t_m by Travel Speed and Age Group

3.2.4 Conclusion and Discussion

This study has examined the braking behavior differences in driver age and gender demographic groups. The study shows that for braking events with a lead vehicle, driver braking deceleration and brake pulse is influenced by driver age and gender, as well as the traffic context, such as current vehicle speed and TTC with the lead vehicle.

The study also shows that, as driver age increases, the maximum braking deceleration increases. A marginal difference in braking deceleration between genders was also detected in the results. Using a linear regression model which controlled for vehicle speed and TTC, the difference between age and gender effect on braking was shown to be statistically significant.

Similarly, the study shows that driver brake pulse varies with the driver demographic and driving context. For all age groups, the maximum braking deceleration decreases as vehicle speed increases. On the other hand, brake pulse were shown to shift towards "rear load" as vehicle speed increases. The shift was not observed in mature drivers, who were observed to "front load" the brakes as vehicle speed increase.

One of the limitations of the study was that the results were based on normal driving data. It is possible that driver braking behavior is entirely different in crash imminent situations, therefore we cannot extend the conclusions from this study to crash imminent situations. In addition, information regarding cruise control activation was not available at the time of the study, which may help distinguish drivers' intention to cancel cruise control from crash avoidance braking. Nevertheless, the results from this study provide a good approximation of driver brake pulses in normal driving, and can still illustrate the differences in braking deceleration across the demographic groups.

The current study shows that there is a clear difference in brake pulse between drivers of different age group and gender. The results of this study can help provide a better understanding of driver braking patterns in normal driving. The results of this study can support future automated braking systems and autonomous vehicle designers to better adapt vehicle driving behavior to be more human-like.

3.3 Effect of Percent Overlap on Car-Following Behavior

3.3.1 Introduction

Previous studies have shown that driver braking behavior differs by driver demographics, such as age and gender [127]. In addition to driver demographics, previous research has shown that driving context factors, e.g., road type, congestion level, and time of day, can also affect driving behavior [128], [129]. One additional driving context factor which may influence driver behavior is the level of overlap between the subject and target vehicle, as shown in Figure 33. Currently, no study has been conducted on driver perception of overlap percentage and its effect on driver braking behavior. In order to improve the effectiveness of future active safety technology, consideration must be taken to assess the effect of overlap level in driver braking behavior. The objectives of the following study was to present a methodology of estimating percentage overlap in NDS data, and characterize the effect of percentage overlap on driver braking behavior.

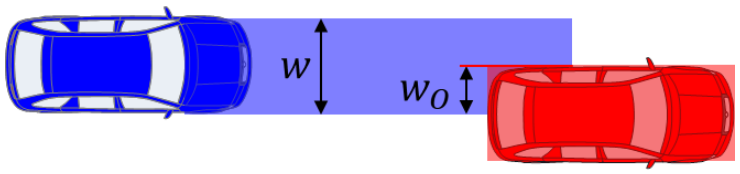

$$\% \text{ Overlap} = \frac{w_O}{w}$$

Figure 33. Calculation of Percent (%) Overlap.

3.3.2 Method

This study was based on examination of car-following behavior using the 100-Car NDS. The overall approach of this study was to characterize the effect of percentage overlap, between the lead vehicle and the instrumented vehicle, in driver braking behavior. In addition, the effect of different driving context was included as covariates in the analysis. Driving context was measured in terms of vehicle speed, time of day (daylight or nighttime), and day of week (weekend or weekday). Vehicle speed was recorded by the vehicle instrumentation equipped for the study. The date was recorded

by the data acquisition system, which was used to determine the day of the week. VTTI determined the time of day by manual examination of the video data from each trip [98]. The cameras in the study sometimes failed or were dislodged from their mounts, making it impossible to determine the time of day. Another possible reason for not being able to determine the time of day was if the entire trip occurred in a covered structure, such as a parking garage. Any trips where the time of day or day of week was unable to be determined were excluded from further analysis.

3.3.2.1 Estimation of Percentage Overlap

The front-facing radar units in the 100-Car study did not store percent overlap. Each tracked object was described by a range, range rate, and azimuth from the equipped vehicle to the center of the target vehicle. The following study utilizes NDS radar instrumentation to estimate the percentage overlap of the lead and instrumented vehicle.

3.3.2.1.1 Step 1: Locating the Lead Vehicle

The method of estimating percentage overlap consists of 3 steps. The first was to locate the lead vehicle with respect to the instrumented vehicle at the time of brake application. This was accomplished by calculating the location of the lead vehicle with respect to the instrumented vehicle, using the recorded radar range and azimuth data, as shown in Figure 34. The equations to calculate the lateral position (x) and the longitudinal position of the lead vehicle (y) are shown in Equation 16 and Equation 17, respectively.

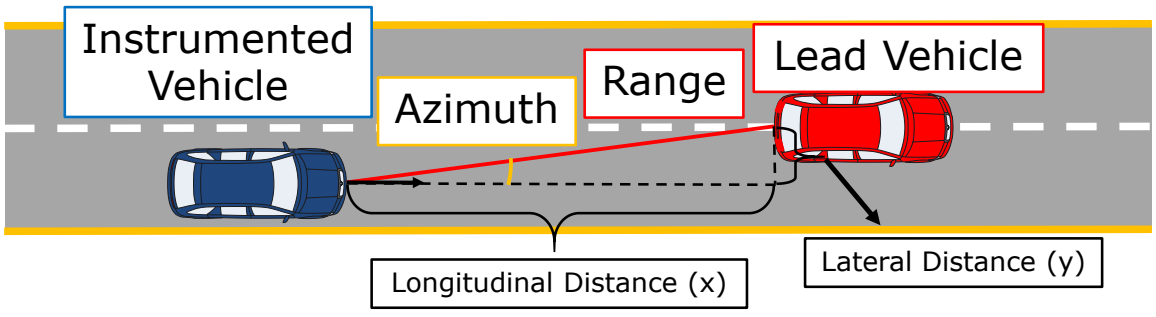

Figure 34. Identify Lead Vehicle Position Using Radar Range and Azimuth

$$x = \cos(Azimuth) * Range \qquad \textbf{Equation 16}$$

$$y = \sin(Azimuth) * Range \qquad \textbf{Equation 17}$$

3.3.2.1.2 Step 2: Reconstruct Instrumented Vehicle Path

The second step of the method reconstructed the path of the instrumented vehicle to the location of the lead vehicle, as shown in Figure 36. The trajectory reconstruction provides a more accurate method of calculating the offset distance between the two vehicles by considering complex roadway geometries. Figure 35 shows an example of braking event with complex roadway geometry. As shown in Figure 35, while the recorded radar range and azimuth is sufficient to accurately calculate the relative position of the lead vehicle on a straight road, but for the roadway presented in the example event, the radar data would indicate that there is no overlap between the two vehicles. Vehicle trajectory reconstruction method therefore provides an improved estimate of overlap percentage by considering roadway geometry.

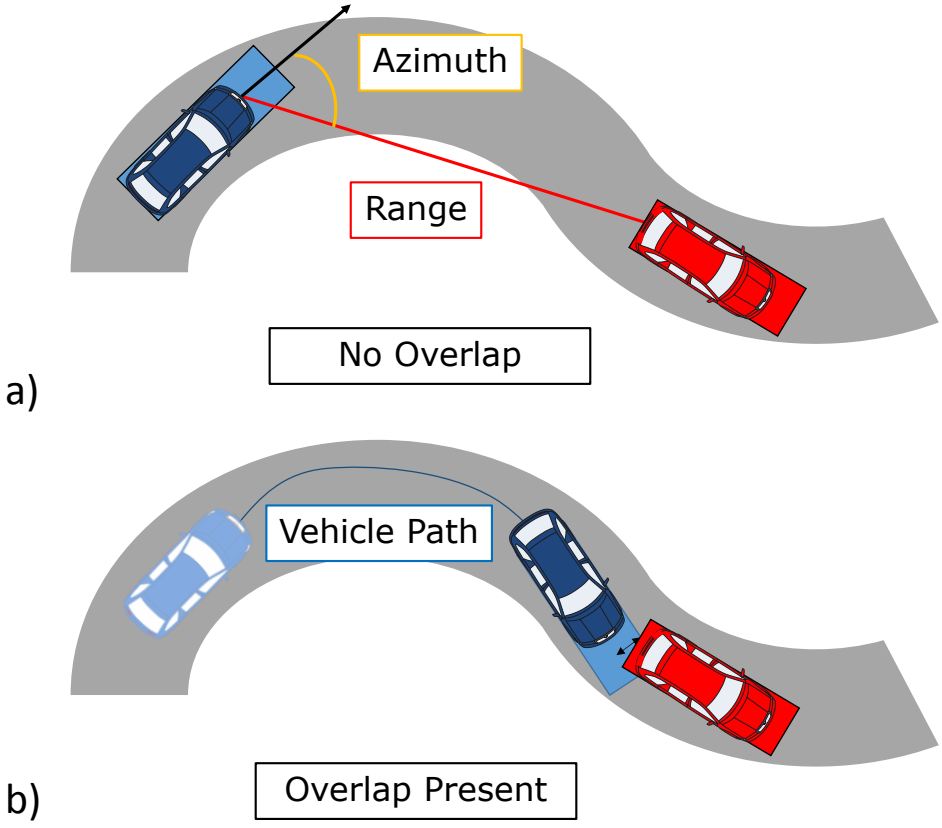

Figure 35. Vehicle Path Reconstruction to Improve Overlap Percentage Estimate

The vehicle trajectory was reconstructed using the recorded vehicle speed and yaw rate. Figure 37 shows the flow chart diagram for vehicle trajectory reconstruction. The instrumented vehicles were assumed to be at x = 0 and y = 0, with a heading of 0 degrees at time of brake application. The remaining heading values were calculated based on trapezoidal integration of the yaw rate, ω, sampled at 0.1 seconds apart. As shown by the diagram, two different methods of calculating travel distance were used for straight and curved trajectories. Time points with vehicle yaw rate greater than $1x10^{-4}$ deg/sec were assumed to have a curved trajectory, in which the distance traveled, l, is calculated based on the radius of curvature, r, and the change in heading angle between the current time point and next time point. Time points with vehicle yaw rate less than $1x10^{-4}$ deg/sec were assumed to have a straight trajectory, and the distance traveled, l, is simply the product of vehicle speed and time duration.

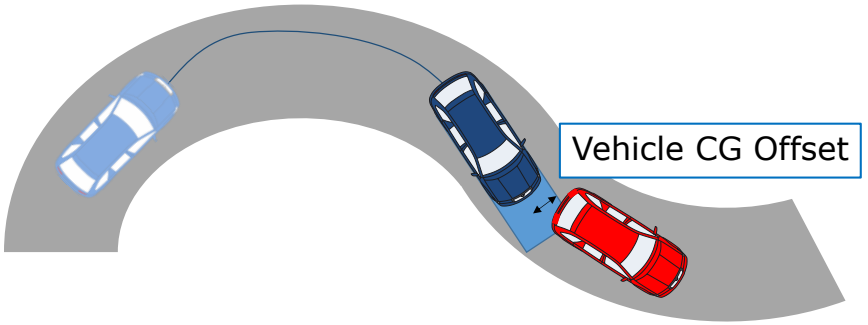

Figure 36. Reconstruction of Vehicle Path

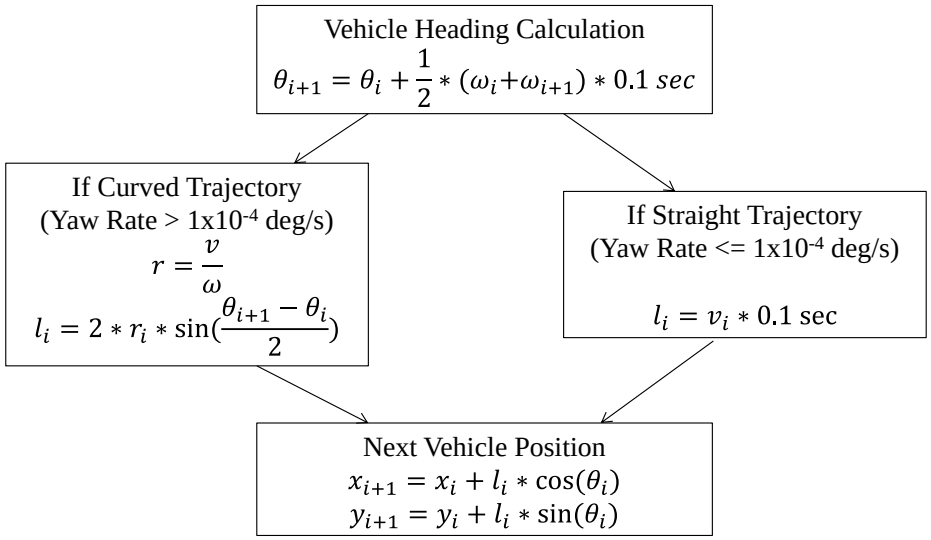

Figure 37. Flow chart for vehicle trajectory reconstruction.

3.3.2.1.3 Step 3: Calculating Overlap Distance and Overlap Percentage

With the instrumented vehicle positioned at the location of the lead vehicle, the last step of the method was to estimate the offset distance between the center of gravity (CG) of the lead vehicle and the instrumented vehicle. Figure 38 illustrates the measurements required to compute vehicle CG offset. The blue rectangle in the graph represents the area occupied by the track width of the instrumented vehicle, and the red rectangle in the graph represents the area occupied by the track width of the lead vehicle, and the purple area represents the intersecting area, or the overlap distance, between the two vehicles. In a hypothetical event, where the lead vehicle stopped and the instrumented vehicle followed its intended path, the intersecting area represents the impact area if the two vehicles were to collide.

Equation 18 and Equation 19 show the calculation of overlap percentage based on the track width of the instrumented vehicle and an assumed track width of the lead vehicle. The track width of all lead vehicles were assumed to be 1.76 m. This was calculated as the average track width of all vehicles in the 100-Car NDS, which we assumed was representative of the track width of the passenger vehicle during the time of data collection. The track width for each instrumented 100-Car vehicle (TW_{int}) was known and recorded by VTTI at the time of data collection. This 3 step process was repeated for each braking event in the sample.

Due to the uncertainty associated with the assumed lead vehicle track width, the following study categorizes overlap percentage as “Small Overlap”, “Some Overlap”, and “Full Overlap”. “Small Overlap” consists of events with an estimated overlap percentage less than 25%. This definition is similar to the Insurance Institute for Highway Safety’s (IIHS) Small Overlap Frontal Crash Test, where the test standard specifies that 25% of the width of test vehicle must be engaged during the crash [130]. The “Some Overlap” category consists of events with overlap percentage between 25% and 75%, and the last “Full Overlap” category consists of events with overlap percentage greater than 75%.

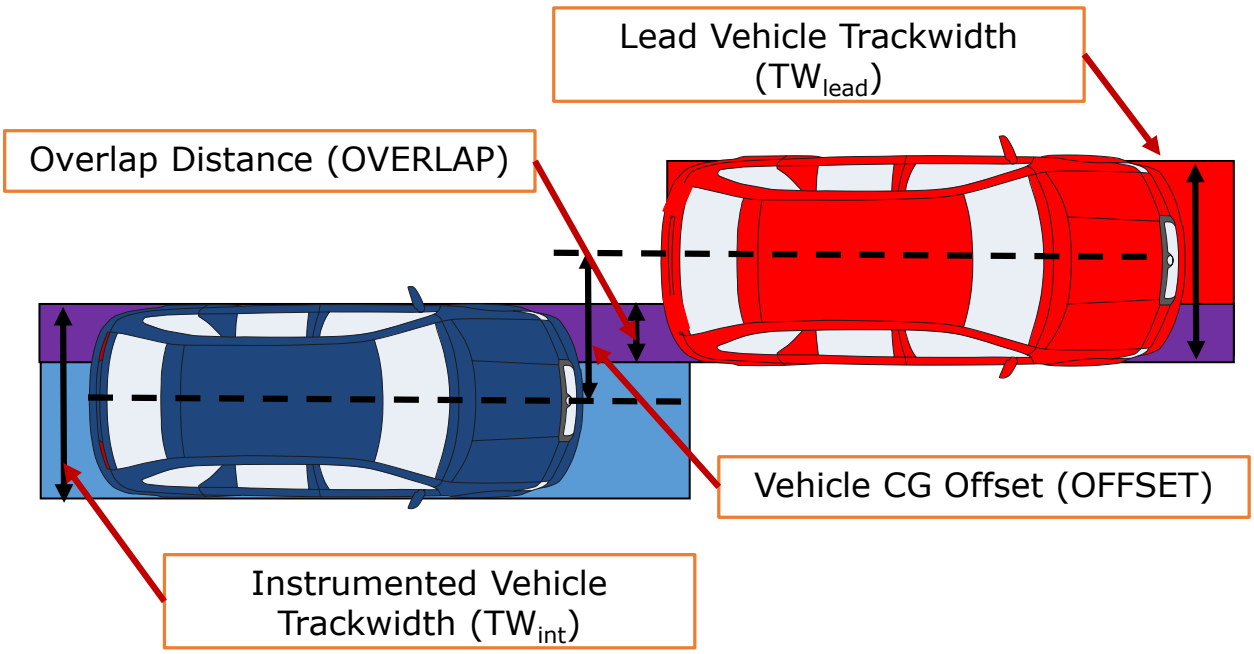

Figure 38. Calculation of Overlap Distance.

$$OVERLAP = (\frac{TW_{lead}}{2} + \frac{TW_{\text{int}}}{2}) - OFFSET \qquad \textbf{Equation 18}$$

$$OverlapPer\,cent = \frac{OVERLAP}{TW_{\text{int}}} \qquad \textbf{Equation 19}$$

3.3.2.1.4 Instrumented Vehicle Lane Change Considerations

For each braking event, we assumed a hypothetical event in which the lead vehicle is stopped in the roadway and the instrumented vehicle follows its intended path, the overlap percentage is then calculated as the intersecting width of the two vehicles when they are at the same location. While the path reconstruction method presented in the previous subsection considers road geometry, it is only valid if the instrumented vehicle remain on the same lane on the roadway. In the event that the instrumented vehicle changes lanes during its path to the lead vehicle's location, the current method shifts the path of the lead vehicle to the original lane and recalculates the overlap percentage.

3.3.2.2 Time to Collision

Time to collision (TTC) calculates the time remaining until impact between two objects. In this study, we define TTC as the time remaining before two vehicles would collide if they continued

at their current trajectory and the relative acceleration remain constant, as shown in Equation 20. This definition of TTC is identical to the Enhanced Time to Collision (ETTC), presented in Chapter 2.6.5. For this study, we characterize driver behavior by the TTC to the lead vehicle at the time when the brakes were applied.

$$TTC = \frac{-V_r - \sqrt{V_r^2 - 2 * A_r * D}}{A_r} \qquad \textbf{Equation 20}$$

To aggregate the behavior of each driver, the minimum TTC at brake application was computed for all combinations of time of day, day of week, vehicle speed (grouped in 10 mph bins), and the category of overlap. For example, a minimum TTC was computed for the scenario of the vehicle traveling between 40 and 50 mph during daylight on a weekday in full overlap braking events. The driver age group was divided into groups of "Novice" 18-20 years, "Young" 21-30 years, "middle" 31-50 years, and "Mature" 51+ years. The age group and gender were included as covariates for TTC in the statistical models.

3.3.2.3 Statistical Methods

In order to determine the effect of driver demographics and driving context upon car following behavior, linear mixed effects models were constructed. Linear mixed effects models are similar to ordinary linear models, but can include random effects variables along with traditional fixed effects. In this study, the driver was treated as a random intercept and the remaining independent variables were modeled as fixed effects. This methodology allowed for the models to take into account between subject variability that an ordinary linear model would not account for. To examine the interaction effects, pairwise contrast were constructed. To test for statistical significant, a Tukey Honestly Significant Difference (HSD) adjustment was made for multiple comparisons. The weighting scheme presented in Table 1 will be used in the statistical analysis to adjust for the demographic sampling bias in the 100-Car NDS.

3.3.3 RESULTS

3.3.3.1 Sample Selection

All trips involving primary drivers, i.e., the owners or lessees of the vehicle, were extracted from the 100-Car study. In order to be included in this study, the drivers had to be operating the vehicle while all required sensors (radar, speed, and yaw rate) were functional for at least 60% of the trips traveled during the study.

In addition to valid sensors, any driving context level, e.g., weekday, during the day, small overlap at 30-40 mph, for a given driver that had fewer than 5 brake applications was excluded from the analysis. Not all drivers enrolled in the study drove frequently during all driving context levels examined for this study. If a driver had very few braking applications at a given driving context level, it was unlikely they had adequate exposure to exhibit a minimum TTC that was representative of their normal behavior.

3.3.3.2 Dataset Summary

Table 14 shows the summery of the final dataset. The final analysis dataset consisted of 809,199 braking events with closing lead vehicle and full driving context information. These braking events were based on 64 drivers over 55,140 trips.

Table 14. Dataset Summery - Overlap Analysis

Group	Drivers	Trips	Number of Braking Events
Trips with Valid Sensor Data	64	64,991	1,501,854
Trips with Closing Braking Events	64	57,257	859,397
Trips with Closing Braking Event and Full Driving Context Information	64	55,140	809,199

Table 15 shows the distribution of all levels of driving context in the analysis. As expected, braking events were more frequent during the day on a weekday. Specifically, weekday, daytime, and full overlap braking events consists of nearly half of all braking events in the analysis (47.9%).

Braking events performed at night on a weekend with small overlap was the least frequent driving context in the analysis, totaling only 2,290 (0.3%) of all braking events.

Table 15. Driving Context Distribution - Overlap Analysis

Driving Context			Number of Braking Events	% of All Braking Events
Day of Week	Daytime	Overlap		
Weekday	Day	Small	20,707	2.6%
Weekday	Day	Some	166,285	20.5%
Weekday	Day	Full	387,249	47.9%
Weekday	Night	Small	5,138	0.6%
Weekday	Night	Some	33,369	4.1%
Weekday	Night	Full	68,647	8.5%
Weekend	Day	Small	4,947	0.6%
Weekend	Day	Some	32,790	4.1%
Weekend	Day	Full	59,879	7.4%
Weekend	Night	Small	2,290	0.3%
Weekend	Night	Some	11,635	1.4%
Weekend	Night	Full	16,263	2.0%

3.3.3.3 Effect of Overlap Percentage in Driver Braking Behavior

Table 16 shows an analysis of variance (ANOVA) for the linear mixed effects model of minimum TTC experienced during the study in each driving context scenario. For the main effects, all of the driving context variables (speed categories, time of day, day of week, and overlap categories), were significant at the $\alpha = 0.05$ confidence level. Age group was statistically significant at the $\alpha = 0.05$ level, while no statistically significant difference were detected between gender groups at the $\alpha = 0.10$ level. The interaction effects of overlap categories and speed ranges were also show to be significant at the $\alpha = 0.10$ level, and will be explored further in the following section.

Table 16. Analysis of Variance for Linear Mixed Effects Model for Minimum TTC

Effect	F Value	Pr (> F)	
Overlap Categories	3.22	0.0402	**
Age Group	22.54	<.0001	***
Gender	1.26	0.2623	
Time of Day	65.26	<.0001	***
Day of Week	39.11	<.0001	***
Speed Categories	545.1	<.0001	***
Overlap Categories*Gender	1.49	0.2259	
Overlap Categories*Age Group	1.77	0.1004	
Overlap Categories*Time of Day	1.12	0.3252	
Overlap Categories*Day of Week	0.83	0.4353	
Overlap Categories*Speed Categories	6.18	<.0001	***
Age Group*Gender	6.01	0.0004	**
Age Group*Time of Day	1.4	0.2409	
Age Group*Day of Week	3.86	0.009	**
Age Group*Speed Categories	1.82	0.0394	**
Gender*Time of Day	1.45	0.2293	
Gender*Day of Week	1.6	0.2055	
Gender*Speed Categories	3.36	0.0094	**
Time of Day*Day of Week	7.7	0.0056	**
Time of Day*Speed Categories	7.81	<.0001	***
Day of Week*Speed Categories	4.91	0.0006	**
Note**: *** = p < 0.0001, ** p < 0.05, * = p < 0.10**			

Table 17 lists the least squared mean estimate of the minimum TTC for each of the main effect variables. The least squared mean estimates of TTC were produced by the regression model averaged across all other factors. As shown in the table, TTC increases with increasing vehicle speed, and also shows slight increase with increasing driver age. However, different levels of overlap categories only show slight difference in the LS mean TTC estimate.

Table 17. Least Squared (LS) Mean Estimates of Minimum TTC by Main Effect Levels

Effect	Level	Estimate
Overlap Categories	Small Overlap	4.34
	Some Overlap	4.50
	Full Overlap	4.40
Speed Categories (mph)	10-20	2.88
	20-30	3.35
	30-40	4.49
	40-50	5.33
	50-60	6.02
Age Group	Novice (18-20)	4.21
	Young (21-30)	4.46
	Middle (31-50)	4.30
	Mature (51+)	4.69
Gender	Female	4.44
	Male	4.39
Time of Day	Day	4.22
	Night	4.61
Day of Week	Weekday	4.26
	Weekend	4.57

3.3.3.4 Minimum TTC by interactions of Driving Context Factors

Figure 39 shows the least squared mean estimate for TTC generated from the linear model by travel speed and overlap categories. The difference in LS Mean TTC was significant across speed ranges, i.e. "Some Overlap" events at 10-20 mph was significantly different than the "Some Overlap" events at 20-30 mph. However, the only speed category with significant difference between different overlap categories was the 20-30 mph group. One hypothesis on the difference in TTC between overlap groups is by lead vehicles cutting into the lane of the instrumented vehicle during slow moving traffic. Vehicles traveling between 20-30 mph are likely in congested traffic in the Washington D.C. area, and the lead vehicle may suddenly change lanes from an adjacent lane to the instrumented vehicle's lane, causing the instrumented vehicle to press the brake and slow down. In this example scenario, the lead vehicle has small overlap with respect to the instrumented vehicle,

and the driver of the instrumented vehicle are forced to press the brake at the last second due to the sudden movement of the lead vehicle lane change.

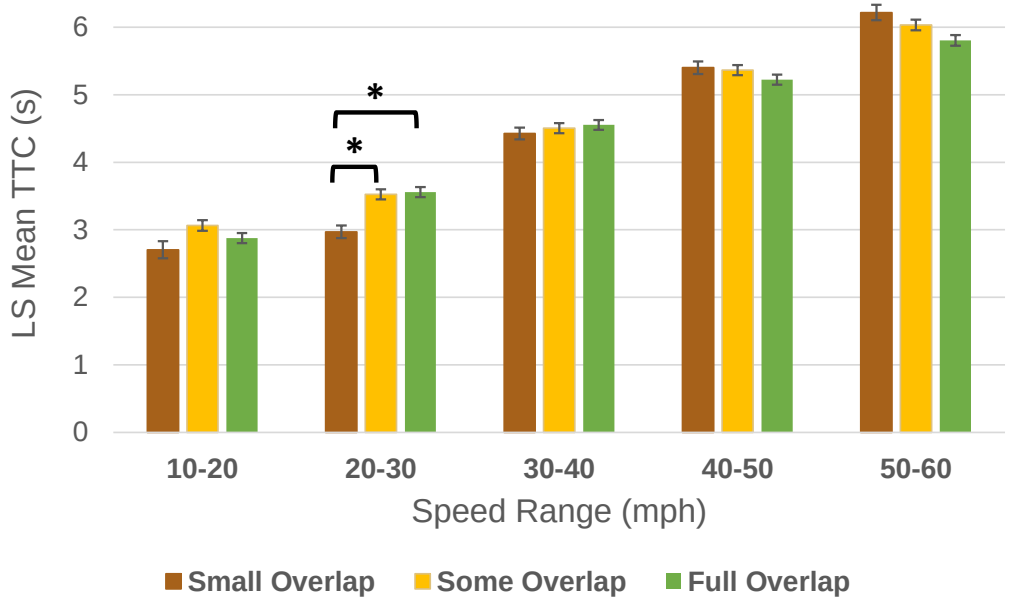

Figure 39. LS Mean Estimates of Minimum TTC by Travel Speed and Overlap Categories

3.3.4 Conclusion and Discussion

This study presents a method of estimating percentage overlap in braking events using only vehicle radar sensors. The method takes into consideration of road geometry between the instrumented vehicle and the lead vehicle, and incorporates considerations for instrumented vehicle lane change scenarios.

In addition, the results of this study show that driving context significantly affects driver braking behavior during car following. Forward crash avoidance systems such as FCW may better match a drivers' expectations if it adapts its warning times to both the driver and the driving context. This adaptation may be possible by utilizing current on-vehicle sensors, such as navigations systems, ambient light sensors, radar, cameras, and vehicle speed sensors. In addition, the result of the study shows that overlap percentage may potentially effect driver braking behavior at vehicle speeds lower than 30 mph. One example scenario, in which overlap percentage may influence driver braking

behavior, is of the lead vehicle suddenly change lane to move in front of the instrumented vehicle. In this scenario, the driver may not have sufficient time to prepare, and may be forced to brake later than usual. Future active safety system and autonomous vehicle systems should consider monitoring nearby vehicle lane keeping behavior, using a method similar to Chapter 6 and overlap percentage to prepare for instance of small overlap events which drivers may not be prepared for.

This study has several important limitations. First, the method utilized in the current study utilizes a constant track width, based on average track width of passenger cars, for all lead vehicles. This assumption do not accurately portrait the range of vehicles present on the roadway.

Second, the resolution of the video in the 100-Car study limits the use of machine vision video analysis and manual video review to determine the accurate track width of the lead vehicle. Future studies may consider using an updated database with improved video quality, such as the SHRP-2 NDS study, to improve the estimation of percentage overlap.

Third, the radar utilized in the 100-Car NDS is limited to ±7 degree azimuth, limiting the range which the radar can potentially "see" lead vehicles. In other words, there are potentially braking events with a lead vehicle present, however the overlap of the lead vehicle was small enough to be outside of the field of view of the radar, and therefore was not correctly identified and included in the analysis.

Lastly, the statistical methodology used for this study aggregated all brake applications during driving context scenarios and took the minimum TTC during each scenario. This aggregation assumes a true minimum that is characteristic of the driver's normal behavior was experienced during each scenario. We observed that if very few brake applications were collected at a given scenario that large variability could be introduced into the results. Typically those scenarios with few brake applications had extremely high TTC, i.e., greater than 20 s. Scenarios with less than 5 brake applications were excluded to attempted to minimize this variability but at the expense of

potentially biasing the results. A possible solution to this challenge would be to use a statistical methodology that uses all the recorded braking data instead of aggregating by scenario.

This study presents a method of estimating percentage overlap in braking events using only vehicle radar sensors. The result from the study shows that in low speed small overlap scenarios during braking events, drivers may delay brake application and create potential near-crash or even crash scenarios. Future active safety systems, therefore, should consider methods of monitoring nearby vehicles to prepare for scenarios such as lead vehicle cut in to assist drivers in avoiding potential crashes.

4 DRIVER BEHAVIOR DURING OVERTAKING MANEUVERS IN CAR FOLLOWING

4.1 INTRODUCTION

Lane changes with the intention to pass the vehicle in front are especially challenging scenarios for FCW designs, because these overtaking maneuvers can occur at high relative vehicle speeds and often involve no brake and/or turn signal application. Therefore, overtaking presents the potential of prematurely triggering the FCW. A better understanding of lane change events can lead to designs which increase driver acceptance of FCW and improve the effectiveness of FCW systems.

Past studies have approached characterizing driver action by modeling driver intention using a simulator environment [131]. Other studies have explored the possibility of predictive systems to track and predict driver intent in real time [132], [133]. Similarly, large scale studies which characterize a population of drivers can benefit automakers who seek to improve driver acceptance of FCW, as well as regulatory agencies seeking to improve FCW vehicle tests. The following study presents the first large scale study of its kind, based on naturalistic driving data to report driver behavior during overtaking maneuvers. The objective of this study was to aid FCW design by characterizing driver behavior during lane change events in the 100-Car naturalistic driving study data.

4.2 METHOD

Our approach for the current study was broken down into three subtasks. The first subtask of the study was to find the lane change maneuvers and determine the start and finish of the lane change events. Since not all lane change events involve braking and/or turn signal use, we developed an algorithm which used the lane tracking instrumentation data to identify lane change events. The second subtask of the study was to identify whether a lead vehicle was present during lane change events, using the algorithm described in Section 2.5. The third and last subtask was to compute

minimum Time to Collision (TTC) for each lane change maneuver. Minimum TTC is often used in research as a safety indicator [134]. In this study, minimum TTC refers to the lowest (closest to zero) recorded TTC for each driver.

4.2.1 *Identification of Lane Change Events*

The identification of lane change events was based on the lane change signal provided by the on-board lane tracking system, Road Scout, developed by VTTI. Road Scout uses the video footage obtained by the on-board camera to determine the distance from the center of the vehicle to the left and right lane markings [135]. Figure 40 shows the diagram of our lane change signal trigger. The lane change signal is triggered when the vehicle center meets the lane edge as the vehicle moves across the lane.

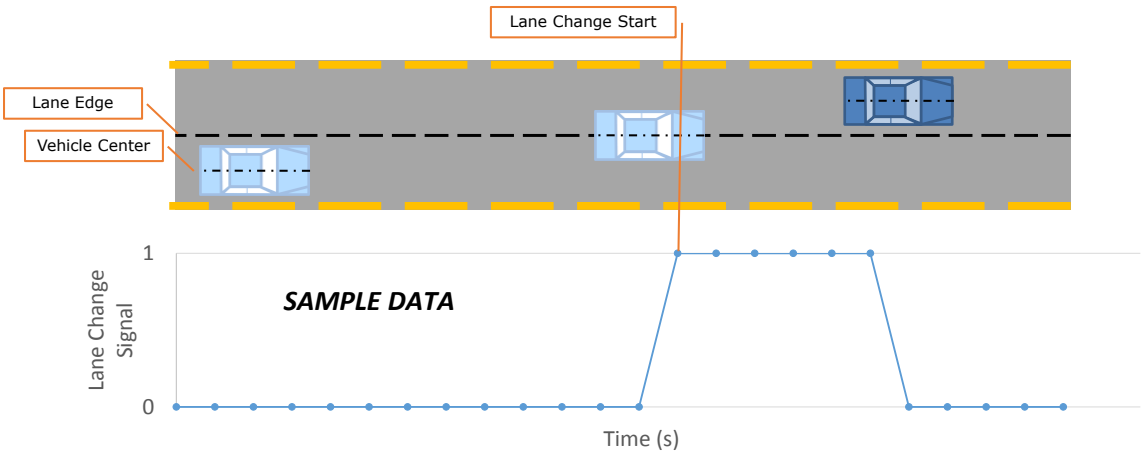

Figure 40. Road Scout Lane Change Signal Trigger Diagram

Our definition of lane departure was based on the International Organization for Standardization (ISO), which defines point of lane/road departure as the instant when the leading edge of the vehicle meets the lane boundary [136]. The start of lane change is calculated by using the track width of each vehicle to determine when the vehicle centerline is one-half track width away from the lane edge. Lane change duration is defined as the time period from when the vehicle's leading edge meet the lane line to when the vehicle is once again within the lane boundary, as shown in Figure 41.

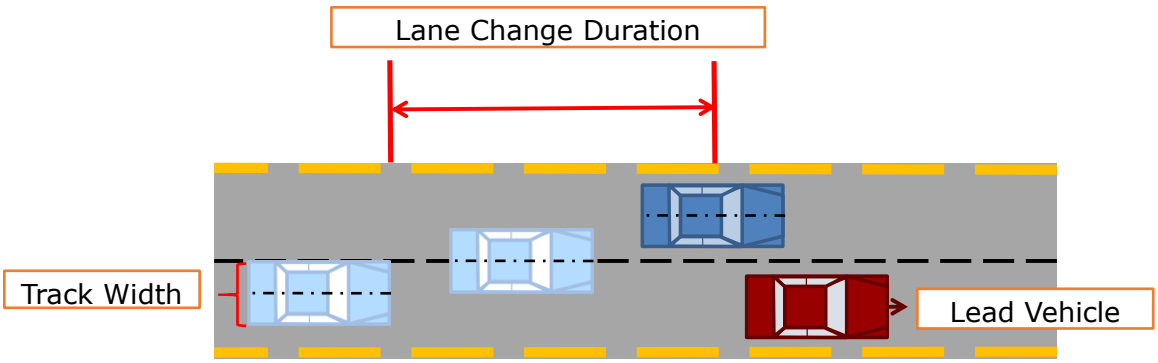

Figure 41. Definition of Lane Change Duration

In order to be included as a valid lane change maneuver, the following conditions have to be met:

1. Lane change duration greater than 0.3 seconds
2. Lane change abort signal not triggered anytime during lane change maneuver. Abort signal are defined in the discussion which follows.
3. Vehicle speed greater than 10 mph at the start of lane change
4. Lane change maneuvers which occurred 1 second apart are combined into one single maneuver

Short duration lane changes (< 0.3 seconds) were assumed to be an erroneous signal trigger and were excluded. This threshold was determined based on the characteristic lane change duration in a random sample of 1,425 lane change events, as shown in Figure 42. The 1,425 lane change events were obtained from a manual review of 126 trip videos. During the review process, the researcher reviewed the entire duration of the trip to determine the time when the vehicle crossed the lane edge (lane change begin) and when the vehicle completed the lane change (lane change ends). Figure 42 shows the distribution of lane change duration in the manually inspected sample. As shown by the figure, the median lane change duration from begin to end was approximately 2.1 seconds. The minimum duration for these events was 0.4 seconds, and 90% of the lane change events in this sample lasted longer than 1.4 seconds.

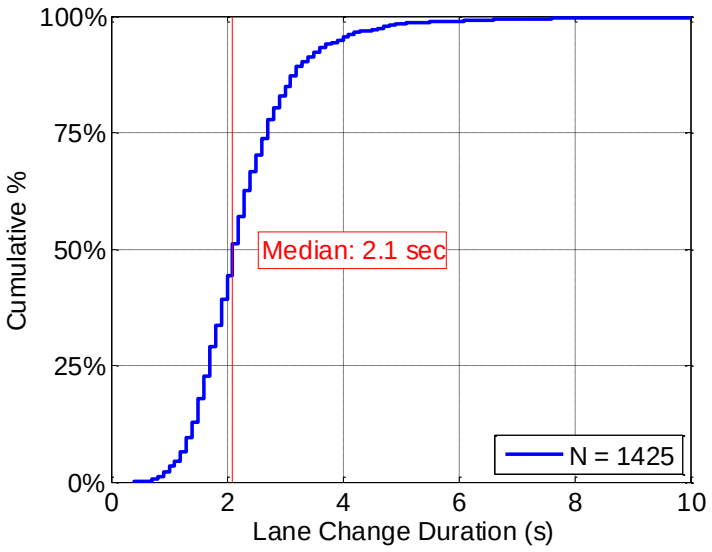

Figure 42. Distribution of Lane Change Duration in Sample of Manually Reviewed Trips

In addition to the lane change signal, Road Scout also indicated when a lane change was initiated by the driver but the maneuver was aborted before the vehicle completely moved into the adjacent lane. In this study, all events which triggered the lane change abort signal at any time during the lane change event were excluded. Any lane change events where the vehicle speed was never above 10 mph have been excluded because these low speed events were not applicable to the current FCAS designs.

4.2.2 Determine Lead Vehicle Search Window

While the on-board machine vision lane tracking system is able to identify the incidence when the vehicle centerline cross the lane edge, the time associated with the lane cross is often much later than the time when driver initiates the lane change maneuver. In a multiple lead vehicle scenario, if we apply the automated lead vehicle search algorithm at the time of vehicle lane crossing, the on-board radar can potentially misidentify the lead vehicle to be the vehicle in the adjacent lane. Figure 43 shows a multiple lead vehicle scenario during lane change. If the lead vehicle identification algorithm was applied at the time of lane crossing, the algorithm can potentially misidentify Lead Vehicle 2 as the actual lead vehicle.

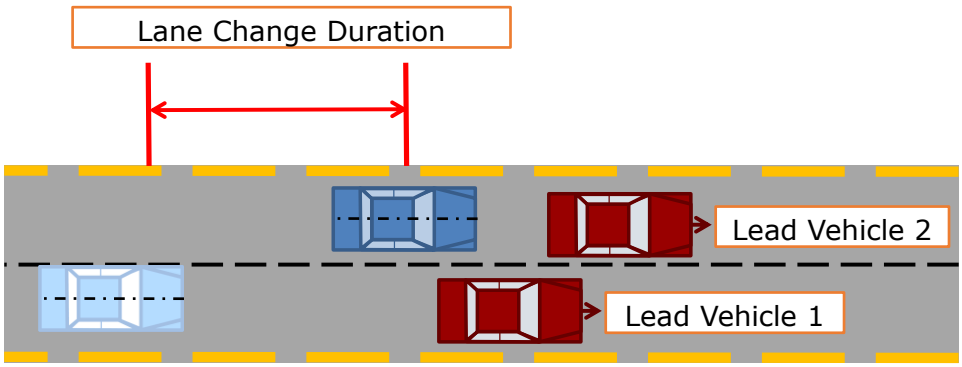

Figure 43. Multiple Lead Vehicles in Lane Change Scenario

In order to improve the accuracy of the lead vehicle identification algorithm, one of the modifications that was made to the lead vehicle search algorithm in this study was to implement a lead vehicle search window, as shown in Figure 44. The lead vehicle search window allows for the algorithm to search for road objects before the vehicle begins to move laterally, therefore improving the accuracy of the algorithm.

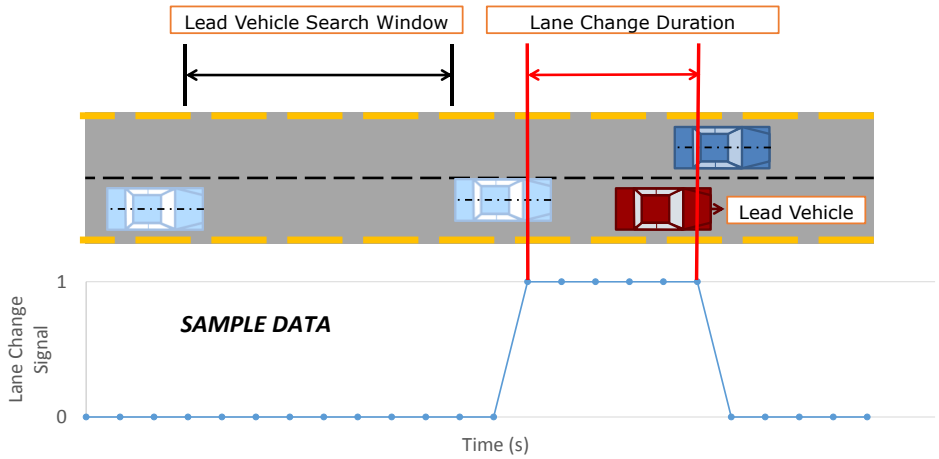

Figure 44. Lead Vehicle Search Window

A search window of 1.5 seconds before lane change start to 1.0 seconds before lane change start was used in the lead vehicle identification algorithm. To determine the appropriate search window for the algorithm, we used the sample of 126 manually reviewed trips to find the earliest time at which the on-board radar detects the lead vehicle. We found that the median of the distribution of lead vehicle detection time to be 3 seconds. We then implemented every permutation

of the time range from 0 to 3 seconds, in increments of 0.5 seconds, in the lead vehicle identification algorithm to find the search window with the highest accuracy rate. Figure 45 shows a sample of the search window ranges and the resultant lead vehicle search algorithm performance. As shown in the figure, the time range of 1.5 seconds before lane change start to 1.0 seconds before lane change start yielded the highest accuracy rate for the lead vehicle identification algorithm. At one second prior to lane change, most vehicles are still within the original lane and following the lead vehicle, resulting in improved performance from the lead vehicle search algorithm.

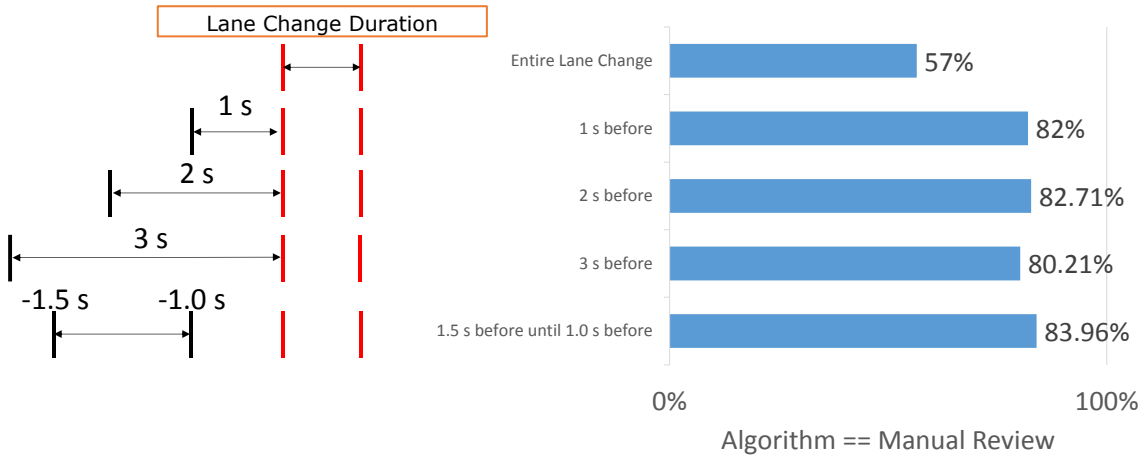

Figure 45. Optimize Lead Vehicle Search Window

4.3 RESULTS

4.3.1 LANE CHANGE DETECTION ALGORITHM VALIDATION

A total of 126 trips, containing nearly 50 hours of video footage was manually examined by the researchers to validate the algorithm. The manual video review procedure identified a total of 1,425 lane change maneuvers.

The performance of lane change detection algorithm was evaluated based on the true positive and false negative matrix shown in Figure 46. The sensitivity (% of correctly detected true positives) and specificity (% of correctly detected true negatives) of the algorithm was calculated as the ratio

of true positive and true negative to the corresponding lane change maneuver, as shown in Equation 21 and Equation 22.

Table 18 summarizes the comparison of the video and lane tracking indicated lane change events. Examining all lane change events, the sensitivity was 0.58 and specificity was 0.97. The reason for the relatively low sensitivity was a high number of false negatives, i.e. "misses" by the lane tracking system. From observation of these events, a lane change event will not be issued by the system if there is low lane tracking probability. For all valid lane changes with sufficient lane tracking information (i.e. lane tracking confidence > 30%, vehicle speed > 10 mph, and headway < 3 s), the lane change detection algorithm performed very well. The sensitivity of the algorithm was 0.87 and the specificity of the algorithm was 0.98.

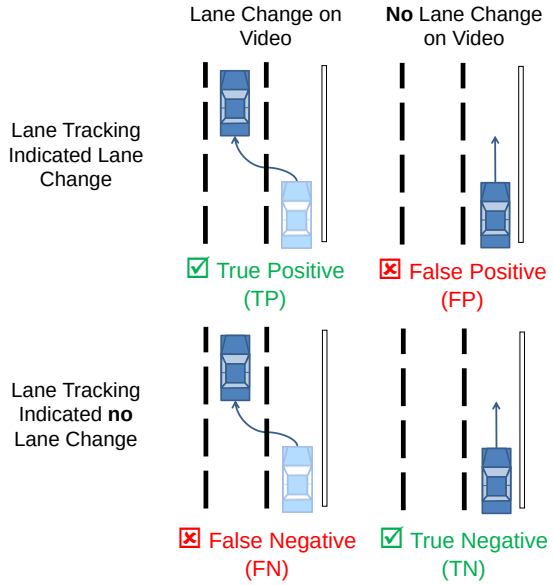

Figure 46: True Positive and False Negative Matrix

$$Sensitivity = \frac{TP}{TP + FN} \qquad \textbf{Equation 21}$$

$$Specificty = \frac{TN}{TN + FP} \qquad \textbf{Equation 22}$$

Table 18. Comparison Results of Video and Lane Tracking Indicated Lane Changes

Measure	All Lane Changes	Exclude Low Probability, Low Speed and > 3 s Headway
Video Lane Changes	1,425	645
Lane Tracking Lane Changes	2,270	850
TP	758	561
FP	543	143
FN	556	84
TN	14,804	8,148
Sensitivity	0.58	0.87
Specificity	0.97	0.98

4.3.2 Lead Vehicle Identification Validation in Lane Change Events

Similar to braking events, the validation of lead vehicle identification in lane change events was done through the comparison of manually identified lane change events against algorithm results. Overall, the lead vehicle detection algorithm correctly identified the car following situation in 84% of the lane changes in the validation sample. Figure 47 shows the lead vehicle identification algorithm performance in five different car following scenarios. Scenario a) is the correct identification of a lead vehicle when there is lead vehicle present, b) is the correct determination of no lead vehicle, c) is the identification of a lead vehicle when no lead vehicle is present, d) is no lead vehicle is identified when a lead vehicle is present, and e) is identifying the wrong vehicle as the lead vehicle.

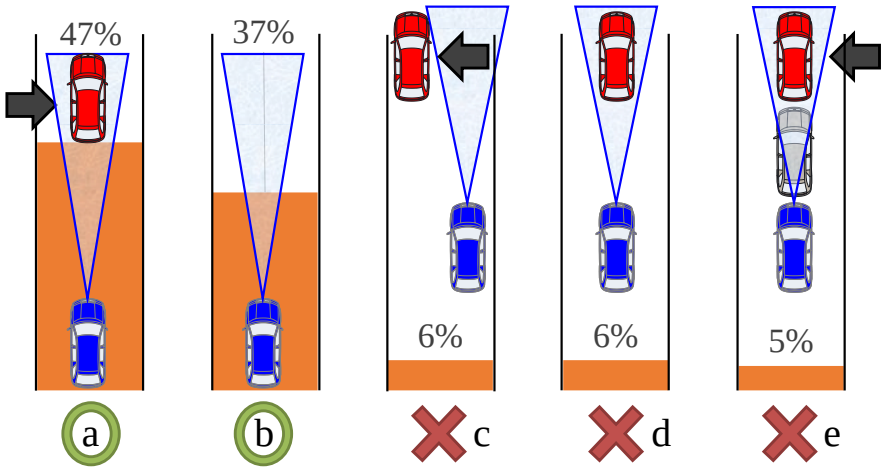

Figure 47: Lead Vehicle Detection Scenarios

4.3.3 *Dataset Summery*

Table 19 summarizes the sample of trips with valid sensor data. A total of 46,250 trips from 45 drivers were used in this study.

Table 19. Driver Selection with Valid Sensor Data

Group	Count
Number of Drivers	45
Number of Trips	46,250
Total Miles Driven	406,606
Median Trip Distance (miles)	4.6
Median Trip Duration (minutes)	11.4

4.3.4 *Population Distribution of TTC at Lane Change*

Table 20 shows the result of applying the lane change detection algorithm to all drivers with valid sensor data, organized by lane change scenarios. A total of 326,238 lane changes were found in the 46,250 trips. The distribution of left side and right side lane changes was essentially the same. A total of 90,639 lane changes involved a closing lead vehicle. Closing lead vehicle events were defined to be lane changes where the driver was moving closer to the lead vehicle. As shown in the table, lane changes with a closing lead vehicle accounted for approximately 28% of all lane change events (All Lane Changes (326,238) divided by Lane Change with Closing Lead Vehicle (90,639) = 28%). Similar to the distribution of all lane change events, left side lane change accounted for approximately 52% of all lane changes with closing lead vehicle, and right side lane changes was approximately 48% of all lane changes with closing lead vehicle.

Table 20. Lane Change Scenario Distribution

Group	All Lane Changes (% of All Lane Changes)	Lane Change with Closing Lead Vehicle (% of Lane Change with Closing Lead Vehicle)
Left Side Lane Changes	171,519 (52.6%)	47,420 (52.3%)
Right Side Lane Changes	154,719 (47.4%)	43,219 (47.7%)
Total Lane Changes	326,238 (100%)	90,639 (100%)

Figure 48 is a box-and-whisker plot that shows the weighted distribution of lane change frequency with a closing lead vehicle within each speed bin. A total of 45 data points (one for each driver) were used to calculate the quantiles in each 10 mph speed bin. Each driver's lane change frequency was normalized by the number of miles traveled within the speed bin as shown in Equation 23, where lane change per miles driven in the i^{th} speed bin was calculated as the total number of lane changes with lead vehicle in the i^{th} speed bin, n_i, divided by the total number of miles driven in the i^{th} speed bin, d_i.

$$\text{lane change per mile driving}_i = \frac{n_i}{d_i} \qquad \textbf{Equation 23}$$

As shown in Figure 48, the median was approximately 0.2 lane changes per mile, or 1 lane change every 5 miles, for typical travel speeds between 20-70 mph. Figure 48 also shows an increase in median lane change frequency with increasing vehicle speed for speeds ranging from 10-50 mph, after which the median begins to decrease with vehicle speed. Very few drivers made overtaking maneuvers in speeds greater than 80 mph. One hypothesis for the relative low instance of lane changes in speed between 10-30 mph is that most U.S. roadways with speed limit less than 25 mph are one lane roads with no opportunity for the driver to change lanes. As speed increase, the number of roadways generally increase allowing for lane change maneuvers. The subsequent decrease in lane change frequency at speeds higher than 50 mph may indicate steady travel speed in less dense traffic, where the driver does not need to change lanes as frequently.

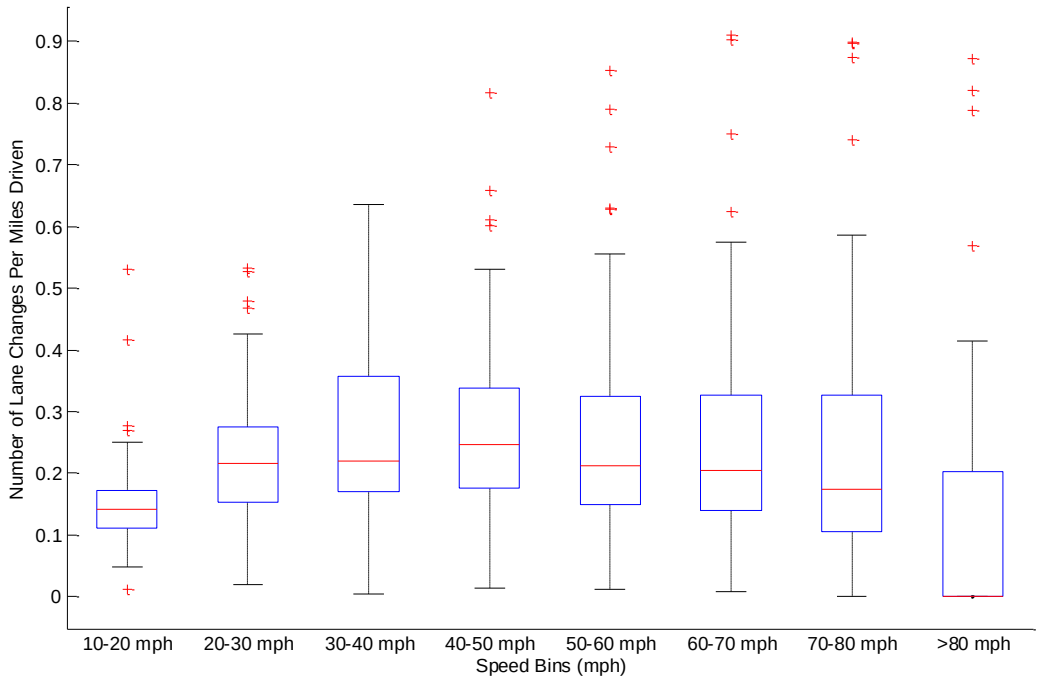

Figure 48. Weighted Distribution of Lane Changes with Closing Lead Vehicle and TTC (90,639 total lane changes)

Figure 49 shows the weighted distribution of minimum TTC by driver in each speed bin. Each driver has one point in each 10 mph speed bin. The cumulative distribution of minimum TTC for each driver are plotted below for each speed bin. In Figure 49, TTC was computed as the TTC at the start of lane change, and minimum TTC for each driver refers to the lowest (closest to zero) TTC for trips within each speed bin.

In general, the minimum TTC increases with travel speed. The variability in minimum TTC between drivers also increases with travel speed. The plot shows the number of drivers who made lane changes with a closing lead vehicle in each speed bin (ex. N = 45 in the 60-70 mph bin). Due to the relatively low percent of lane changes at high speeds, not all drivers had lane changes with a closing lead vehicle in the >80 mph speed range.

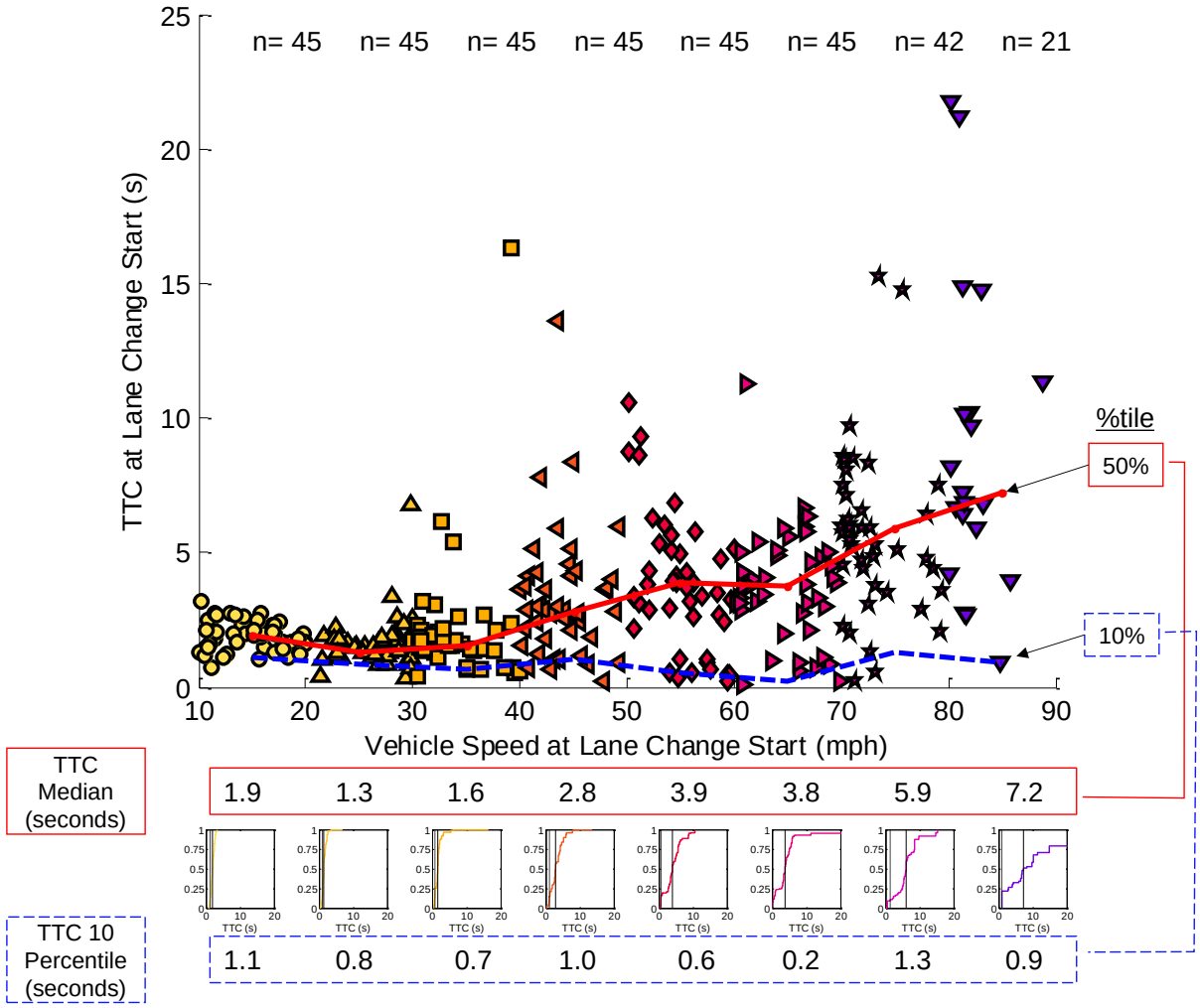

Figure 49. Weighted Distribution of Minimum TTC for Each Driver by Travel Speed Bin (n =90,639 lane changes)

4.4 Conclusion and Discussion

The objective of this study was to aid FCW design by characterizing driver behavior during overtaking events. This study presented a methodology to detect lane change events and a methodology to identify lead vehicle in lane change events in the 100-Car NDS. The performance of these two algorithms was validated against 126 trips, in which the researchers manually examined the video footage to determine the time frame of lane change and lead vehicle presence. Finally these algorithms were applied to the 100-Car NDS dataset to obtain the distribution of TTC at lane change with a lead vehicle in front of the subject car.

In 126 randomly selected validation trips, the researcher manually reviewed the trip videos and identified 1,425 lane change events. Within the sample of manually identified lane change events, 420 events were found to be overtaking events, in which the video showed a driver passing a lead vehicle. A total of 439 merging lane changes were found in the sample, in which a closing lead vehicle was present in about 42% of the merging events. For lane change events other than overtaking and merging (566 events), a closing lead vehicle was present in 37% of these events. Overall, the lane change detection algorithm performed very well. For lane changes with sufficient lane tracking information, the validation process showed that the automated lane change algorithm had a sensitivity of 0.87 and a specificity of 0.983. The lead vehicle identification algorithm also performed reasonably well, and correctly identified the car following situation in 84% of the validation sample of lane change events. Our lane change detection algorithm is highly dependent on the presence of lane markings, therefore our analysis was restricted to marked roadways. It is uncertain how our results may generalize to roads with poor lane markings.

A total of 326,238 lane change events were identified by the algorithm in 46,250 trips, totaling over 400,000 miles of driving. In addition, the breakdown of lane change frequency by speed bin also shows that drivers increase lane changes for travel speeds ranging from 10-50 mph. The lower lane change frequency in the lower speed range bins can potentially be due to several reasons. First, it is likely that lane changes events in lower speed ranges (i.e. lower than 30 mph) were on roads with lower speed limits and were 2-lane roads with no adjacent lanes to change into. We also hypothesize that when drivers initiate lane change maneuvers in lower speed ranges, they were more likely to speed up and thus are grouped into higher speed bin ranges. An example scenario would be during congested traffic conditions in the Washington D.C. area, the instrumented vehicle was in a lane with slow moving traffic but sped up to change into the adjacent lane in order to move ahead of traffic.

The distribution of TTC showed that minimum TTC, as well as variability of TTC between drivers, generally increased with travel speed. The increase in TTC can be attributed to drivers generally becoming more cautious and increasing following distance as travel speed increases. As drivers begin to increase following distance, lead vehicles are more likely to be outside of the range of the front radar. Although our study was highly dependent on the radar to detect lead vehicle, the results are biased towards what the radar can "see". However, the results are still relevant in improving the effectiveness of a FCW system in a crash imminent situation.

The characterization of lane change events presented in the current study will provide active safety system designers with an enhanced understanding of driver action in overtaking maneuvers and can improve designs of FCW systems in several areas. First, the results of this study show that the frequency and TTC in lane change events vary by vehicle speed. This implies that the warning threshold for FCW systems needs to adapt to current vehicle speed. Second, the large variability in minimum TTC between drivers shows the need for FCW systems to implement several different warning thresholds depending on different driving style. For example, FCW systems may give driver the option to select different warning settings for "aggressive" or "conservative" driving style.

5 COMPARISON OF TTC AT BRAKING WITH TTC AT OVERTAKING

5.1 INTRODUCTION

In normal car following situations, the driver can either apply the brake or change lanes to avoid a collision with a slow moving vehicle in front. In order to design a FCW system which anticipates driver actions, the designers need a distribution of driver car following behavior which incorporates the potential of either braking or lane change maneuvers.

In Chapter 3.1 of this dissertation, we determined the distribution of Time to Collision (TTC) during car following for vehicle braking events. Similarly, Chapter 3 of this dissertation analyzed driver behavior during overtaking maneuvers. In both studies, driver behavior was characterized based on Time to Collision (TTC). TTC refers to the time remaining until collision, assuming that the two objects maintain constant velocity and trajectory. In previous studies, TTC has been shown to be a useful metric for driver perception of risk [109]. However, it is unknown whether driver risk perception changes with respect to vehicle speed. In other words, will a driver who is aggressive at 30 mph remain aggressive at higher speeds? In addition, does a driver who shows aggressive braking characteristics initiate aggressive lane change maneuvers as well? The objective of this study was to combine driver braking characteristics and lane change characteristics to examine the potential change in driver behavior between braking and lane change maneuvers in car-following.

5.2 METHOD

The overall approach of this study was to combine the results presented in previous studies analyzing driver braking and lane change maneuvers in the 100-Car NDS, and examine the potential difference in driver behavior between the two car following maneuvers. In order to extract braking and lane change events from the large 100-Car NDS, and correctly identify the car-following scenarios, we utilized a previously developed automated search algorithm [49], [67]. In order to assess the accuracy of the automated search algorithm, our researchers manually examined video

footages from 323 trips containing 3,765 miles of travel and 115 hours of data. For each braking event, the results of the automated search algorithm were compared to the results of the manual video review. The comparison between the algorithm output and the manual inspection shows that our automated search algorithm was able to correctly identify the lead vehicle in 90% of the validation sample.

5.3 THEORY/CALCULATION

5.3.1 TIME TO COLLISION

Time to Collision (TTC) was used in both the braking and lane change events in car-following to characterize driver behavior. Shown in Equation 24, TTC is calculated as the ratio of the range (x) between vehicles and the rate of change of range ($\dot{x}$).

In addition, the difference in TTC between lane change and braking events was characterized using ΔTTC, as shown in Equation 25.

$$TTC = \frac{x}{\dot{x}} \qquad \textbf{Equation 24}$$

$$\Delta TTC = TTC\ at\ Start\ of\ Braking - TTC\ at\ Start\ of\ Lane\ Change \qquad \textbf{Equation 25}$$

5.3.2 RELATIVE FREQUENCY

Equation 26 shows a relative frequency metric, which is used in the following study to characterize driver braking and lane change frequency by normalizing the number of lane change events by the number of braking events.

$$Relative\ Frequency = \frac{\#\ of\ Lane\ Change\ Events}{\#\ of\ Braking\ Events} \qquad \textbf{Equation 26}$$

5.3.3 *Probability Density Function*

Probability density functions characterize the probability of occurrence of a continuous random variable, such as TTC. In this study, probability density functions were used to characterize the probability of braking and lane change initiation for each driver.

5.3.4 *Model Selection Criterion*

The approach to finding the distribution which best fit the TTC values associated with each driver's braking and lane change events was to compare a number of common probability density distributions, shown in Table 21. Model selection was determined based on minimizing two statistical criteria, the Akaike's information criterion (AIC) [110], and the Bayesian information criterion (BIC) [111]. If a model is constructed based on a sample of training data, AIC and BIC provides an estimate of the model performance on a similar sample of testing data. In order to avoid the addition of parameters which will overfit the model to the training data, both AIC and BIC control for the number of parameters in a model using a penalty term, as seen in Equation 27 and Equation 28, where n is the number of observations, and k is the number of parameters in the model. The *likelihood* term in both equations denotes the likelihood function, which measures the agreement between the model and the observed data.

Table 21. List of Common Probability Density Distributions

Distribution Name
Generalized Extreme Value
Log-logistic
Log-normal
Inverse Gaussian
Birnbaum-Saunders
Generalized Pareto
t Location-Scale
Weibull
Gamma
Exponential
Nakagami
Logistic
Normal
Rayleigh
Rician
Extreme Value

$$AIC = -2 * \ln(likelihood) + 2 * k \qquad \textbf{Equation 27}$$

$$BIC = -2 * \ln(likelihood) + k * \ln(n) \qquad \textbf{Equation 28}$$

5.4 RESULTS

5.4.1 DATASET SUMMARY

Table 22 summarizes the number of trips and miles traveled by all primary drivers in their primary vehicles, as well as drivers with valid sensor data. A total of 46,250 trips from 45 drivers were used in this study.

Table 22. Driver Selection with Valid Sensor Data

Group	Drivers	Number of Trips	Miles
All Trips (Primary Drivers/Vehicles)	106	132,721	1,118,905
Drivers with >60% Valid Sensor Data	45	58,121	528,440
Trips with Valid Data	45	46,250	406,607

5.4.2 *Automated Search Algorithm Results*

Using our automated search algorithm, we were able to identify any potential lead vehicle in car following events and calculate the TTC to determine whether the vehicles are closing. Table 23 shows the summary of brake events with a closing lead vehicle. A total of 641,759 braking events were identified as have a closing lead vehicle. Similarly, a total of 91,413 lane change events were identified as having a closing lead vehicle. Based on the event count in Table 23, we can see that, in general, drivers initiate braking maneuvers more frequently than lane change maneuvers.

Table 23. Brake Events with Lead Vehicle

Measure	Count
Number of braking events with a closing lead vehicle	641,759
Number of lane change events with a closing lead vehicle	91,413

5.4.3 *Lane Change and Braking Frequency*

Figure 50 shows the cumulative distributions of the relative frequency of braking and lane change events. Braking and lane change events were divided into 9 speed bins based on the vehicle speed at the time of the braking or lane change event. Relative frequency was computed as the ratio of lane change events to braking events. A relative frequency less than 1 would indicate that braking was more frequent for the driver within the particular speed bin, and a relative frequency greater than 1 would indicate that lane change was more frequent within the speed bin.

As shown by Figure 50, the median of the relative frequency generally increases with increasing vehicle speed. For vehicle speeds less than 50 mph, nearly all drivers perform more braking than lane change maneuvers. As the speed increases to the 70-80 mph speed bin, the median is nearly 1, meaning that about half the drivers are more likely to brake than change lanes, and the other half are more likely to do the opposite.

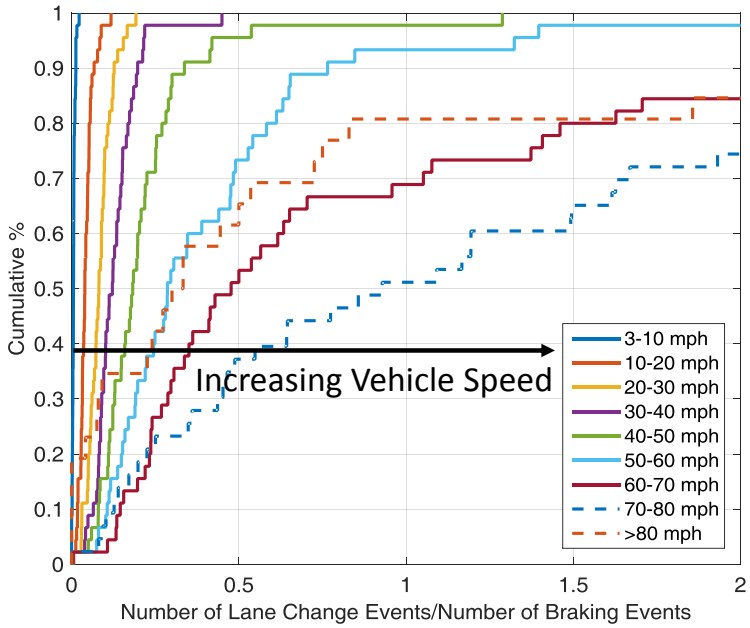

Figure 50. Lane Change and Braking Frequency Ratio.

5.4.4 Comparison of TTC at Braking and Lane Change

Figure 51 shows a scatter plot of the ΔTTC metric. Similar to Figure 50, the events were divided into 9 speed bins based on the speed of the vehicle at the start of the braking event. For all braking and lane change maneuvers with a closing lead vehicle in each speed bin, we first computed all TTC at the start of the braking or lane change events, and then computed the 10th percentile TTC for each driver. The ΔTTC for each driver was computed by taking the difference between the 10th percentile TTC at the start of braking and the 10th percentile TTC at the start of lane change. Unlike minimum values, the 10th percentile provides the valuable lower end time threshold for driver behavior, and eliminates extreme values which may be captured by calculating the minimum. Each data point in the speed bin represents the ΔTTC for one driver, and the "n=" note on top of the figure denotes the number of drivers which was represented in each speed bin. The number of drivers do not always equal to the full sample of 45 drivers due to the fact that not all drivers initiated both braking and lane change events in all speed bins. The figure also shows the median and 10th

percentile of all data points in each speed bin, connected by the solid and dashed lines, respectively. In addition, the values of the medians and 10th percentiles are tabulated in Table 24.

As shown in Figure 51, the median ΔTTC in each speed bins are approximately zero for all vehicle speeds, suggesting that the difference between braking and lane change TTC is small. However, there is a great deal of variability in ΔTTC from driver to driver. The figure shows that the variability between drivers increase with increasing vehicle speed. For example, in the 60-70 mph speed range, driver ΔTTC can vary between approximately -8 seconds to 8 seconds.

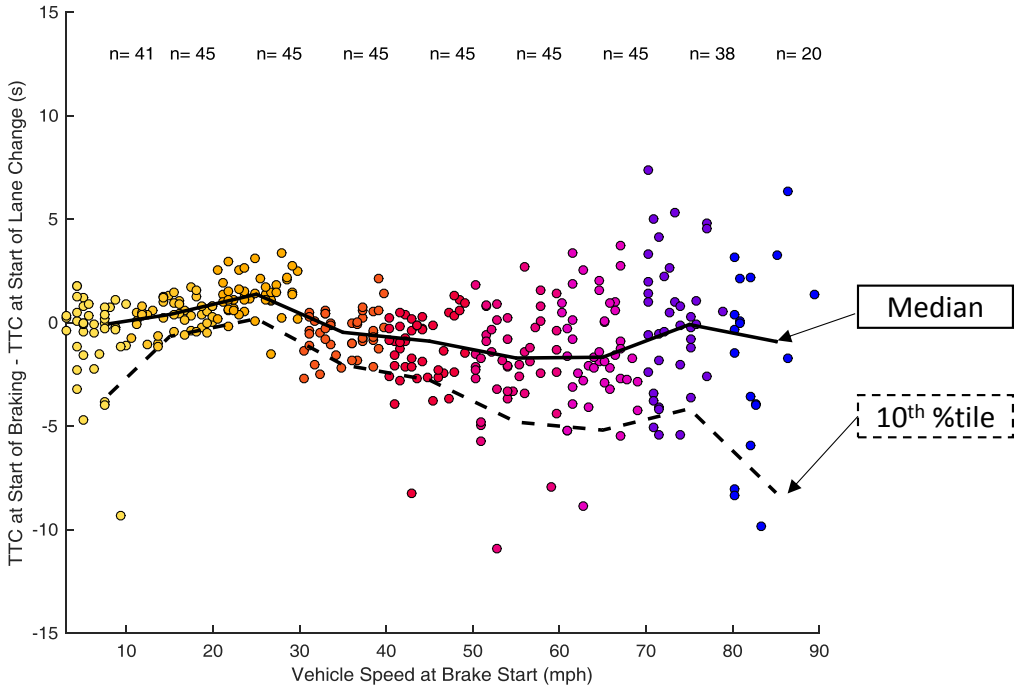

Figure 51. 10th Percentile TTC at Braking and Lane Change.

Table 24. 10th Percentile TTC at Braking and Lane Change

Measure	3-10 mph	10-20 mph	20-30 mph	30-40 mph	40-50 mph	50-60 mph	60-70 mph	70-80 mph	80+ mph
Median	-0.05	0.40	1.37	-0.47	-0.89	-1.71	-1.67	-0.09	-0.91
10th Percentile	-3.47	-0.67	0.19	-2.03	-2.77	-4.80	-5.19	-4.16	-8.22

5.4.5 RANKING OF DRIVER TTC

One method of comparing driver aggressiveness across speed bins and between braking and lane change events is by ranking the drivers. Figure 52 shows a series of driver ranking, based on 10th percentile TTC in braking and lane change events, for the first 9 drivers in the sample. Figures are broke up into 9 separate plots to increase clarity, the rankings for the remaining drivers can be found in Appendix A - Driver Ranking of 10th Percentile TTC at Braking and Lane Change Events. For each speed bin, the drivers with lower TTC (i.e. aggressive driving), receives a higher ranking, and drivers with higher TTC (i.e. conservative driving) receives a lower ranking. Each driver is assigned a Driver ID and shown in the legend of each plot. The figures only shows ranking for speeds between 10-70 mph in order to include a complete ranking, where all drivers initiated both lane change and braking maneuvers.

Similar to the results shown in Figure 51, the rankings in Figure 52 show that driver behavior varies greatly between drivers. Drivers do not all consistently stay aggressive across speed bins, as well as between lane change and braking events. The rankings in the figures can be generalized into 4 categories: “Increasing”, where the driver ranking increase with vehicle speed, indicating driver becoming more aggressive with increasing vehicle speed; “Decreasing”, where the driver ranking decreases with vehicle speed, indicating that driver is becoming more conservative with increasing vehicle speed; “Constant”, denotes when drivers are consistent in their ranking throughout the speed ranges; and lastly “Varying”, which denotes that driver’s ranking changes with no particular pattern.

We can see examples of all four types of ranking changes in the following figure. For example, the braking ranking of driver 1005 shows increasing trend with increasing vehicle speed in part a). Similarly, the braking ranking of driver 1002 shows a decreasing trend. One of the most prominent examples of consistent ranking can be seen in driver 1050 in Appendix A part d), where the driver shows consistently the most aggressive braking and lane change behavior. In addition to trends in ranking across speed ranges, several drivers show similar trend between braking and lane change events. For example, driver 1033 in part d) shows a "Decreasing" trend in braking events as well as lane change events, while drivers 1062 in part e) shows generally increase in aggressiveness in both braking and lane change.

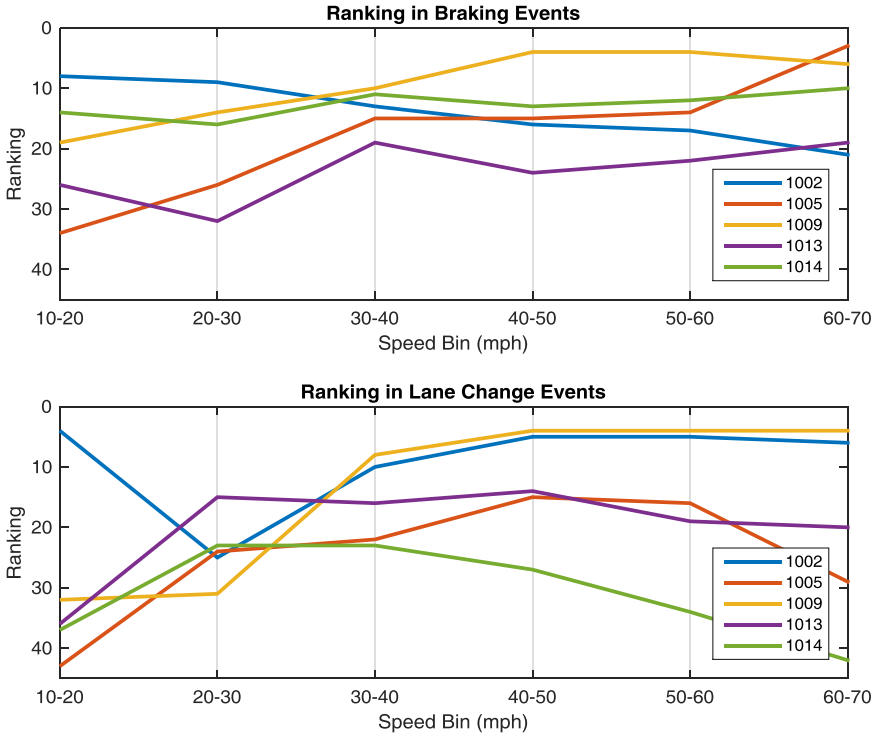

Figure 52. Driver Ranking of 10th Percentile TTC at Braking and Lane Change Events

5.4.6 DRIVER SPECIFIC PROBABILITY DISTRIBUTION OF TTC IN LANE CHANGE AND BRAKING

The results thus far have shown that driver behavior in car following events varies greatly between drivers. The frequency of braking and lane change events have been shown to vary between drivers. Driver perception of risk, as measured by TTC at braking and lane change events, have been shown to vary with vehicle speed, and more importantly, the pattern at which driver perceive risk in car following event has also shown to be highly variable. In other words, a driver who shows aggressive braking at low speeds may not necessarily exhibit similar aggressively behavior at higher speeds braking events or lane change events at similar speeds. Therefore, one potential solution in designing an effective FCW system is to predict when each driver may normally brake or change lanes, in order to issue warning only when necessary.

Figure 53 and Figure 54 shows the probability distribution of TTC for Driver 1002's braking and lane change events across different vehicle speeds. As shown by the figure, the probability distribution describes the probability of the driver applying the brake or change lanes at different TTC threshold. Each curve in the figures has a distinguishable peak, which represent the TTC that correspond with the maximum probability of driver initiating a braking or lane change maneuver.

Table 25 shows a summary of the maximum probable TTC for both braking and lane change events.

As shown by Figure 53, the peak probability braking TTC decreases with increasing vehicle speed, suggesting that drivers initiate braking maneuvers less frequently in higher speeds. In contrast, the lane change probability distribution shown in Figure 54 do not show a similar decrease in max with respect to vehicle speed. This finding corresponds to the relative frequency distribution shown in Figure 50, which showed braking frequency decreased with increasing vehicle speed.

Similar maximum probable TTC values have been generated for the remaining drivers of the study sample. A summary of the maximum probable TTC values for all drivers and speed ranges are presented in Appendix B.

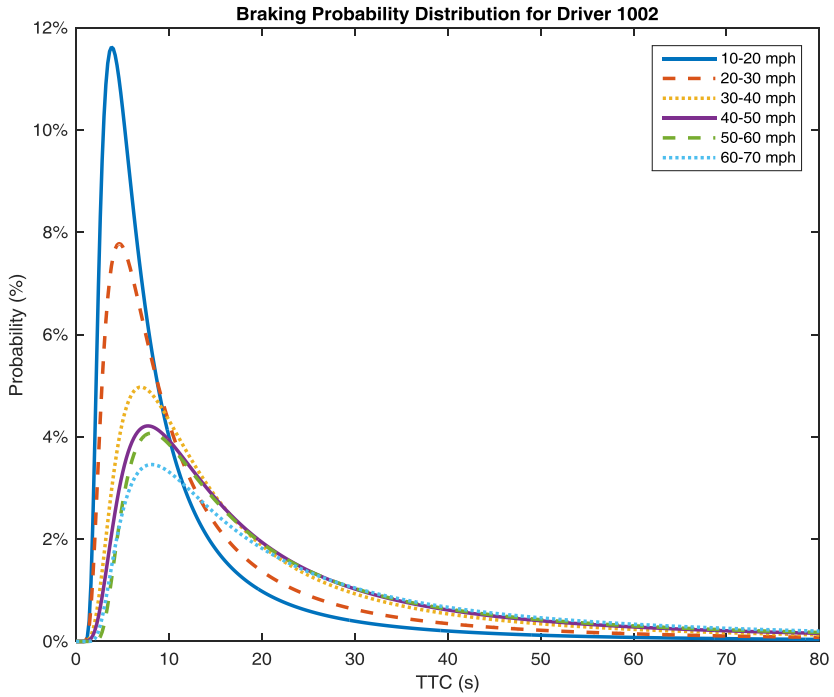

Figure 53. Probability Distribution of Brake Application by TTC for Driver 1002

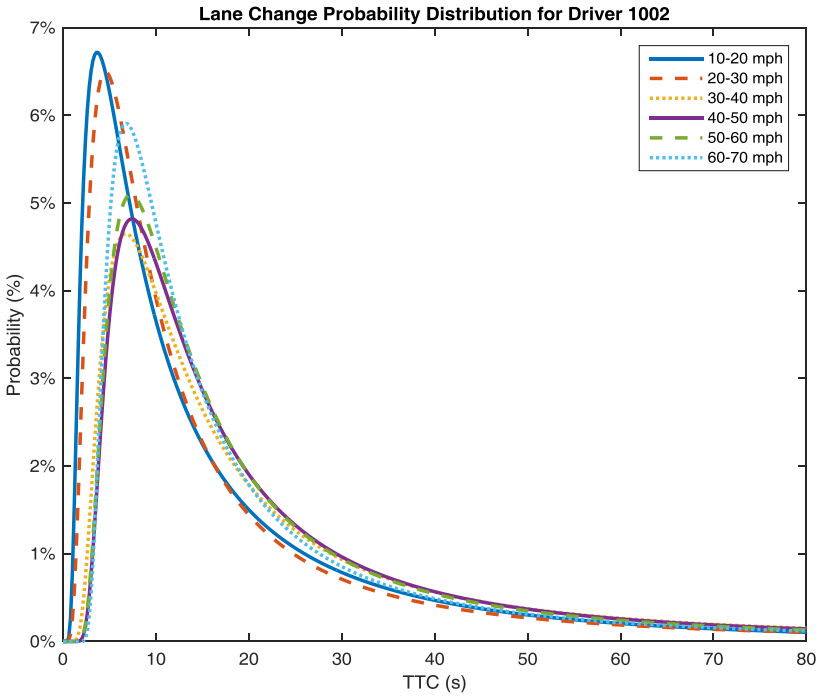

Figure 54. Probability Distribution of Lane Change Initiation by TTC for Driver 1002

Table 25. Driver 1002 Max Probability TTC Summary

Maneuver	10-20 mph	20-30 mph	30-40 mph	40-50 mph	50-60 mph	60-70 mph
Braking	3.80	4.60	7.01	7.81	8.01	8.21
Lane Change	3.60	4.60	6.81	7.41	7.21	6.81

5.5 Conclusion and Discussion

This study compared driver braking and lane change behavior in normal car-following events. The result of the study was based upon the 100-Car NDS and included 45 drivers and over 400,000 miles of driving data. Using an automated search algorithm, we first extracted all braking and lane change maneuvers from the dataset and characterized driver braking and lane change behavior in car following events in previous reports. The research objective of this study was to combine driver braking characteristic and lane change characteristics to examine the potential change in driver behavior between braking and lane change maneuvers in car-following.

Several characteristics of driver behavior in braking and lane change events were presented in the results. First, we examined the relative frequency of braking and lane change events across different vehicle speeds. The result shows that in lower speeds, between 3-40 mph, drivers in the study sample all initiated more braking events than lane change events. In addition, as vehicle speed increases, the ratio of number of lane change events and number of braking events begin to increase. The median of the relative frequency for vehicle speed between 70-80 mph was approximately 1. The increase in relative frequency suggests that drivers initiate the majority of the braking events in lower vehicle speeds, such as while driving on small rural roads, or congested traffic. In higher speed, such as during travel on interstate highways, drivers are more likely to initiate lane changes to overtake vehicles and maintain current travel speed. The relative frequency result also shows that braking and lane change frequency are highly variable by driver, especially in vehicle speeds near highway speeds. Half of the drivers in the sample performed more braking events and the other half performed more lane change events during vehicle speeds between 70-80 mph. This is indicative that driver behavior in car following begins to increase in variability in higher vehicle speeds.

The second part of the results analyzed the difference in TTC during braking and lane change events. In order to eliminate extreme values which may be capture by the minimum TTC, the comparison of TTC during braking and lane change was based upon 10^{th} percentile TTC for each driver. The resultant scatter plot of ΔTTC between braking and lane change, shown in Figure 51, suggests that the median difference between driver lane change and braking TTC are largely centered at 0. However, as vehicle speed increases, the variability between drivers also increase similar to the relative frequency distribution shown in Figure 50.

Given the large variability between drivers, exhibited thus far by both the difference in frequency of lane change and braking events, as well as the perception of risk during car following events, as indicated by the largely varied TTC, our next question was to address whether a driver

who was aggressive in low speed braking would continue to exhibit aggressive braking behavior in higher speed braking events or lane change events. The results of this section was presented as a series of 9 rankings, shown in Figure 52 and Appendix A, in which each driver was ranked from 1 (most aggressive) to 45 (least aggressive), based on the TTC at braking and lane change. The results shows that, although several drivers show consistent trend in car following behavior, not all drivers' behavior can be generalized or categorized.

The last section of the results explored the potential of creating driver specific TTC for both braking and lane change events. The approach was to find the probability density functions with the best fit for TTC values associated with each driver's braking and lane change events. For each driver the maximum probable TTC value for braking and lane change event in each speed bin has been presented in Appendix B. The results from this section are similar to the rankings established in the previous section. As indicated by the TTC values in each speed bin, driver risk perception varies by both driver and vehicle speed, and each individualized probability density function can potentially help tailor the timing of FCW warnings to driver preference.

6 DISTRIBUTION OF TTC AND ETTC AT START OF STEERING DURING OVERTAKING

6.1 INTRODUCTION

The study presented in this section is based on the methodology and results presented in Chapter 4 "Driver Behavior in Overtaking Maneuvers in Car Following". In Chapter 4, we developed an algorithm to identify lane change events, and defined the start of lane change as the time when the leading vehicle edge contacted the lane edge, as shown in Figure 55. Although the orginal definition of start of lane change provided a reasonable representation of the lane change event, it may not fully capture the driving scenario when the driver initiated the lane change event. In the following study, we present a newly developed methodology to improve estimation of start of lane change, by using start of steering maneuver as the beginning of the lane change event. The overall objective of this study was to extract time of steering initiation for all previously identified lane change events, and to characterize driver lane change behavior at start of lane change by TTC and ETTC.

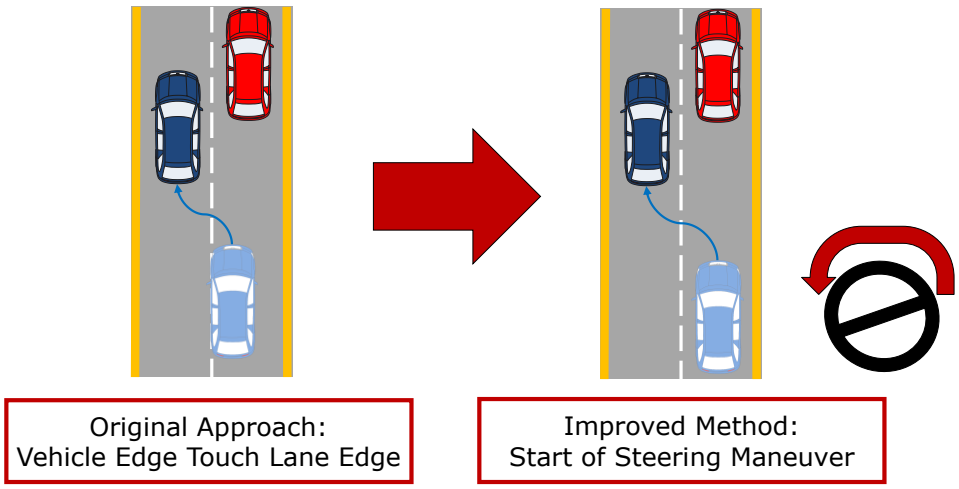

Figure 55. Improved Method of Determining Start of Lane Change Event

6.2 METHODS

6.2.1 OVERALL APPROACH

The overall approach of this study was to modify the methodology developed in Chapter 4, "Driver Behavior during Overtaking Maneuvers in Car Following", to estimate the start of steering maneuver in lane change events in the 100-Car NDS.

One of the major challenges in determining the start of steering maneuver in the 100-Car NDS is the fact that the 100-Car study does not directly record steering wheel input for the participating vehicles. Therefore, the following study utilizes vehicle lane position to estimate start of steering in lane change events. Figure 56 shows the two vehicle kinematic parameters used in this study. Distance to Lane Boundary (DTLB) measures the distance between the vehicle edge and the lane edge and is measured and recorded by the on-board lane tracking software in the 100-Car NDS. Lateral Velocity measures the rate of change of the distance to lane boundary, and is computed by taking the rate of change of DTLB.

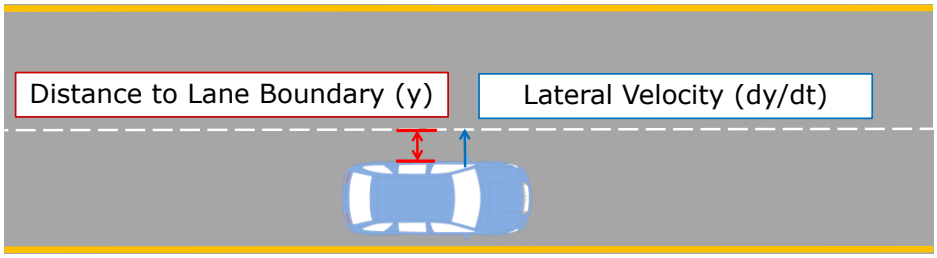

Figure 56. Vehicle Kinematic Parameters Used to Estimate Start of Lane Change

Another challenge associated with determining the start of steering maneuver in the 100-Car NDS is that there are a wide variety of driving scenarios and driving personalities in each lane change event. Different drivers may have different timing in lane change events, and different scenarios may prompt the drivers to complete the lane change faster or slower. Therefore, our algorithm for finding the start of steering maneuver must be dynamic and capable of adapting to each lane change event.

Our solution to developing an adaptive steering maneuver detection algorithm is based on the idea that if we observe the driver's "normal" lane keeping behavior for a period of time, then we may be able to detect when driver lane keeping behavior falls outside of what is "normal" for each specific event. We defined normal driving behavior in this study using a technique adapted from Fujishiro and Takahashi [138]. Figure 57 shows an example from the Fujishiro and Takahashi study, in which driver lane keeping behavior was characterized as a function of distance to lane boundary and later velocity. In the Fujishiro and Takahashi study, a bivariate normal distribution was constructed using the DTLB and lateral velocity time series data, and normal driving behavior was defined as any data within the contour line representing 99% probability, as shown by the magenta circle.

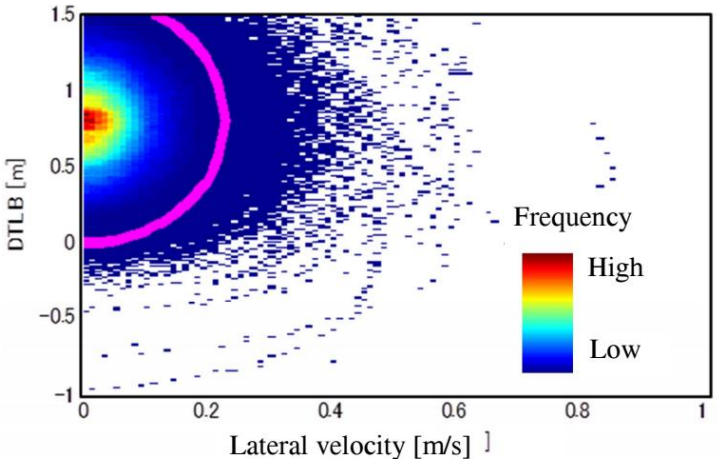

Figure 57. Lateral Velocity and Distance to Lane Boundary (DTLB) Distribution from Fujishiro and Takahashi [138] **(Reproduced with Permission from Authors)**

6.2.2 BIVARIATE NORMAL DISTRIBUTION

The bivariate normal distribution is an extension of the univariate normal distribution. Similar to univariate normal distribution, the bivariate extension computes the probability distribution as a function of two variables, and has probability of density function of the following form:

$$f(x,y) = \frac{1}{2\pi\sigma_x\sigma_y\sqrt{1-\rho^2}}\exp(-\frac{1}{2}Q(x,y)) \qquad \textbf{Equation 29}$$

where the function Q takes the form:

$$Q(x,y) = \frac{1}{1-\rho^2}[(\frac{x-\mu_x}{\sigma_x})^2 + (\frac{y-\mu_y}{\sigma_y})^2 - 2\rho\frac{(x-\mu_x)(y-\mu_y)}{\sigma_x\sigma_y}] \qquad \textbf{Equation 30}$$

The parameters σ_x σ_y and μ_x μ_y represents the standard deviation and mean of the variable x and y, respectively. The parameter ρ is the population correlation coefficient, which measures the dependence of two variables and is computed based on the covariance of the variables x and y and their respective standard deviation, as shown in Equation 31.

$$\rho(x,y) = \frac{COV(x,y)}{\sigma_x\sigma_y} \qquad \textbf{Equation 31}$$

The probability of each x and y combination is calculated by taking a surface integral of Equation 31, as shown in Equation 32. Lastly, the desired contour boundary is determined by finding x and y values of the same probability.

$$P(x,y) = \iint_s f(x,y)dS \qquad \textbf{Equation 32}$$

6.2.3 STEERING MANEUVER DETECTION ALGORITHM

The steering maneuver detection algorithm follows the 3 steps shown in Figure 58. For each lane change event identified in Chapter 4, the current algorithm first extracts the lane change start time and lane change end time, as shown in Figure 58 (a). The lane change start time identified in the old method refers to the time when vehicle's leading edge first crosses the lane edge, as shown in Figure 58 (a).

The next step of the algorithm takes available time series data from 60 seconds before vehicle lane crossing to 5 seconds before vehicle lane crossing and models normal driver lane keeping behavior by DTLB and lateral velocity, as shown in Figure 58 (b). Similar to the Fujishiro and Takahashi study, we defined normal driving behavior by creating a bivariate normal distribution of

the DTLB and lateral velocity data prior to vehicle lane crossing and an associated 95% probability contour line. If the lane change event occurred less than 60 seconds from the start of the trip, then the algorithm utilizes any available data to model normal driving behavior, if the lane change event occurred less than 5 seconds from the start of the trip, then the particular event is omitted from the analysis, as not enough data is available to model driver lane keeping behavior. Lastly, if the prior lane change event occurred within 60 second of the current event, the algorithm only uses the available data after the last lane change event to characterize lane keeping behavior for the current event.

The last step of the algorithm, shown in Figure 58 (c), takes the available time series data from 5 seconds before vehicle lane crossing to time of vehicle lane crossing to determine the earliest time point at which the lane keeping behavior is outside of the 95% boundary established in step (b). The process shown in Figure 58 was repeated for each lane change event to create a unique "normal" lane keeping threshold for each event.

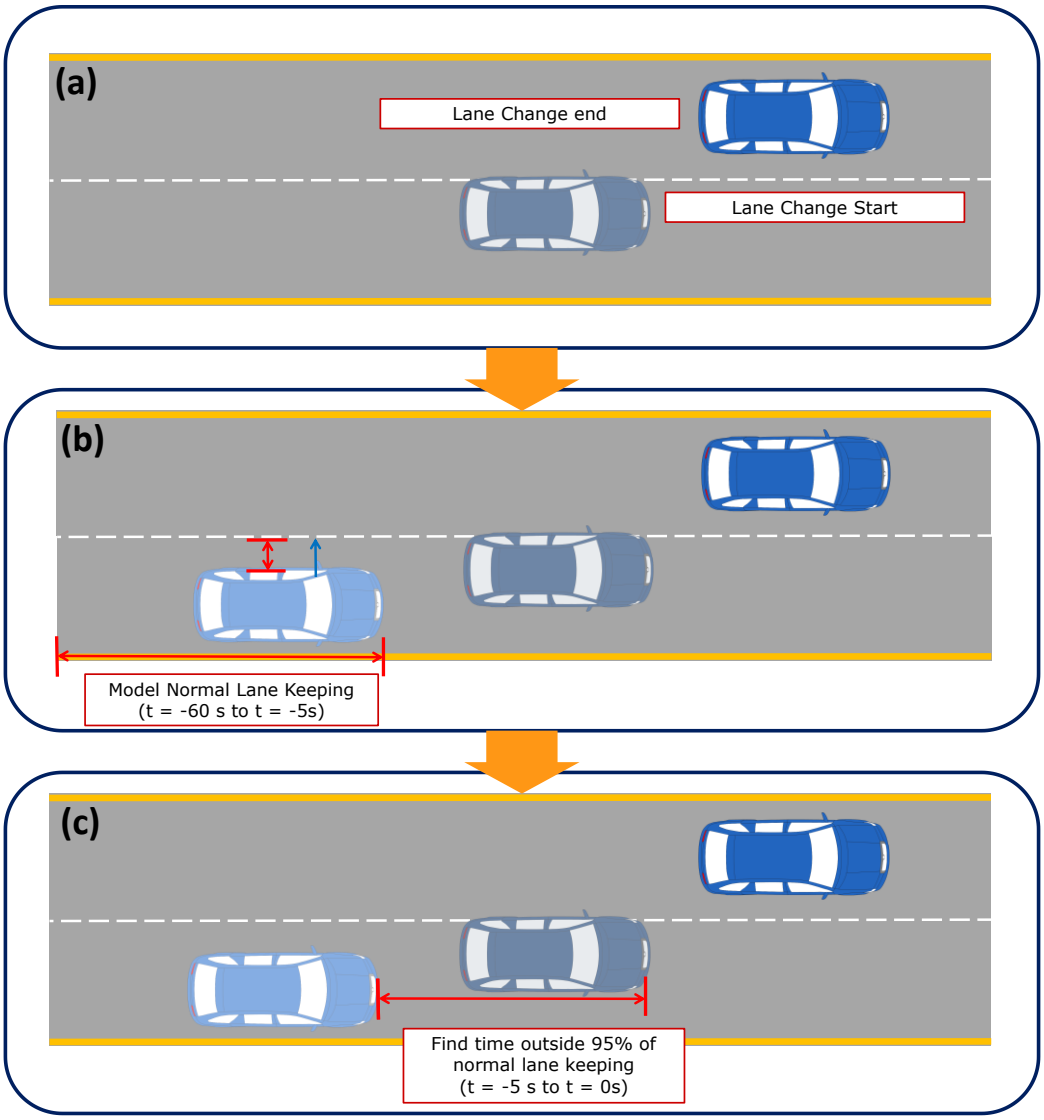

Figure 58. Steering Maneuver Detection Algorithm Procedure

6.2.4 Data Signal Processing

In order to select only the reliable lane tracking data, the following selection criteria were enforced:

- Lane tracking confidence > 30%
- Lane tracking reports positive lane width
- Exclude potential outliers by Cook's Distance

The 100-Car NDS provides confidence levels for both left and right lanes in the on-board lane tracking software. For the current study, in order to include sufficient data to model normal lane keeping behavior while retaining reasonable data quality, we required greater than 30% lane tracking confidence and positive lane width for all data points included in the analysis.

After filtering out the unreliable lane tracking data points, we created a multilinear regression model based the remaining DTLB and lateral velocity data and calculated the Cook's Distance for each data point. Cook's Distance measures the influence of each point on the regression model if the data point was excluded from the model, higher Cook's Distance indicates significant influence on the regression and be used to identify potential outliers. Previous studies have utilized Cook's Distance greater than 3 times the average Cook's Distance of the sample as an indication of outlier [139]. The following study excludes data points with Cook's Distance that are greater than 5 times the average Cook's Distance in order to exclude extreme data points and retain sufficient information.

6.2.5 ALGORITHM VALIDATION

In order to validate the results reported by our algorithm, we compared the algorithm results to manual inspection of video footage of selected lane change events in the 100-Car NDS.

A total of 131 randomly selected lane change events from 112 trips were extracted as the validation sample. For each lane change event, the undergraduate intern in our lab group reviewed the over-the-shoulder camera view in VTTI's secure enclave to determine the time stamp when the driver begins to initiate steering maneuver. In certain low lighting lane change events, such as nighttime or shadows created by nearby objects, time of steering initiation could not be determined by manual inspection, and therefore was not included in the validation sample.

Figure 59. Algorithm Validation with Manual Video Review

6.2.6 RESULTS

6.2.6.1 Algorithm Validation

Figure 60 shows the comparison of lead time as estimated by the algorithm and as observed by video review. In this comparison, lead time is defined as the time from start of steering maneuver and first vehicle lane crossing, as shown in Figure 61.

The cumulative distribution of lead time compares the result from visual inspection validation sample and the algorithm results from the same events. Only 66 events of the 131 events from the validation sample included sufficient data to estimate start of steering maneuver. As shown in Figure 60, the medium lead time based on validation data is approximately 1.6 seconds, while the median lead time based on algorithm results was approximately 0.8 seconds. Both the validation results and the algorithm results shows that all lead time in the sample were less than 5 seconds.

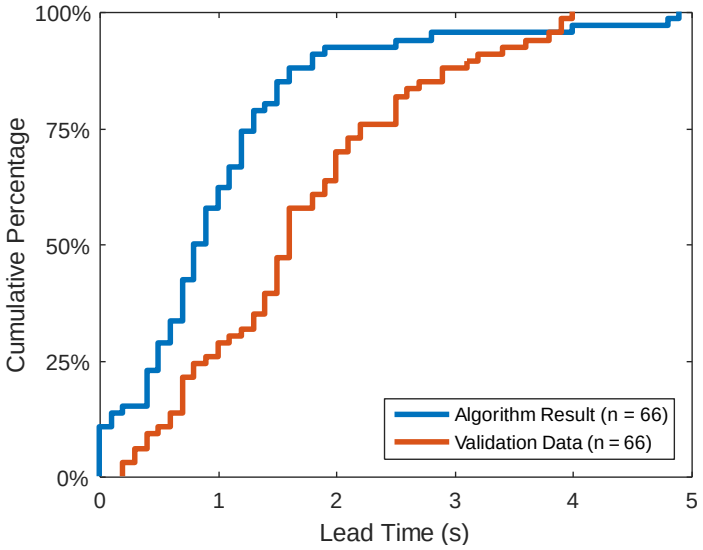

Figure 60. Cumulative Distribution of Lead Time

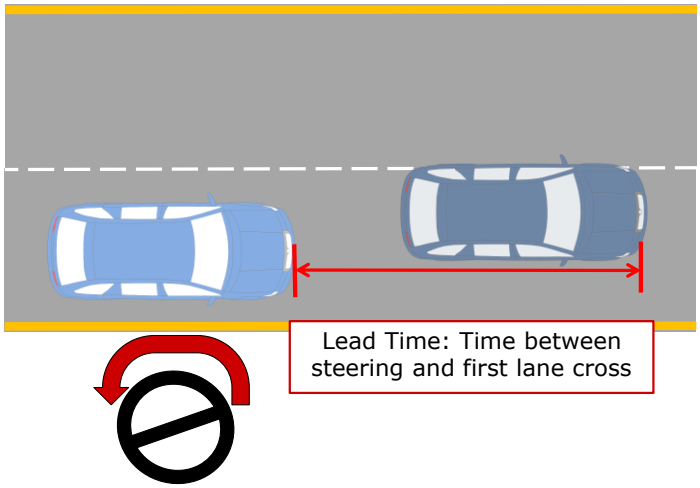

Figure 61. Definition of Lead Time

The next step was to determine the boundary between normal lane-keeping and start of the lane change. We assumed that a bivariate normal distribution which captures 95% of the normal lane-keeping behavior to be the boundary between normal lane-keeping and lane change initiation. Figure 62 shows the average percentage error of lead time for each confidence interval. Average percentage error is computed as the average of the percentage error, calculated as shown in Equation

33, of all events in the validation sample. As shown in Figure 62, confidence interval of 95% produces the lowest average percentage error of 17%.

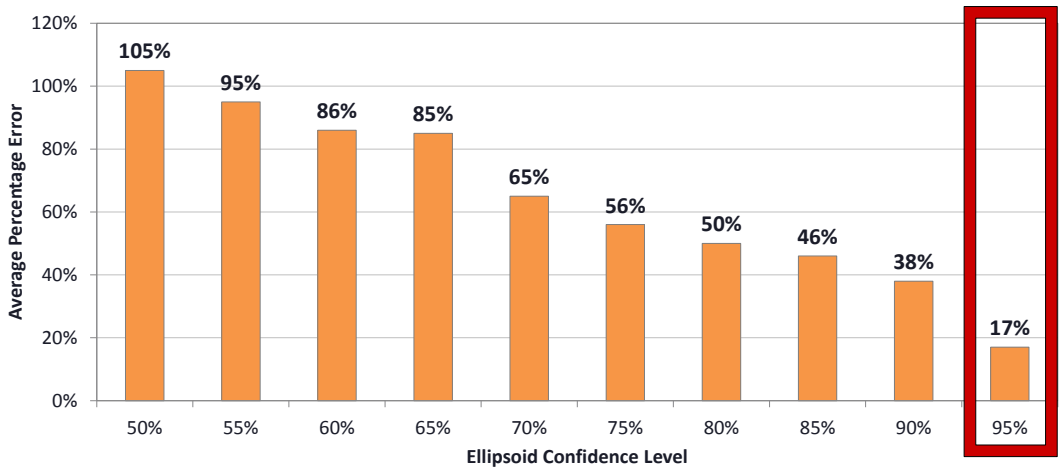

Figure 62. Sensitivity Analysis of Confidence Interval

$$Percentage\,Error = \frac{|\,Leadtime_{algorithmm} - Leadtime_{validation}\,|}{Leadtime_{validation}} \qquad \textbf{Equation 33}$$

6.2.6.2 Sample Algorithm Result

Figure 63 shows the steering maneuver detection algorithm performance on a sample trip. The horizontal axis shows the vehicle lateral velocity and the vertical axis shows the distance past edge, or DTLB. The red circle represents the data points used in modeling normal lane keeping behavior, the blue ellipse represents the boundary which captures 95% of the normal lane-keeping behavior, and the blue cross represents the data 5 seconds prior to lane crossing used to determine the start of steering maneuver. The yellow arrow in Figure 63 shows the time progression of driver initiating the lane change maneuver.

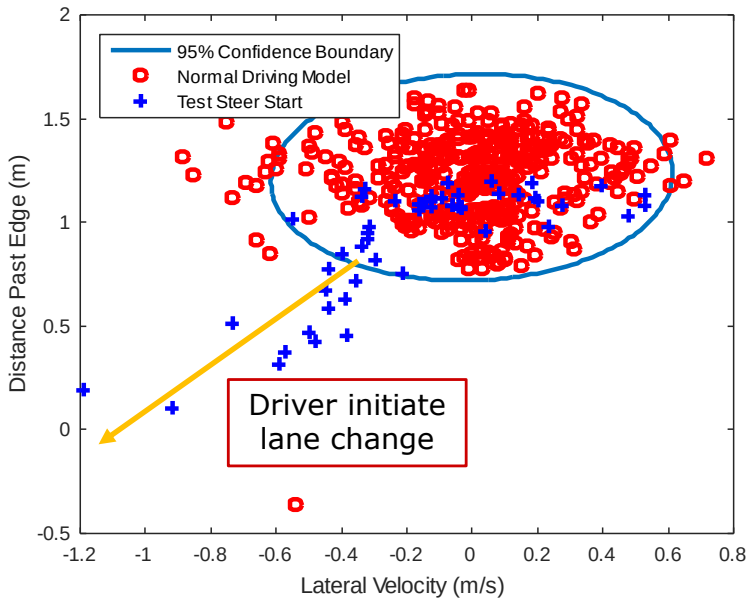

Figure 63. Sample Validation Result

Figure 64 and Figure 65 shows the DTLB and lateral distance for the sample event shown in Figure 63. The orange line in the figure shows the time when the algorithm determined that the data is outside of the normal lane-keeping boundary, while the yellow line in the figure shows when the visual inspection indicated that the driver begin to initiate the steering maneuver. As shown in the figures, the difference in the time of steering maneuver initiation between the algorithm and the visual inspection was approximately 0.2 seconds.

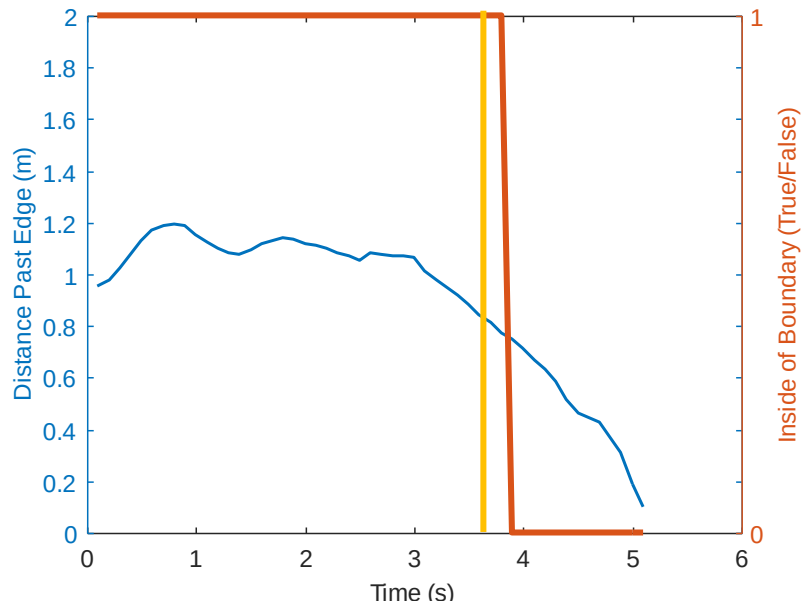

Figure 64. Sample Event Distance Past Edge

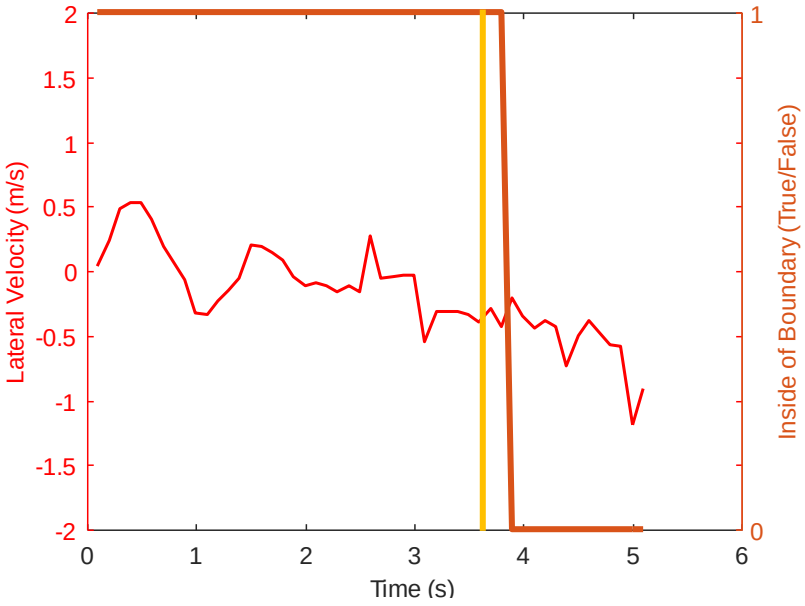

Figure 65. Sample Event Lateral Velocity

6.2.6.3 Dataset Composition

Table 26 shows the dataset composition of the lane change events with steering time and lead vehicle. A total of 326,238 lane change events were identified in the study "Driver Behavior during Overtaking Maneuvers in Car Following", presented in Chapter4. Using the steering maneuver detection algorithm, we were able to compute steering initiation time for 55,144 of the previously identified lane change events, and 53,615 lane change events had both a valid steering initiation time and lead vehicle data. The following results characterizes driver lane change behavior based on the 53,615 lane change events with both steering initiation time and lead vehicle.

Table 26. Dataset Composition

Group	Drivers	Trips	Number of Lane Change Events
Trips with Lane Change Events	45	32,350	326,238
Lane Changes with Steering Initiation Time	32	15,369	55,144
Lane Changes with Steering Time and Lead Vehicle	32	15,187	53,615

6.2.6.4 Distribution of Lead Time

Figure 66 shows the cumulative distribution of lead time between steering start and lane edge crossing. An illustration of lead time can be found in Figure 61. As shown in Figure 66, the median lead time in the population of lane change was approximately 1 second.

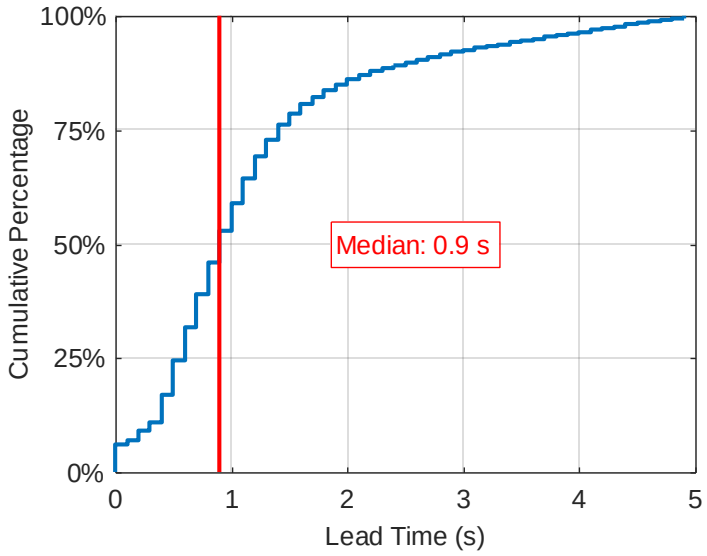

Figure 66. Cumulative Distribution of Lead Time

6.2.6.5 Driver Lane Change Behavior at Start of Steering

Figure 67 shows the distribution of 10th percentile ETTC at the start of steering maneuver as a function of vehicle speed. Vehicle speed was divided into 8 10 mph bins. For each driver, we extracted lane change events with closing ETTC for each speed bin, and plotted the ETTC and the respective vehicle speed. The solid black line shows the median ETTC of the population, similarly the dashed black line shows the 10th percentile of the population ETTC.

Figure 67 shows that, as vehicle speed increased, the median and the 10th percentile population ETTC at the start of the steering maneuver generally increases with vehicle speed. Figure 67 also shows the number of drivers included in each speed bin (ex. N = 31 in the 60-70 mph bin). Due to the relatively low percent of lane change at high speeds, not all drivers had lane changes with a closing lead vehicle in the >80 mph speed range.

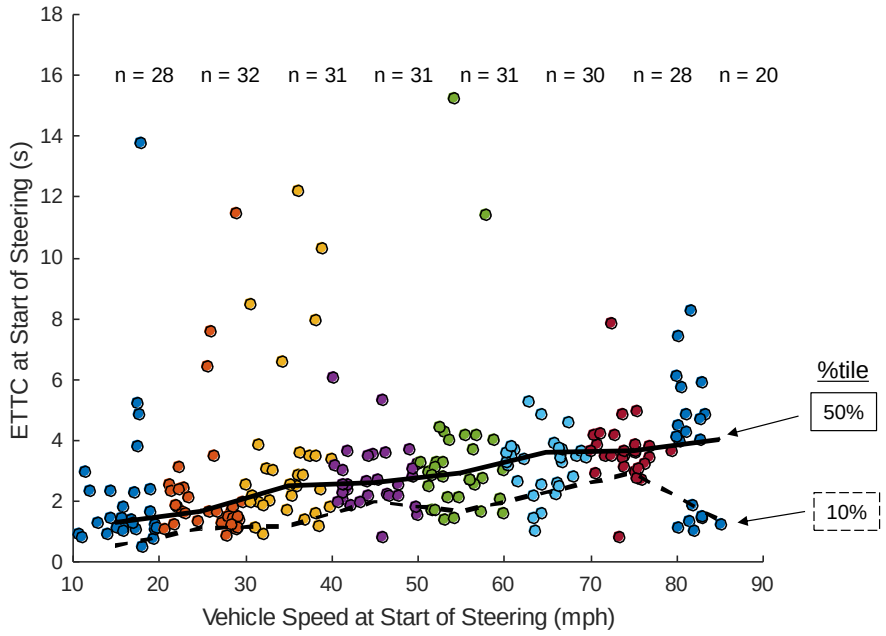

Figure 67. Distribution of 10th Percentile ETTC at Start of Steering Maneuver

Similarly, Figure 68 shows the distribution of 10th percentile TTC at the start of steering maneuver as a function of vehicle speed. In general, the TTC distribution shows higher population median and 10th percentile as compared to the ETTC distribution. The number of drivers which were included in each speed bin is slightly different between the TTC and ETTC distribution. The difference in the number of drivers was due to the fact that ETTC calculation considers relative acceleration, and the same event may be considered to be a closing event by ETTC but not TTC.

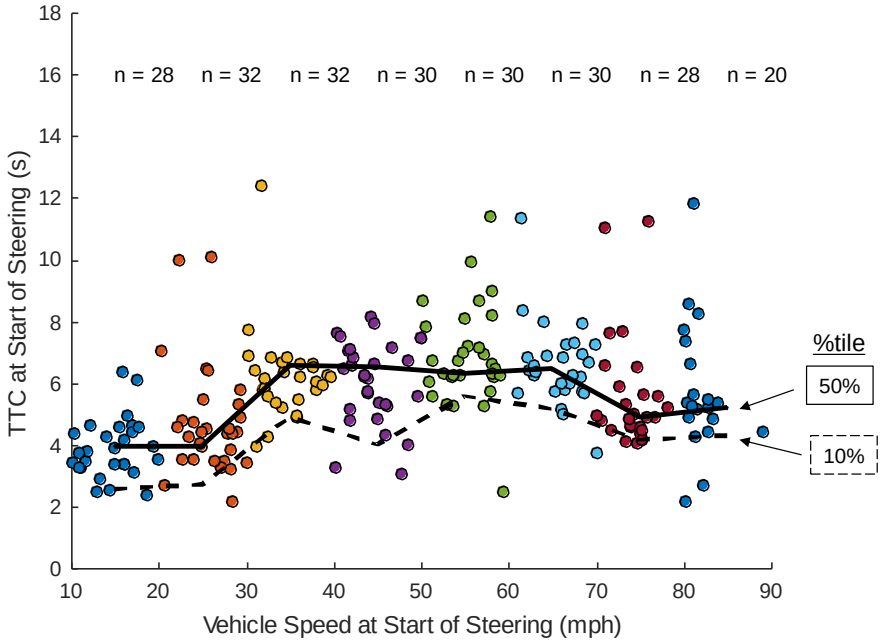

Figure 68. Distribution of 10th Percentile TTC at Start of Steering Maneuver

Figure 69 shows the distribution of relative velocity corresponding to each 10th percentile driver ETTC. For each data point in Figure 67, Figure 69 shows the relative velocity at the time of steering initiation and the corresponding ETTC.

As shown in Figure 69, the majority of the lane change events corresponding to 10th percentile ETTC occur with relative velocity lower than 5 m/s (~11 mph). However, in one events, relative velocity was 25 m/s (~56 mph), while the ETTC value was only 2.5 seconds.

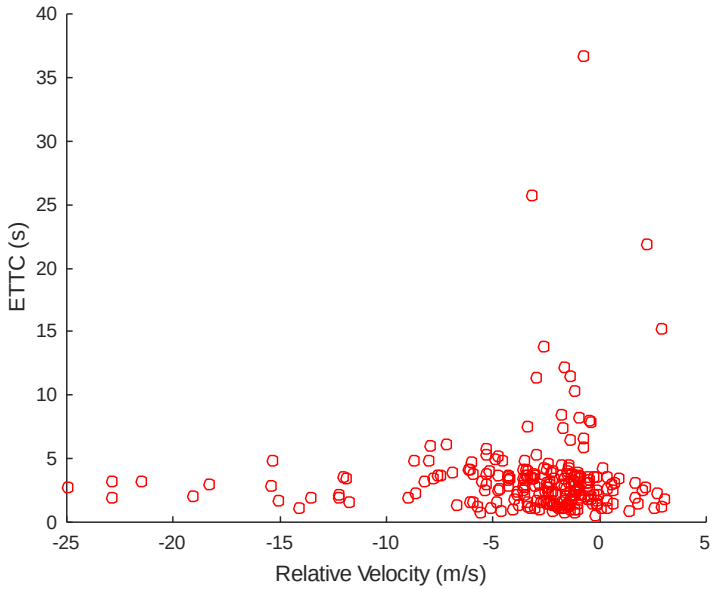

Figure 69. Distribution of Relative Velocity and ETTC at Start of Steering in 10th Percentile ETTC Lane Change Events

Overtaking events with large relative velocity and small ETTC values are especially concerning for FCW systems due to the potential of falsely triggering the warning. We further investigated the events with large relative velocities by examining the relative distance between the vehicles at the start of steering maneuver. Figure 70 shows the distribution of distance and relative velocity at the time of steering initiation. The result from the distribution of distance shows that in overtaking events, the relative distance generally increases with relative velocity. For the event with relative velocity of 25 m/s, the distance between the vehicles was approximately 70 m.

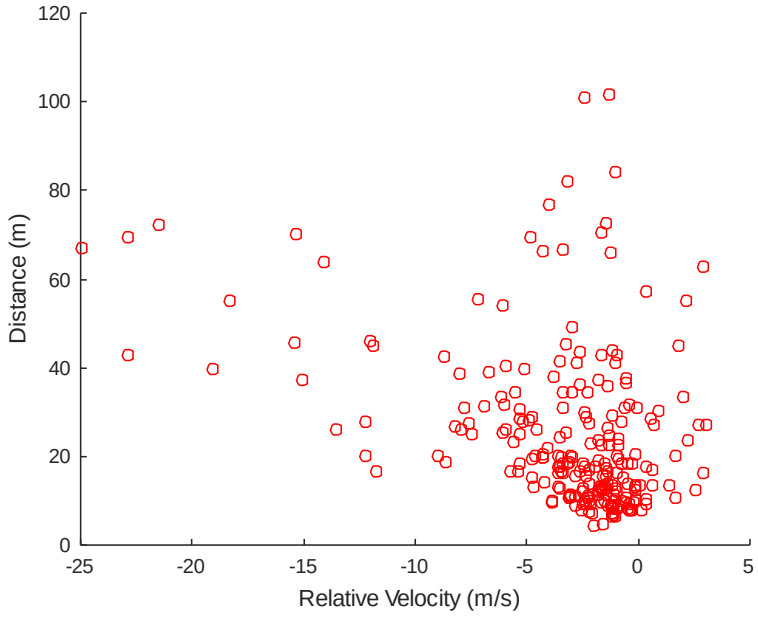

Figure 70. Distribution of Relative Velocity and Distance at Start of Steering in 10th Percentile ETTC Lane Change Events

6.2.6.6 Probability Distribution of ETTC and TTC

In addition to calculating the 10th percentile ETTC and TTC, we also constructed probability distribution for the population ETTC and TTC values. Using a method described in Chapter 3.1, the general extreme value (GEV) distribution was selected as the best fit probability density function to characterize the distribution.

Figure 71 and Figure 72 show the GEV distribution of ETTC and TTC at the start of steering maneuver. The distributions were computed separately for each 10 mph vehicle speed. For each vehicle speed bin, the GEV distribution provides continuous probability of steering initiation with respect to ETTC and TTC.

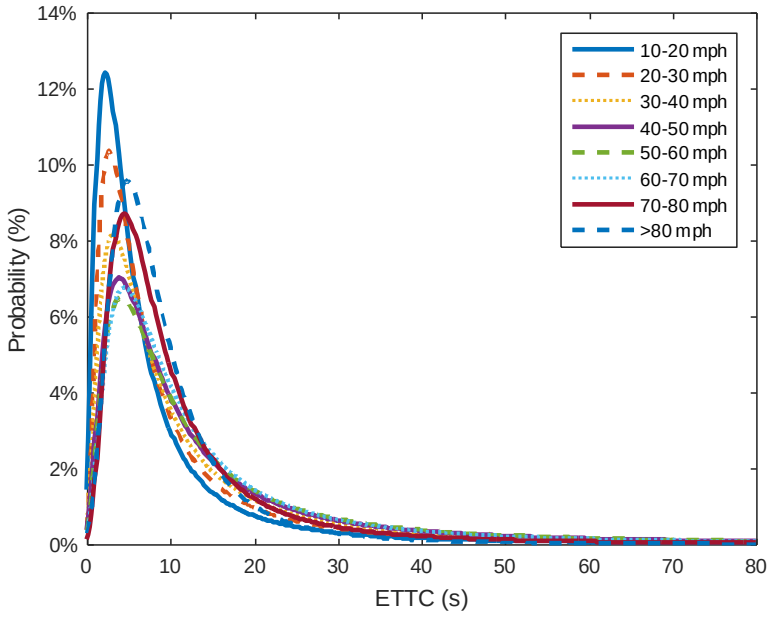

Figure 71. GEV Distribution of ETTC at Start of Steering Maneuver

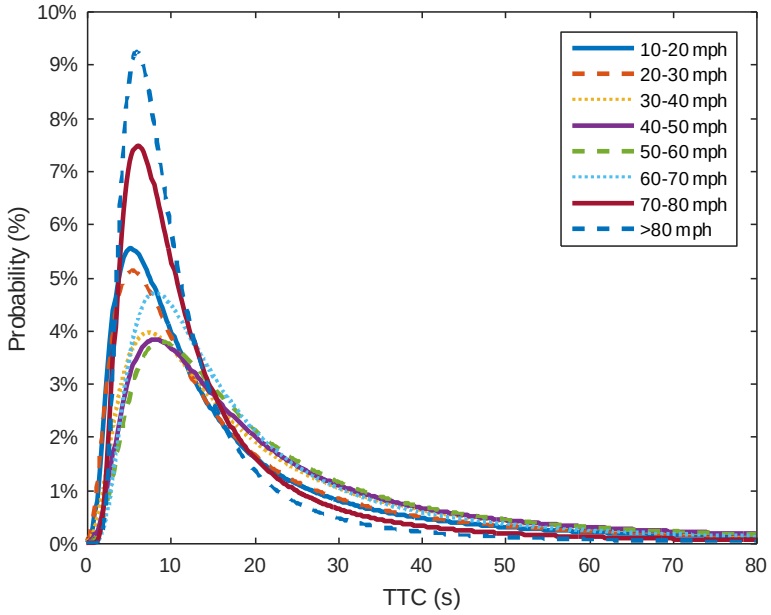

Figure 72. GEV Distribution of TTC at Start of Steering Maneuver

6.2.6.7 Comparison of Driver Behavior at Lane Crossing and Steering Initiation

The GEV distributions shown in Figure 71 and Figure 72 can also be characterized by their mode, or the ETTC or TTC values corresponding to the maximum probability in each distribution. Figure 73 shows the modes of GEV distributions of ETTC values at the start of steering and start of lane crossing. GEV distributions were constructed for ETTC at the start of lane crossing.

The comparison of GEV distributions modes between the start of lane crossing and start of steering shows that the modes of the ETTC distributions are higher at the start of steering for all speed ranges, and the modes generally increase with vehicle speed.

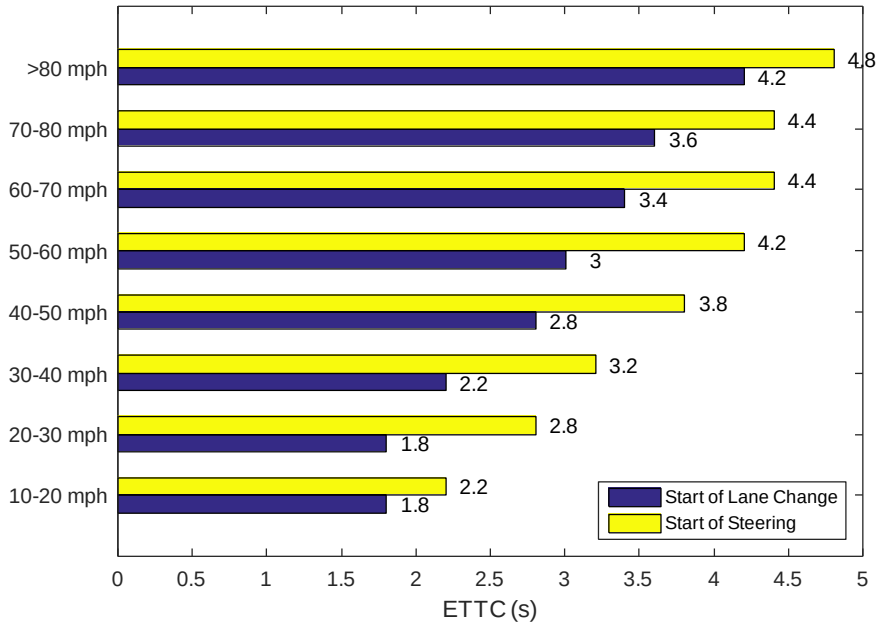

Figure 73. Comparison Modes of GEV Distributions for ETTC in Lane Change

Similarly, Figure 74 shows the comparison of GEV distributions of TTC values at the start of steering and start of lane crossing. Similar to the ETTC distributions, shown in Figure 73, modes of GEV distributions for TTC at the start of steering were higher at the start of steering as compared to the start of lane crossing for all speed ranges. However, modes of GEV distribution for TTC values do not show a continuous increase with respect to speed.

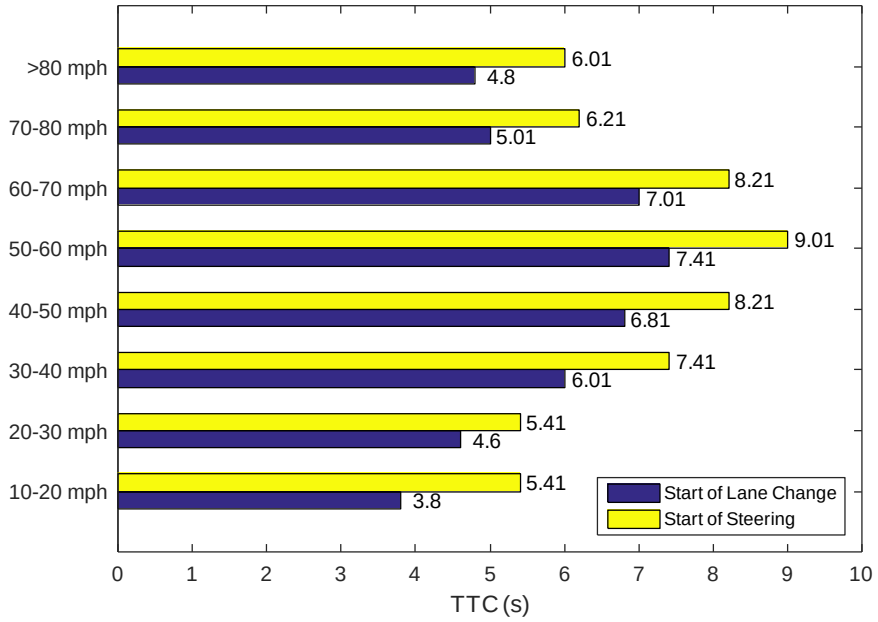

Figure 74. Comparison Modes of GEV Distributions for TTC in Lane Change

6.3 Conclusion and Discussion

The overall objective of the current study was to extract time of steering initiation for all previously identified lane change events, and to characterize driver lane change behavior at start of lane change by TTC and ETTC. In the current study, we developed a methodology to extract start of steering maneuver for lane change events previously identified in Chapter 4. The current study improves the estimation of start of lane change, by using start of steering maneuver as the beginning of the lane change event. The overall approach in the methodology was to model the normal lane keeping behavior using the distance to lane boundary and lateral velocity of the vehicle prior to the lane change event, and start of steering maneuver was estimated as the first time when driver lane keeping behavior reaches outside 95% of normal lane keeping behavior.

The results of the algorithm were validated against manual video inspection of 131 randomly selected lane change events. During the manual inspection, the researcher review of the over-the-shoulder camera view to determine when the driver initiated the steering maneuver during the lane

change. In certain low light lane change events, such as night time driving or shadows casted over the driver, time of steering maneuver could not be determined.

The comparison of lead time, or the time between the start of the steering maneuver and the vehicle crossing the lane edge, showed that the median lead time for the algorithm was approximately 0.8 seconds shorter than the lead time reported by visual inspection. We hypothesize that the difference in lead time is largely due to the play in the steering wheel and the fact that vehicles do not immediately respond to steering wheel input. In addition, lead time was less than 5 seconds for all lane change events in the validation sample, suggesting that detecting steering wheel input within 5 seconds prior to lane crossing was a reasonable assumption in our algorithm.

The algorithm validation sample was also utilized in a sensitivity analysis of the confidence interval. Confidence intervals between 50% and 95% was selected to represent normal lane keeping behavior, and the performance of the algorithm was compared against the results from the manual inspection. According to the average percentage error of lead time between the algorithm output and the manual inspection, a 95% confidence level best described the normal lane keeping behavior in our algorithm, and was therefore selected in the final methodology.

A total of 326,238 lane change events were previously identified in "Driver Behavior during Overtaking Maneuvers in Car Following". Using the steering maneuver detection algorithm, we were able to compute steering initiation time for 55,144 of the previously identified lane change events, and 53,615 lane change events had both a valid steering initiation time and lead vehicle data. The large number of reduction in lane change events is largely due to the unavailable or unreliable lane tracking information. In most rural or suburban driving environments, lane lines are poorly marked or not available, therefore our algorithm did not have sufficient information to model normal driver lane keeping behavior.

The distribution of lead time, or the time between steering initiation and first lane crossing, was approximately 1 second. In approximately 5% of the events, the lead time identified by the algorithm was 0, suggesting that in a small percentage of events, driver are very close to the target lane when they initiate the lane change maneuver. For all lane change events, the result of the algorithm shows that drivers begin steering maneuver for a lane change within 5 seconds of the vehicle crossing the lane. This shows that, in certain cases, we can potentially detect drivers' intent to change lanes as far as 5 seconds in advance.

The distribution of 10^{th} percentile ETTC at the start of steering maneuver shows that the population median generally increases with vehicle speed. In other words, driver generally have higher ETTC at the start of lane change events with higher vehicle speed, suggesting that drivers are becoming more cautious and leaving more space during lane change events. However, in a small number of events, driver had ETTC of nearly 1 second while the vehicle speed was greater than 40 mph.

We further investigated these events by calculating the distribution of relative speed and range between vehicles at the start of the steering maneuver. The result shows that events with small ETTC are generally associated with low relative speed, indicating that drivers are maintaining similar speed as the lead vehicle during overtaking maneuvers. In several events, the relative speed was positive, indicating that the following vehicle was traveling at a slower speed than the lead vehicle, and accelerating to overtake the lead vehicle.

Lastly, probability distribution was generated for the population of ETTC and TTC values using the general extreme value distribution. The modes, or peaks of the probability distributions, shows that ETTC generally increase with vehicle speed. The comparison of modes of probability distribution shows drivers have higher ETTC at the start of steering maneuver than the first lane

cross. This suggests that drivers generally decrease the following distance between vehicles as the overtake maneuver progresses.

In summary, the current study developed a valuable methodology to estimate the start of steering maneuver in lane change events in the 100-Car NDS. Steering input was not directly recorded in the 100-Car NDS, and the current method provides an important tool in improving driver lane change characterization, and the resultant characterization of lane change events at the start of steering improves the previous study using first lane cross as the start of steering maneuver.

7 CONCLUSIONS

The overall research objective of this dissertation was to characterize normal driver behavior in car following events. The dissertation presents the first large scale study of its kind, based on naturalistic driving data to report driver behavior during a variety of car-following events. The overall goal of this dissertation was to provide a better understanding of driver behavior in normal car-following driving conditions, which can benefit automakers who seek to improve FCAS effectiveness in rear impact avoidance, as well as regulatory agencies seeking to improve FCAS vehicle tests. Second 1 of this chapter summarizes the key points from the results of each study. The following sections details the discussion and conclusion from each chapter of the dissertation.

7.1 KEY POINTS

The key points from each study presented in this dissertation are summarized in the following chapter.

7.1.1 COMPARISON OF TTC AND ETTC

- Distribution of minimum TTC and ETTC generally increase with increasing vehicle speed
- Between drivers variability in the distribution of minimum TTC are generally greater than that of the minimum ETTC distribution
- Only about 1/3 of all braking events had zero relative acceleration.
- General Extreme Value Distribution was found to be the best fit to describe both TTC and ETTC distribution

- Probability Distribution Model Parameters for ETTC Distribution

Speed Range (mph)	Distribution Name	Parameter Estimates		
		k	σ	μ
3-10	GEV	0.522	1.953	3.135
10-20	GEV	0.597	2.337	4.224
20-30	GEV	0.592	3.147	5.261
30-40	GEV	0.604	4.322	6.824
40-50	GEV	0.596	5.213	8.066
40-60	GEV	0.603	6.124	9.108
60-70	GEV	0.625	6.961	9.873
70-80	GEV	0.631	7.394	10.330
80+	GEV	0.514	7.134	10.277

- Probability Distribution Model Parameters for TTC Distribution

Speed Range (mph)	Distribution Name	Parameter Estimates		
		k	σ	μ
3-10	GEV	0.607	3.934	5.009
10-20	GEV	0.666	5.177	7.345
20-30	GEV	0.649	7.298	9.582
30-40	GEV	0.654	9.244	12.221
40-50	GEV	0.658	9.993	13.338
40-60	GEV	0.666	10.824	14.167
60-70	GEV	0.699	11.637	14.500
70-80	GEV	0.724	11.381	13.684
80+	GEV	0.569	9.533	12.558

- ETTC GEV Probability Model Characteristics

Speed Range (mph)	Mode (%)	Max ETTC (s)	10 %tile (s)	50 %tile (s)	90 %tile (s)
3-10	21.2	2.402	1.982	3.666	12.647
10-20	18.3	3.203	2.779	4.984	16.380
20-30	13.6	4.004	3.331	6.265	20.936
30-40	9.9	5.005	4.161	8.225	29.478
40-50	8.2	6.006	4.824	9.754	35.400
50-60	8.0	6.607	5.305	11.06	42.358
60-70	6.2	7.007	5.546	12.18	49.055
70-80	5.9	7.207	5.629	12.96	51.403
80+	5.8	7.608	5.621	12.56	43.213

- TTC GEV Probability Model Characteristics

Speed Range (mph)	Mode (%)	Max TTC (s)	10 %tile (s)	50 %tile (s)	90 %tile (s)
3-10	10.9	3.403	2.503	6.543	24.167
10-20	8.5	5.205	4.002	9.472	34.762
20-30	6.0	6.406	4.990	12.317	49.000
30-40	4.8	8.208	6.464	15.599	63.583
40-50	4.4	9.009	7.080	17.018	69.532
50-60	4.1	4.409	7.332	18.317	76.087
60-70	3.9	9.409	7.087	19.421	80.429
70-80	4.0	8.609	6.278	18.968	78.879
80+	4.4	8.809	6.171	16.340	58.664

7.1.2 AGE AND GENDER DIFFERENCES IN BRAKE PULSE IN CAR FOLLOWING

- The median braking duration in car-following was approximately 2.6 seconds. Approximately 20% of the braking events were found to be less than 1 second, and 90% of the braking events lasted less than 11 seconds.
- The median braking deceleration in car-following was approximately 0.08 g. In 90% of the braking events, the maximum braking deceleration was less than 0.2 g.
- The median change in vehicle velocity was approximately 4 mph. Approximately 20% of raking events in the sample had a change in vehicle speed of less than 1 mph.
- Mean Maximum Braking Deceleration for drivers of different age and gender groups

Groups	LS Mean Braking Force (g)
Novice (18-20)	0.084
Young (21-30)	0.093
Middle (31-50)	0.115
Mature (51+)	0.107
Male	0.093
Female	0.107

- Mean brake pulse shape (centroid location) between drivers of different age and gender groups

Groups	t_c/t_m
Novice(18-20)	0.542
Young (21-30)	0.529
Middle (31-50)	0.518
Mature (51+)	0.526
Male	0.538
Female	0.519

7.1.3 Effect of Percent Overlap on Car-following Behavior

- Full overlap were among the most frequent scenario during braking in car-following.
- Age group, time of day, day of week, and speed categories were significant factors in influencing driver braking behavior (TTC) at alpha = 0.05.
- No practical significance were detected in TTC between overlap categories.
- Marginal difference were detected in TTC between overlap categories at vehicle speeds of 20-30 mph.

7.1.4 Driver Behavior during Overtaking Maneuvers in Car-following

- Driver lane change in car-following was evenly distributed between left side and right side lane change (~50% left side lane change, ~50% right side lane change).
- Approximately 28% of lane change events in car-following had a closing lead vehicle.
- The median lane change frequency was approximately 0.2 lane changes per mile, or 1 lane change every 5 miles, for typical travel speeds between 20-70 mph. Almost no drivers initiated lane change at vehicle speeds above 80 mph.
- Minimum driver TTC in lane change increases with increasing vehicle speed, the variability between drivers also increase with increasing vehicle speed.

7.1.5 Comparison of TTC at Braking with TTC at Overtaking

- Relative frequency between braking and overtaking were found to change with respect to vehicle speed. For vehicle speeds less than 50 mph, nearly all drivers perform more braking than lane change maneuvers. As the speed increases, drivers begin to change lanes for frequently. 30% of the drivers change lanes more than they brake at speeds greater than 70 mph.
- Each driver's lane change and braking characteristic was characterized using a Generalized Extreme Value distribution and presented in the Appendix.

7.1.6 Distributing of TTC and ETTC at Start of Steering during Overtaking

- Drivers were found to start initiating steering within 5 seconds of crossing the lane line in lane change events.
- Drivers were shown to have higher TTC and ETTC at the start of the steering maneuver as compared to the time of first lane crossing. In other words, drivers generally decrease the following distance between vehicles as the overtake maneuver progresses.

7.2 Comparison of TTC and ETTC during Normal Driving

The objective of this study was to calculate the ETTC for all braking events with a lead vehicle in the 100-Car NDS. In addition, we determined the probability distribution functions which best fit both samples of ETTC and TTC. The model selection criterion was based upon AIC and BIC.

This study was based on a total of number of 64 drivers which had sufficient valid sensor data to be included, resulting in a total of 72,380 trips with 609,620 miles of travel in the study. A total of 1,682,093 braking events with a valid lead vehicle were identified using the automated search algorithm. Using TTC as a metric, 985,259 of the braking events were identified as having a closing

lead vehicle. Using ETTC as a metric, a total of 876,619 of the braking events were identifed as having a closing lead vehicle.

The braking events with a closing lead vehicle identified by ETTC and TTC were used to compute the 10th percentile ETTC and TTC values for each driver. The ETTC and TTC distributions both increased with vehicle speed. The variance of both distributions also increase with vehicle speed. However, the median and 10th percentile across all drivers was higher for TTC values than ETTC values. In addition, the variance for drivers within each speed range was also higher for TTC values than ETTC values.

The result of the relative acceleration distribution shows that only 1/3 of the braking events had zero relative acceleration. Approximately 65% of the braking events contained positive relative acceleration, indicating increasing closing speed and resulting in lower time remaining until collision than considering relative velocity alone. The result shows that the addition of relative acceleration in the ETTC calculation provides a more accurate measurement of time remaining until collision.

The generalized extreme value model was found to be the best fit distribution for both ETTC and TTC values based on AIC and BIC score. The distribution fits showed close correlation with the underlying data. Probability density distribution of ETTC showed a higher peak probability, or mode, than TTC. The higher mode was evident across all speed ranges.

In summary, this study compared ETTC and TTC as metrics of characterizing driver braking behavior in car following. ETTC possesses an advantage over TTC by incorporating relative acceleration in calculating the time to collision. The results of this study shows that ETTC distributions have lower variance between drivers across all vehicle speed ranges. In addition, we found that both distributions of ETTC and TTC can be represented by a GEV distribution. The distributions provides the probability of occurrence across a range of continuous ETTC and TTC values. The results from this study provides a better understanding of driver behavior in car

following events, and can be used to improve various driver models, such as normal braking time threshold, and driver perception of risk in car following events.

7.3 Age and Gender Difference in Braking Behavior during Car Following

This study has examined the braking behavior difference in driver age and gender demographic groups. The study shows that for braking events with a lead vehicle, driver braking deceleration and brake pulse is influenced by driver age and gender, as well as the traffic context, such as current vehicle speed and TTC with the lead vehicle.

The study also shows that, as driver age increases, the maximum braking deceleration increases. A marginal difference in braking deceleration between male and female drivers was also detected in the results. Using a linear regression model which controlled for vehicle speed and TTC, the difference between age and gender effect on braking was shown to be statistically significant.

Similarly, the study shows that driver brake pulse varies with the driver demographic and driving context. For all age groups, the maximum braking deceleration decreases as vehicle speed increases. On the other hand, brake pulse were shown to shift towards "rear load" as vehicle speed increases. The shift was not observed in mature drivers, who were shown to "front load" the brakes as vehicle speed increase.

One of the limitations of the study was that the results were based on normal driving data. It is possible that driver braking behavior is entirely different in crash imminent situations, therefore we cannot extend the conclusions from this study to crash imminent situations. In addition, information regarding cruise control activation was not available at the time of the study, which may help distinguish drivers' intention to cancel cruise control from crash avoidance braking. Nevertheless, the results from this study provides an good approximation of driver brake pulses in normal driving, and can still illustrate the differences in braking deceleration across the demographic groups.

The current study shows that there is a clear difference in brake pulse between drivers of different age group and gender. The results of this study can help provide a better understanding of driver braking patterns in normal driving. The results of this study can support future automated braking systems and autonomous vehicle designers to better adapt vehicle driving behavior to be more human-like.

7.4 Effect of Percent Overlap on Car-Following Behavior

The results of this study show that driving context significantly affects driver braking behavior during car following. Forward crash avoidance systems such as FCW may better match a drivers' expectations if it adapts its warning times to both the driver and the driving context. This adaptation may be possible by utilizing current on-vehicle sensors, such as navigations systems, ambient light sensors, radar, cameras, and vehicle speed sensors. In addition, the result of the study shows that overlap percentage may potentially effect driver braking behavior at vehicle speeds lower than 30 mph. One example scenario, in which overlap percentage may influence driver braking behavior, is of the lead vehicle suddenly change lane to move in front of the instrumented vehicle. In this scenario, the driver may not have sufficient time to prepare, and may be forced to brake later than usual. Future active safety system and autonomous vehicle systems should consider monitoring nearby vehicle lane keeping behavior, using the method presented in this dissertation, and overlap percentage to prepare for instance of small overlap events which drivers may not be prepared for.

This study has several important limitations. First, the 100-Car NDS data was not linked to roadway data. Previous characterizations of driving behavior using NDS data have found that speeding was a significant indicator of crash risk. This study did not have access to the speed limits on the roads and thus could not assess whether drivers were speeding. The analysis in this study could be improved if NDS data with linked roadway data were available.

Second, the method utilized in the current study utilizes a constant track width, based on average track width of passenger cars, for all lead vehicles. This assumption do not accurately portrait the range of vehicles present on the roadway. Furthermore, the resolution of the video in the 100-Car study limits the use of machine vision video analysis and manual video review to determine the accurate track width of the lead vehicle. Future studies may consider using an updated database with improved video quality, such as the SHRP-2 NDS study, to improve the estimation of percentage overlap.

Third, the radar utilized in the 100-Car NDS is limited to ±7 degree azimuth, limiting the range which the radar can potentially "see" lead vehicles. In other words, there are potentially braking events with a lead vehicle present, however the overlap of the lead vehicle was small enough to be outside of the field of view of the radar, and therefore was not correctly identified and included in the analysis.

Lastly, the statistical methodology used for this study aggregated all brake applications during driving context scenarios and took the minimum TTC during each scenario. This aggregation assumes a true minimum that is characteristic of the driver's normal behavior was experienced during each scenario. We observed that if very few brake applications were collected at a given scenario that large variability could be introduced into the results. Typically those scenarios with few brake applications had extremely high TTC, i.e., greater than 20 s. Scenarios with less than 5 brake applications were excluded to attempted to minimize this variability but at the expense of potentially biasing the results. A possible solution to this challenge would be to use a statistical methodology that uses all the recorded braking data instead of aggregating by scenario.

This study presents a method of estimating percentage overlap in braking events using only vehicle radar sensors. The result from the study shows that in small overlap scenarios during braking events, drivers may delay brake application and create potential near-crash or even crash scenarios.

Future active safety systems, therefore, should consider methods of monitoring nearby vehicles to prepare for scenarios such as lead vehicle cut in to assist drivers in avoiding potential crashes.

7.5 Driver Behavior during Overtaking Maneuvers in Car Following

The objective of this study was to aid FCW design by characterizing driver behavior during overtaking events. This study presented a methodology to detect lane change events and a methodology to identify lead vehicle in lane change events in the 100-Car NDS. The performance of these two algorithms was validated against 126 trips, in which the researchers manually examined the video footage to determine the time frame of lane change and lead vehicle presence. Finally these algorithms were applied to the 100-Car NDS dataset to obtain the distribution of TTC at lane change with a lead vehicle in front of the subject car.

In 126 randomly selected validation trips, the researcher manually reviewed the trip videos and identified 1,425 lane change events. Within the sample of manually identified lane change events, 420 events were found to be overtaking events, in which the video showed a driver passing a lead vehicle. A total of 439 merging lane changes were found in the sample, in which a closing lead vehicle was present in about 42% of the merging events. For lane change events other than overtaking and merging (566 events), a closing lead vehicle was present in 37% of these events. Overall, the lane change detection algorithm performed very well. For lane changes with sufficient lane tracking information, the validation process showed that the automated lane change algorithm had a sensitivity of 0.87 and a specificity of 0.983. The lead vehicle identification algorithm also performed reasonably well, and correctly identified the car following situation in 84% of the validation sample of lane change events. Our lane change detection algorithm is highly dependent on the presence of lane markings, therefore our analysis was restricted to marked roadways. It is uncertain how our results may generalize to roads with poor lane markings.

A total of 326,238 lane change events were identified by the algorithm in 46,250 trips, totaling over 400,000 miles of driving. In addition, the breakdown of lane change frequency by speed bin also shows that drivers increase lane changes for travel speeds ranging from 10-50 mph. The lower lane change frequency in the lower speed range bins can potentially be due to several reasons. First, it is likely that lane change events in lower speed ranges (i.e. lower than 30 mph) were on roads with lower speed limits and were 2-lane roads with no adjacent lanes to change into. We also hypothesize that when drivers initiate lane change maneuvers in lower speed ranges, they were more likely to speed up and thus are grouped into higher speed bin ranges. An example scenario would be during congested traffic conditions in the Washington D.C. area, the instrumented vehicle was in a lane with slow moving traffic but sped up to change into the adjacent lane in order to move ahead of traffic.

The distribution of TTC showed that minimum TTC, as well as variability of TTC between drivers, generally increased with travel speed. The increase in TTC can be attributed to drivers generally becoming more cautious and increasing following distance as travel speed increases. As drivers begin to increase following distance, lead vehicles are more likely to be outside of the range of the front radar. Although our study was highly dependent on the radar to detect lead vehicle, therefore biased towards what the radar can "see", the results are still relevant in improving the effectiveness of a FCW system in a crash imminent situation.

The characterization of lane change events presented in the current study will provide active safety system designers with an enhanced understanding of driver action in overtaking maneuvers and can improve designs of FCW systems in several areas. First, the results of this study show that the frequency and TTC in lane change events vary by vehicle speed. This implies that the warning threshold for FCW systems needs to adapt to current vehicle speed. Second, the large variability in minimum TTC between drivers shows the need for FCW systems to implement several different

warning thresholds depending on different driving style. For example, FCW systems may give driver the option to select different warning settings for "aggressive" or "conservative" driving style.

7.6 Comparison of TTC at Braking with TTC at Overtaking

This study compared driver braking and lane change behavior in normal car-following events. The result of the study was based upon the 100-Car NDS and included 45 drivers and over 400,000 miles of driving data. Using an automated search algorithm, we first extracted all braking and lane change maneuvers from the dataset and characterized driver braking and lane change behavior in car following events in previous reports. The research objective of this study was to combine driver braking characteristic and lane change characteristics to examine the potential change in driver behavior between braking and lane change maneuvers in car-following.

Several characteristics of driver behavior in braking and lane change events were presented in the results. First, we examined the relative frequency of braking and lane change events across different vehicle speeds. The result shows that in lower speeds, between 3-40 mph, drivers in the study sample all initiated more braking events than lane change events. In addition, as vehicle speed increases, the ratio of number of lane change events and number of braking events begin to increase. The median of the relative frequency for vehicle speed between 70-80 mph was approximately 1. The increase in relative frequency suggests that drivers initiate the majority of the braking events in lower vehicle speeds, such as while driving on small rural roads, or congested traffic. In higher speed, such as during travel on interstate highways, drivers are more likely to initiate lane changes to overtake vehicles and maintain current travel speed. The relative frequency result also shows that braking and lane change frequency are highly variable by driver, especially in vehicle speeds near highway speeds. Half of the drivers in the sample performed more braking events and the other half performed more lane change events during vehicle speeds between 70-80 mph. This is indicative that driver behavior in car following begins to increase in variability in higher vehicle speeds.

The second part of the results analyzed the difference in TTC during braking and lane change events. In order to eliminate extreme values which may be capture by the minimum TTC, the comparison of TTC during braking and lane change was based upon 10^{th} percentile TTC for each driver. The resultant scatter plot of ΔTTC between braking and lane change suggests that the median difference between driver lane change and braking TTC are largely centered at 0. However, as vehicle speed increases, the variability between drivers also increase.

Given the large variability between drivers, exhibited thus far by both the difference in frequency of lane change and braking events, as well as the perception of risk during car following events, as indicated by the largely varied TTC, our next question was to address whether a driver who was aggressive in low speed braking would continue to exhibit aggressive braking behavior in higher speed braking events or lane change events. The results of this section was presented as a series of 9 rankings in which each driver was ranked from 1 (most aggressive) to 45 (least aggressive), based on the TTC at braking and lane change. The results shows that, although several drivers show consistent trend in car following behavior, not all drivers' behavior can be generalized or categorized.

The last section of the results explored the potential of creating driver specific TTC for both braking and lane change events. The approach was to find the probability density functions with the best fit for TTC values associated with each driver's braking and lane change events. For each driver the maximum probable TTC value for braking and lane change event in each speed bin has been presented in Appendix B. The results from this section are similar to the rankings established in the previous section. As indicated by the TTC values in each speed bin, driver risk perception varies by both driver and vehicle speed, and each individualized probability density function can potentially help tailor the timing of FCW warnings to driver preference.

7.7 Distribution of TTC and ETTC at Start of Steering during Overtaking

This study extracted time of steering initiation for all previously identified lane change events, and to characterized driver lane change behavior at start of lane change by TTC and ETTC. In this study, we developed a methodology to extract the start of steering maneuver for lane change events. This study improves the estimation of start of lane change, by using start of steering maneuver as the beginning of the lane change event. The overall approach in the methodology was to model the normal lane keeping behavior using the distance to lane boundary and lateral velocity of the vehicle prior to the lane change event, and start of steering maneuver was estimated as the first time when driver lane keeping behavior reaches outside 95% of normal lane keeping behavior.

The results of the algorithm were validated against manual video inspection of 131 randomly selected lane change events. During the manual inspection, the researcher reviewed of the over-the-shoulder camera view to determine when the driver initiated the steering maneuver during the lane change. In certain low light lane change events, such as night time driving or shadows casted over the driver, time of steering maneuver could not be determined.

The comparison of lead time, or the time between the start of the steering maneuver and the vehicle crossing the lane edge, showed that the median lead time for the algorithm was approximately 0.8 seconds shorter than the lead time reported by visual inspection. We hypothesize that the difference in lead time is largely due to the play in the steering wheel and the fact that vehicles do not immediately respond to steering wheel input. In addition, lead time was less than 5 seconds for all lane change events in the validation sample, suggesting that detecting steering wheel input within 5 seconds prior to lane crossing was a reasonable assumption in our algorithm.

The algorithm validation sample was also utilized in a sensitivity analysis of the confidence interval. Confidence intervals between 50% and 95% was selected to represent normal lane keeping behavior, and the performance of the algorithm was compared against the results from the manual inspection. According to the average percentage error of lead time between the algorithm output

and the manual inspection, a 95% confidence level best described the normal lane keeping behavior in our algorithm, and was therefore selected in the final methodology.

7.8 PUBLICATION SUMMARY

A summary of publications in support of the current dissertation is shown in Table 27.

Table 27. Summary of Relevant Publications

Publication Citation	Relevant Chapter
"Population Distribution of Time to Collision at Brake Application during Car Following from Naturalistic Driving Data" K.D. Kusano, J. Montgomery, **R. Chen**, and H. C. Gabler, *Journal of Safety Research*, December 2014	3 Driver Behavior during Braking in Car Following
"Driver Behavior during Overtaking Maneuvers from the 100-Car Naturalistic Driving Study" **R. Chen**, and H. C. Gabler, *Traffic Injury Prevention*, March 2015	4 Driver Behavior during Overtaking Maneuvers in Car Following
"Driver Behavior During Lane Change from the 100-Car Naturalistic Driving Study", **R. Chen**, K.D. Kusano, and H.C. Gabler, 24th International Technical Conference on the Enhanced Safety of Vehicles, Gothenburg, Sweden, June 8-11, 2015	4 Driver Behavior during Overtaking Maneuvers in Car Following
"Age and Gender Difference in Braking Behavior from the 100-Car Naturalistic Driving Study: The Implication for Autonomous Braking System Design" **R. Chen**, K. D. Kusano, and H. C. Gabler. Proceedings of the 3rd FAST-zero Conference, Gothenburg, Sweden, September 2015.	3.2 Age and Gender Difference in Braking Behavior during Car Following
"Comparison of Time to Collision and Enhanced Time to Collision at Brake Application during Normal Driving" **R. Chen**, Rini Sherony, and H. C. Gabler, SAE Technical Paper No. 2016-01-1448	3.1 Comparison of TTC and ETTC during Normal Braking Events
"Method of Predicting Adjacent Vehicle Lane Change Maneuver" **R. Chen**, H. C. Gabler, IEEE Transaction on Intelligent Transportation Systems, (Proposed)	6 Distribution of TTC and ETTC at Start of Steering during Overtaking

8 REFERENCES

[1] W. T. Hollowell, H. C. Gabler, S. L. Stucki, S. Summers, and R. Hackney, James, "Updated Review of Potential Test Procedures of FMVSS No. 208," National Highway Traffic Safety Administration. Washington, DC, 1999.

[2] Office of Regulatory Analysis and Evaluation, "FMVSS No. 214 - Amending Side Impact Dynamic Test Adding Oblique Pole Test," National Highway Traffic Safety Administration. Washington, DC, 2007.

[3] C. Kahane, "Lives Saved by Vehicle Safety Technologies and Associated Federal Motor Vehicle Safety Standards , 1960 to 2012 Passenger Cars and LTVs," p. DOT HS 812 069, 2015.

[4] National Highway Traffic Safety Administration, "Traffic Safety Facts 2014 - A Compilation of Motor Vehicle Crash Data from the Fatality Analysis Reporting System and the General Estimates System," DOT HS 8120261, 2016.

[5] R. Chen and H. C. Gabler, "Risk of thoracic injury from direct steering wheel impact in frontal crashes.," *J. Trauma Acute Care Surg.*, vol. 76, no. 6, pp. 1441–6, Jun. 2014.

[6] F. S. Gayzik, R. S. Martin, H. C. Gabler, J. J. Hoth, S. M. Duma, J. W. Meredith, and J. D. Stitzel, "Characterization of crash-induced thoracic loading resulting in pulmonary contusion.," *J. Trauma*, vol. 66, no. 3, pp. 840–9, Mar. 2009.

[7] H. C. Gabler, K. H. Digges, B. N. Fildes, and L. Sparke, "Side Impact Injury Risk for Belted Far Side Passenger Vehicle Occupants," *SAE Trans. J. Passeng. Car - Mech. Syst.*, vol. 114, no. 2005–01–0287, 2005.

[8] O. Bostrom, H. C. Gabler, K. H. Digges, B. N. Fildes, and S. S., "Injury Reduction Opportunities of Far Side Impact Countermeasures," *Ann. Adv. Automot. Med.*, vol. 52, pp. 289–300, 2008.

[9] H. C. Gabler, "The Evolution of Side Crash Compatibility Between Cars, Light Trucks and Vans," *SAE Trans. J. Passeng. Car - Mech. Syst.*, vol. 112, no. 6, pp. 2003–01–0899, 2003.

[10] H. C. Gabler and W. T. Hollowell, "The Aggressivity of Light Trucks and Vans in Traffic Crashes," *SAE Trans. J. Passeng. Cars*, vol. 107, no. 6, p. 980908, 1998.

[11] D. E. Lefler and H. C. Gabler, "The Fatality and Injury Risk of Light Truck Impacts with Pedestrians in the United States," *Accid. Anal. Prev.*, vol. 36, pp. 295–304, 2004.

[12] B. N. Fildes, H. C. Gabler, D. Otte, A. Linder, and L. Sparke, "Pedestrian Impact Priorities Using Real-World Crash Data and Harm," in *Proceedings of the 2004 International IRCOBI Conference on the Biomechanics of Impact*, 2004.

[13] B. N. Fildes, A. Linder, A. Clarke, D. Otte, H. C. Gabler, Y. Y., R. Fredrikkson, Y. Fujita, D. Cessari, K. Yang, L. Sparke, and S. Smith, "Pedestrian Safety: International Collaborative Research Based on Real World Crash Data," in *Proceedings of the International Expert Symposium on Accident Research (ESAR)*, 2004.

[14] A. Daniello and H. C. Gabler, "Characteristics of Injuries in Motorcycle-to-Barrier Collisions in Maryland," *Transp. Res. Rec. J. Transp. Res. Board*, pp. 92–98, Dec. 2012.

[15] A. Daniello and H. C. Gabler, "The Effect of Barrier Type on Injury Severity in Motorcycle to

Barrier Collisions in North Carolina, Texas, and New Jersey," *Transp. Res. Rec. J. Transp. Res. Board*, pp. 144–151, 2011.

[16] A. Daniello and H. C. Gabler, "Fatality Risk in Motorcycle Collisions with Roadside Objects in the United States," *Accid. Anal. Prev.*, vol. 43, pp. 1167–1170, 2011.

[17] N. S. Johnson and H. C. Gabler, "Injury Outcome in Crashes with Guardrail End Terminals," *Traffic Inj. Prev.*, vol. 16, no. sup2, pp. S103–S108, Oct. 2015.

[18] N. S. Johnson, R. Thomson, and H. C. Gabler, "Improved method for roadside barrier length of need modeling using real-world trajectories," *Accid. Anal. Prev.*, vol. 80, pp. 162–171, Jul. 2015.

[19] N. Johnson and H. Gabler, "Injury Risk Posed by Side Impact of Nontracking Vehicles into Guardrails," *Transp. Res. Rec. J. Transp. Res. Board*, vol. 2377, pp. 21–28, Dec. 2013.

[20] C. E. Hampton and H. C. Gabler, "Crash Performance of Strong-Post W-Beam Guardrail with Missing Blockouts," *Int. J. Crashworthiness*, vol. 17, no. 1, pp. 93–103, 2012.

[21] D. J. Gabauer, K. D. Kusano, D. Marzougui, K. Opeila, M. Hargrave, and H. C. Gabler, "Pendulum Testing as a Means of Assessing the Crash Performance of Longitudinal Barrier with Minor Damage," *Int. J. Impact Eng.*, vol. 37, pp. 1121–1137, 2010.

[22] D. C. Viano, *Role of the Seat in Rear Crash Safety*. Warrendale, PA: SAE International, 2002.

[23] N. Nishimura, C. K. Simms, and D. P. Wood, "Impact characteristics of a vehicle population in low speed front to rear collisions," *Accid. Anal. Prev.*, vol. 79, pp. 1–12, 2015.

[24] N. Yoganandan, B. D. Stemper, and R. D. Rao, "Patient Mechanisms of Injury in Whiplash-Associated Disorders," *Semin. Spine Surg.*, vol. 25, no. 1, pp. 67–74, 2013.

[25] S. Norris and I. Watt, "The Prognosis Rear-End Neck Injuries Resulting Vehicle Collisions," *J. bone Jt. Surg. Br. Vol.*, vol. 65, no. 5, pp. 608–611, 1983.

[26] D. C. Viano, "Influence of seat properties on occupant dynamics in severe rear crashes.," *Traffic Inj. Prev.*, vol. 4, no. 4, pp. 324–336, 2003.

[27] J. Foret-Bruno, X. Trosseille, J.-F. Huere, J.-Y. Le Coz, F. Bendjellal, and A. Diboine, "Comparison of Thoracic Injury Risk in Frontal Car Crashes for Occupant Restrained without Belt Load Limiters and Those Restrained with 6 kN and 4 kN Belt Load," *Stapp Car Crash J.*, vol. 45, no. November, 2001.

[28] F. Tagliaferri, C. Compagnone, N. Yoganandan, and T. A. Gennarelli, "Traumatic Brain Injury After Frontal Crashes: Relationship With Body Mass Index," *J. Trauma Inj. Infect. Crit. Care*, vol. 66, no. 3, pp. 727–729, Mar. 2009.

[29] H. Araki, K. Yamada, Y. Hiroshima, and T. Ito, "Development of rear-end collision avoidance system," in *Proceedings of the 1996 IEEE Intelligent Vehicles Symposium*, 1996, pp. 224–229.

[30] P. Barber and N. Clarke, "Advanced collision warning systems," *IEE Colloq. Ind. Autom. Control Appl. Automot. Ind.*, vol. 1998, pp. 2–2, 1998.

[31] P. Seiler, B. Song, and J. K. Hedrick, "Development of a Collision Avoidance System," *SAE Tech. Pap.*, p. 980853, Feb. 1998.

[32] K. D. Kusano and H. C. Gabler, "Safety Benefits of Forward Collision Warning, Brake Assist, and Autonomous Braking Systems in Rear-End Collisions," *IEEE Trans. Intell. Transp. Syst.*, vol. 13, no. 4, pp. 1546–1555, Dec. 2012.

[33] National Highway Traffic Safety Administration, *Forward Collision Warning System Confirmation Test*. Washington, DC: U.S. Department of Transportation, 2013.

[34] A. Doi, "Development of a rear-end collision avoidance system with automatic brake control," *JSAE Rev.*, vol. 15, no. 4, pp. 335–340, Oct. 1994.

[35] J. B. Cicchino, "Effectiveness of Forward Collision Warning Systems with and without Autonomous Emergency Braking in Reducing Police-Reported Crash Rates," Arlington, VA: Insurance Institute for Highway Safety, 2016.

[36] "Google Self-Driving Car Project Monthly Report July 2015," Mountain View, CA, 2015.

[37] M. Blanco, J. Atwood, S. Russell, T. Trimble, J. McClafferty, and M. Perez, "Automated Vehicle Crash Rate Comparison Using Naturalistic Data," Blacksburg, VA: Virginia Tech Transporation Institute, 2016.

[38] "Audi piloted driving," *Audi 04 Journal*. [Online]. Available: http://www.audi.com/content/com/brand/en/vorsprung_durch_technik/content/2014/10/piloted-driving.html. [Accessed: 18-Aug-2015].

[39] N. Ungerleider, "BAIDU AND BMW PLAN TO LAUNCH SELF-DRIVING CAR THIS YEAR," *Fast Feed*. [Online]. Available: http://www.fastcompany.com/3047411/fast-feed/baidu-and-bmw-plan-to-launch-self-driving-car-this-year. [Accessed: 18-Aug-2015].

[40] "Nissan Announces Unprecedented Autonomous Drive Benchmarks," *Nissan News*. [Online]. Available: http://nissannews.com/en-US/nissan/usa/releases/nissan-announces-unprecedented-autonomous-drive-benchmarks. [Accessed: 18-Aug-2015].

[41] "Volvo Will Stest Self-Driving Cars with Real Customers in 2017." [Online]. Available: http://www.wired.com/2015/02/volvo-will-test-self-driving-cars-real-customers-2017/. [Accessed: 18-Aug-2015].

[42] A. H. Eichelberger and A. T. Mccartt, "Toyota Drivers ' Experiences with Dynamic Radar Cruise Control , the Pre-Collision System , and Lane-Keeping Assist," *J. Safety Res.*, vol. 56, no. March, pp. 67–73, 2014.

[43] J. B. Cicchino and A. T. Mccartt, "Experiences of Model Year 2011 Dodge and Jeep Owners With Collision Avoidance and Related Technologies," *Traffic Inj. Prev.*, vol. 16, no. April 2016, pp. 298–303, 2015.

[44] K. A. Braitman, A. T. McCartt, D. S. Zuby, and J. Singer, "Volvo and Infiniti Drivers' Experiences with Select Crash Avoidance Technologies," *Traffic Inj. Prev.*, vol. 11, no. 3, pp. 270–278, 2010.

[45] A. H. Eichelberger and A. T. McCartt, "Volvo drivers' experiences with advanced crash avoidance and related technologies.," *Traffic Inj. Prev.*, vol. 15, no. 2, pp. 187–95, 2014.

[46] J. P. Bliss and S. a. Acton, "Alarm mistrust in automobiles: How collision alarm reliability affects driving," *Appl. Ergon.*, vol. 34, no. 6, pp. 499–509, 2003.

[47] G. Abe and J. Richardson, "The influence of alarm timing on braking response and driver trust in low speed driving," *Saf. Sci.*, vol. 43, no. 9, pp. 639–654, 2005.

[48] A. H. Jamson, F. C. H. Lai, and O. M. J. Carsten, "Potential benefits of an adaptive forward collision warning system," *Transp. Res. Part C Emerg. Technol.*, vol. 16, no. 4, pp. 471–484, 2008.

[49] K. Lee and H. Peng, "Evaluation of automotive forward collision warning and collision avoidance algorithms," *Veh. Syst. Dyn.*, vol. 43, no. 10, pp. 735–751, 2005.

[50] J. M. Scanlon, K. Page, R. Sherony, and H. C. Gabler, "Using Event Data Recorders from Real-World Crashes to Evaluate the Vehicle Detection Capability of an Intersection Advanced Driver Assistance System," *SAE Tech. Pap.*, no. 2016–01–1457, 2016.

[51] T. R. Johnson, R. Chen, R. Sherony, and H. C. Gabler, "Investigation of Driver Lane Keeping Behavior in Normal Driving based on Naturalistic Driving Study Data," *SAE Int. J. Transp. Saf.*, vol. 4, no. 2, 2016.

[52] K. D. Kusano and H. C. Gabler, "Comparison of Expected Crash and Injury Reduction from Production Forward Collision and Lane Departure Warning Systems," *Traffic Inj. Prev.*, vol. 16, no. sup2, pp. S109–S114, Oct. 2015.

[53] K. D. Kusano and H. C. Gabler, "Target Population for Intersection Advanced Driver Assistance Systems in the U.S.," *SAE Int. J. Transp. Saf.*, vol. 3, no. 1, pp. 2015–01–1408, Apr. 2015.

[54] J. M. Scanlon, K. D. Kusano, R. Sherony, and H. C. Gabler, "POTENTIAL SAFETY BENEFITS OF LANE DEPARTURE WARNING AND PREVENTION SYSTEMS IN THE U.S. VEHICLE FLEET," *Proc. 24th Enhanc. Saf. Veh. Conf.*, pp. 15–0080, 2015.

[55] R. Chen, K. D. Kusano, and H. C. Gabler, "Driver Behavior During Overtaking Maneuvers from the 100-Car Naturalistic Driving Study," *Traffic Inj. Prev.*, vol. 16, no. sup2, pp. S176–S181, Oct. 2015.

[56] R. Chen, K. D. Kusano, and H. C. Gabler, "Age and Gender Difference in Braking Behavior from the 100-Car Naturalistic Driving Study: The Implication for Autonomous Braking System Design," in *Proceedings of the 3rd International Symposium on Future Active Safety Technology Towards zero traffic accidents*, 2015, pp. 463–469.

[57] M. a. Goodrich and E. R. Boer, "Designing Human-Centered Automation: Tradeoffs in Collision Avoidance System Design," *IEEE Trans. Intell. Transp. Syst.*, vol. 1, no. 1, pp. 40–54, 2000.

[58] L. Bainbridge, "Ironies of automation," *Automatica*, vol. 19, no. 6, pp. 775–779, 1983.

[59] T. Gordon, H. Sardar, D. Blower, M. Ljung Aust, Z. Bareket, M. BArnes, A. Blankespoor, I. Isaksson-Hellman, J. Ivarsson, B. Juhas, K. Nobukawa, and H. Theander, "Advanced Crash Avoidance Technologies (ACAT) Program – Final Report of the Volvo-Ford- UMTRI Project : Safety Impact Methodology for Lane Departure Warning – Method Development And Estimation of Benefits," p. DOT HS 811 405, 2010.

[60] K. Kusano, T. I. Gorman, R. Sherony, and H. C. Gabler, "Potential Occupant Injury Reduction in the U.S. Vehicle Fleet for Lane Departure Warning–Equipped Vehicles in Single-Vehicle Crashes," *Traffic Inj. Prev.*, vol. 15, no. sup1, pp. S157–S164, Sep. 2014.

[61] K. D. Kusano, H. Gabler, and T. I. Gorman, "Fleetwide Safety Benefits of Production Forward Collision and Lane Departure Warning Systems," *SAE Int. J. Passeng. Cars - Mech. Syst.*, vol. 7, no. 2, pp. 2014–01–0166, Apr. 2014.

[62] S. B. McLaughlin, J. M. Hankey, and T. a. Dingus, "A method for evaluating collision avoidance systems using naturalistic driving data," *Accid. Anal. Prev.*, vol. 40, no. 1, pp. 8–16, 2008.

[63] R. R. Knipling, M. Mironer, D. L. Hendricks, L. Tijeripa, and J. Everson, "Assessment of IVHS Countermeasures for Collision Avoidance: Rear-End Crashes," p. DOT HS 807 995, 1993.

[64] J. S. Wang and R. R. Knipling, "Lane Change / Merge Crashes : Problem Size Assessment and Statistical Description," p. DOT HS 808 075, 1994.

[65] K. Kusano and H. C. Gabler, "Target Population for Injury Reduction from Pre-Crash Systems," 2010.

[66] D. Smith L, W. Najm G, and a Lam H, "Analysis of Braking and Steering Performance in Car-Following Scenarios," *SAE Tech. Pap. Ser.*, p. 8 p., 2003.

[67] F. Bella and R. Russo, "A collision warning system for rear-end collision: A driving simulator study," *Procedia - Soc. Behav. Sci.*, vol. 20, pp. 676–686, 2011.

[68] D. V. McGehee, E. N. Mazzae, and G. H. S. Baldwin, "Driver Reaction Time in Crash Avoidance Research: Validation of a Driving Simulator Study on a Test Track," *Proc. Hum. Factors Ergon. Soc. Annu. Meet.*, vol. 44, no. 20, pp. 3–320–3–323, 2000.

[69] H. C. Gabler, J. Hinch, and J. Steiner, *Event Data Recorders: A Decade of Innovation*. Warrendale, PA: SAE International, 2008.

[70] C. E. Hampton and H. C. Gabler, "Evaluation of the Accuracy of NASS/CDS Delta-V Estimates from the Enhanced WinSmash Algorithm.," *Ann. Adv. Automot. Med.*, vol. 54, pp. 241–52, 2010.

[71] C. E. Hampton and H. C. Gabler, "NASS/CDS delta-V estimates: the influence of enhancements to the WinSmash crash reconstruction code.," *Ann. Adv. Automot. Med.*, vol. 53, pp. 91–102, Oct. 2009.

[72] J. R. Funk, J. M. Cormier, and H. C. Gabler, "Effect of delta-V errors in NASS on frontal crash risk calculations.," *Ann. Adv. Automot. Med.*, vol. 52, pp. 155–64, Oct. 2008.

[73] P. Niehoff and H. C. Gabler, "The accuracy of WinSmash delta-V estimates: the influence of vehicle type, stiffness, and impact mode.," *Annu. Proc. Assoc. Adv. Automot. Med.*, vol. 50, pp. 73–89, 2006.

[74] H. C. Gabler, C. E. Hampton, and J. Hinch, "Crash Severity: A Comparison of Event Data Recorder Measurements with Accident Reconstruction Estimates," *SAE Tech. Pap.*, no. 2004–03–08, Mar. 2004.

[75] H. C. Gabler, C. E. Hampton, and T. A. Roston, "Estimating Crash Severity: Can Event Data Recorders Replace Crash Reconstruction?," in *Proceedings of the 18th Enhanced Safety of Vehicles Conference International Conference on Enhanced Safety of Vehicles*, 2003, p. 490.

[76] A. H. Tsoi and H. C. Gabler, "Evaluation of Vehicle-Based Crash Severity Metrics," *Traffic Inj. Prev.*, vol. 16, no. sup2, pp. S132–S139, Oct. 2015.

[77] K. Kusano and H. C. Gabler, "Comparison and Validation of Injury Risk Classifiers for Advanced Automated Crash Notification Systems," *Traffic Inj. Prev.*, vol. 15, no. sup1, pp. S126–S133, Sep. 2014.

[78] D. J. Gabauer and H. C. Gabler, "Comparison of roadside crash injury metrics using event data recorders.," *Accid. Anal. Prev.*, vol. 40, no. 2, pp. 548–58, Mar. 2008.

[79] D. J. Gabauer and H. C. Gabler, "Evaluation of Acceleration Severity Index Threshold Values Utilizing Event Data Recorder Technology," *Transp. Res. Rec. J. Transp. Res. Board*, vol. 1904, pp. 37–45, 2005.

[80] D. J. Gabauer and H. C. Gabler, "A Methodology to Evaluate the Flail Space Model Utilizing Event Data Recorder Technology," *Transp. Res. Rec. J. Transp. Res. Board*, vol. 1890, pp. 49–57, 2004.

[81] H. C. Gabler and J. Hinch, "Evaluation of advanced air bag deployment algorithm performance using event data recorders.," *Ann. Adv. Automot. Med.*, vol. 52, pp. 175–84, Oct. 2008.

[82] H. C. Gabler and J. Hinch, "Characterization of Advanced Air Bag Field Performance using Event Data Recorders," in *Proceedings of the 12th International Conference on Enhanced Safety of Vehicles*, 2007, pp. 07–0349.

[83] A. Tsoi, J. Hinch, R. Ruth, and H. Gabler, "Validation of Event Data Recorders in High Severity Full‐Frontal Crash Tests," *SAE Int. J. Transp. Saf.*, vol. 1, no. 1, Apr. 2013.

[84] A. Tsoi, N. Johnson, and H. C. Gabler, "Validation of Event Data Recorders in Side-Impact Crash Tests," *SAE Int. J. Trans. Saf.*, vol. 2, no. 1, pp. 130–164, 2014.

[85] N. S. Johnson and H. C. Gabler, "Evaluation of NASS-CDS side crash delta-V estimates using event data recorders.," *Traffic Inj. Prev.*, vol. 15, no. 8, pp. 827–34, 2014.

[86] A. H. Tsoi, J. Hinch, and H. Gabler, "Analysis of Event Data Recorder Survivability in Crashes with Fire, Immersion, and High Delta-V," in *SAE Int. J. Trans. Safety*, 2015, vol. 563, no. September 2012.

[87] A. H. Tsoi, J. Hinch, M. Winterhalter, and H. Gabler, "Survivability of Event Data Recorder Data in Exposure to High Temperature, Submersion, and Static Crush," in *SAE Int. J. Trans. Safety*, 2015.

[88] K. D. Kusano, R. Sherony, and H. C. Gabler, "Methodology for Using Advanced Event Data Recorders to Reconstruct Vehicle Trajectories for Use in Safety Impact Methodologies (SIM).," *Traffic Inj. Prev.*, vol. 14 Suppl, pp. S77–86, Jan. 2013.

[89] J. M. Scanlon, K. D. Kusano, and H. C. Gabler, "Analysis of Driving Behavior Prior to Intersection Crashes Using EDRs," in *59th Annual Scientific Conference of the Association for the Advancedment of Automotive Medicine*, 2015.

[90] J. M. Scanlon, K. D. Kusano, and H. C. Gabler, "A Preliminary Model of Driver Acceleration Behavior prior to Real-World Straight Crossing Path Intersection Crashes Using EDRs," in *Proceedings of the 2015 IEEE Intelligent Transportation Systems Conference*, 2015.

[91] K. D. Kusano, R. Chen, A. H. Tsoi, and H. C. Gabler, "Comparison of Event Data Recorder and Naturalistic Driving Data for the Study of Lane Departure Events," *Proc. 24th Enhanc. Saf. Veh. Conf.*, no. 15–0149, 2015.

[92] K. D. Kusano and H. C. Gabler, "Real-world Driver Crash Avoidance Maneuvers in Rear-end Collisions using Event Data Recorders," in *Proceedings of the 2013 Road Safety and Simulation International Conference*, 2013.

[93] H. C. Gabler and J. Hinch, "Feasibility of using Event Data Recorders to Characterize the Pre-Crash Behavior of Drivers in Rear-End Collisions," in *Proceedings of the 21st International Conference on Enhanced Safety of Vehicles*, 2009, pp. 09–0452.

[94] National Highway Traffic Safety Administration, *Event Data Recorders - Final Rule*. 2012, pp. 233–245.

[95] T. A. Dingus, F. Guo, S. Lee, J. F. Antin, M. Perez, M. Buchanan-King, and J. Hankey, "Driver crash risk factors and prevalence evaluation using naturalistic driving data," *Proc. Natl. Acad. Sci. U. S. A.*, vol. 113, no. 10, pp. 2636–2641, 2016.

[96] R. Chen, R. Sherony, and H. C. Gabler, "Comparison of Time to Collision and Enhanced Time to Collision at Brake Application during Normal Driving," *SAE Tech. Pap.*, no. 2016–01–1448, 2016.

[97] A. M. Noble, K. D. Kusano, J. M. Scanlon, Z. R. Doerzph, and H. C. Gabler, "Driver Approach and Traversal Trajectories for Signalized Intersections Using Naturalistic Data," in *Proceedings of the 95th Annual Meeting of the Transportation Research Board*, 2016, pp. 16–1490.

[98] T. Dingus, S. Klauer, V. Neale, A. Petersen, S. E. Lee, J. Sudweeks, M. Perez, J. Hankey, D. Ramsey, S. Gupta, C. Bucher, Z. . Doerzaph, J. Jermeland, and R. . Knipling, "The 100-Car Naturalistic Driving Study, Phase II – Results of the 100-Car Field Experiment," no. DOT HS 810 593, 2006.

[99] A. Blatt, J. Pierowicz, M. Flanigan, P. Lin, A. Kourtellis, P. Jovanis, J. Jenness, J. Wilaby, J. Campbell, C. Richard, D. Good, N. Czar, and M. Hoover, "SHRP2 Naturalistic Driving Study; Collection of Naturalistic Driving Data," 2014.

[100] J. Sayer, S. Bogard, M. Buonarosa, D. J. LeBlanc, D. S. Funkhouser, S. Bao, D. Blankespoor, Adam, and C. B. Winkler, "Integrated Vehicle-Based Safety Systems Light-Vehicle Field Operational Test Key Findings Report," no. DOT HS 811 416, 2011.

[101] J. McClafferty and J. Hankey, "100-Car Reanalysis : Summary of Primary and Secondary Driver Characteristics." The National Surface Transportation Safety Center for Excellence, Blacksburg, VA, p. Report Number 10–UT–007, 2010.

[102] Federal Highway Adminstration, "Distribution of licensed drivers – 2012 by sex and percentage in each age group and relation to population." [Online]. Available: http://www.fhwa.dot.gov/policyinformation/statistics/2012/dl20.cfm. [Accessed: 01-Apr-2015].

[103] K. D. Kusano, J. Montgomery, and H. C. Gabler, "Methodology for identifying car following events from naturalistic data," *IEEE Intell. Veh. Symp.*, pp. 281–285, 2014.

[104] TRB, *Highway Capacity Manual 2010*. Washington, DC: Transportation Research Board, 2010.

[105] T. Wada, S. Doi, and K. Imai, "Analysis of Drivers' Behaviors in Car Following Based on a Performance," *SAE Tech. Pap.*, no. 2007–01–0440, pp. 776–790, 2007.

[106] H. Aoki, N. V. Q. Hung, and H. Yasuda, "Perceptual risk estimate (PRE): an index of the

longitudinal risk estimate," in *Proceedings of the 22nd Enhanced Safety of Vehicles Conference*, 2011, pp. 11–0121.

[107] M. T. Phan, V. Fremont, I. Thouvenin, M. Sallak, and V. Cherfaoui, "Estimation of driver awareness of pedestrian based on Hidden Markov Model," in *Proceedings of the 2015 IEEE Intelligent Vehicles Symposium*, 2015, pp. 970–975.

[108] V. L. Neale, M. A. Perez, Z. R. Doerzph, S. E. Lee, S. Stone, and T. A. Dingus, "FINAL CONTRACT REPORT INTERSECTION DECISION SUPPORT: EVALUATION OF A VIOLATION WARNING SYSTEM TO MITIGATE STRAIGHT CROSSING PATH COLLISIONS," Charlottesvill, VA: Virginia Transportation Research Council, 2006.

[109] D. N. Lee, "A theory of visual control of braking based on information about time-to-collision.," *Perception*, vol. 5, no. 4, pp. 437–459, 1976.

[110] H. Akaike, "A new look at the statistical model identification," *IEEE Trans. Automat. Contr.*, vol. 19, no. 6, 1974.

[111] G. Schwarz, "Estimating the Dimension of a Model," *Ann. Stat.*, vol. 6, no. 2, pp. 461–464, Mar. 1978.

[112] R. A. Fisher and L. H. C. Tippett, "Limiting forms of the frequency distribution of the largest or smallest member of a sample," *Math. Proc. Cambridge Philos. Soc.*, vol. 24, pp. 180–190, 1927.

[113] A. F. Jenkinson, "The Frequency Distribution of the Annual Maximum (or Minimum) of Meteorological Elements," *Q. J. R. Meterorological Soc.*, vol. 81, no. 348, pp. 158–171, 1955.

[114] A. Torrielli, M. Pia, and G. Solari, "Extreme wind speeds from long-term synthetic records," *Jnl. Wind Eng. Ind. Aerodyn.*, vol. 115, pp. 22–38, 2013.

[115] W. Fernandes and M. Naghettini, "A Bayesian approach for estimating extreme flood probabilities with upper-bounded distribution functions," pp. 1127–1143, 2010.

[116] M. Rocco, "Extreme Values in Finance: A Survey," *J. Econ. Surv.*, vol. 28, no. 1, pp. 82–108, 2014.

[117] P. Songchitruksa and A. P. Tarko, "The extreme value theory approach to safety estimation," *Accid. Anal. Prev.*, vol. 38, pp. 811–822, 2006.

[118] J. Zheng, K. Suzuki, and M. Fujita, "Predicting driver's lane-changing decisions using a neural network model," *Simul. Model. Pract. Theory*, vol. 42, pp. 73–83, Mar. 2014.

[119] K. D. Kusano, R. Chen, J. Montgomery, and H. C. Gabler, "Population distributions of time to collision at brake application during car following from naturalistic driving data," *J. Safety Res.*, vol. 54, pp. 95.e29–104, Sep. 2015.

[120] T. Wada, S. Doi, N. Tsuru, K. Isaji, and H. Kaneko, "Modeling of Expert Driver's Braking Behavior and Its Application to an Automatic Braking System," in *Retina*, 2009.

[121] M. Kassaagi, G. Brissart, and J. Popieul, "a Study on Driver Behavior During Braking on Open Road," *Proc. 18th Enhanc. Saf. Veh. Conf.*, pp. 03–340, 2003.

[122] J. Lee, J. Hoffman, T. Brown, and D. McGehee, "Comparison of Driver Braking Responses in a High-Fidelity Simulator and on a Test Track," *Transp. Res. Rec.*, vol. 1803, no. 1, pp. 59–65,

2002.

[123] D. C. Gazis, R. Herman, and R. W. Rothery, "Nonlinear Follow-the-Leader Models of Traffic Flow," *Oper. Res.*, vol. 9, no. 4, pp. 545–567, Aug. 1961.

[124] T. Hiraoka, T. Kunimatsu, O. Nishihara, and H. Kumamoto, "Modeling of driver following behavior based on minimum-jerk theory," *Intell. Transp. Soc. Am. - 12th World Congr. Intell. Transp. Syst. 2005*, vol. 4, no. November, pp. 1989–2000, 2009.

[125] J. E. Morley, A. M. Abbatecola, J. M. Argiles, V. Baracos, J. Bauer, S. Bhasin, T. Cederholm, A. J. Stewart Coats, S. R. Cummings, W. J. Evans, K. Fearon, L. Ferrucci, R. a. Fielding, J. M. Guralnik, T. B. Harris, A. Inui, K. Kalantar-Zadeh, B. A. Kirwan, G. Mantovani, M. Muscaritoli, A. B. Newman, F. Rossi-Fanelli, G. M. C. Rosano, R. Roubenoff, M. Schambelan, G. H. Sokol, T. W. Storer, B. Vellas, S. von Haehling, S. S. Yeh, and S. D. Anker, "Sarcopenia With Limited Mobility: An International Consensus," *J. Am. Med. Dir. Assoc.*, vol. 12, pp. 403–409, 2011.

[126] A. E. J. Miller, J. D. MacDougall, M. A. Tarnopolsky, and D. G. Sale, "Gender differences in strength and muscle fiber characteristics," *Eur. J. Appl. Physiol. Occup. Physiol.*, vol. 66, pp. 254–262, 1993.

[127] J. Montgomery, K. D. Kusano, and H. C. Gabler, "Age and Gender Differences in Time to Collision at Braking From the 100-Car Naturalistic Driving Study," *Traffic Inj. Prev.*, vol. 15, no. sup1, pp. S15–S20, Sep. 2014.

[128] A. B. Ellison, S. P. Greaves, and M. C. J. Bliemer, "Driver behaviour profiles for road safety analysis," *Accid. Anal. Prev.*, vol. 76, pp. 118–132, 2015.

[129] A. Ellison, S. Greaves, and M. Bliemer, "Examining Heterogeneity of Driver Behavior with Temporal and Spatial Factors," *Transp. Res. Rec. J. Transp. Res. Board*, vol. 2386, pp. 158–167, Dec. 2013.

[130] "Insurance Institute for Highway Safety Highway Loss Data Institute - Frontal Crash Tests." [Online]. Available: http://www.iihs.org/iihs/ratings/ratings-info/frontal-crash-tests. [Accessed: 10-May-2016].

[131] L. Bi, C. Wang, X. Yang, M. Wang, and Y. Liu, "Detecting Driver Normal and Emergency Lane-Changing Intentions With Queuing Network-Based Driver Models," *Int. J. Hum. Comput. Interact.*, vol. 31, no. March, pp. 139–145, 2015.

[132] A. Doshi, B. T. Morris, and M. M. Trivedi, "On-road prediction of driver's intent with multimodal sensory cues," *IEEE Pervasive Comput.*, vol. 10, pp. 22–34, 2011.

[133] J. McCall and D. Wipf, "Lane change intent analysis using robust operators and sparse Bayesian learning," *IEEE Trans. Intell. Transp. Syst.*, vol. 8, no. 3, pp. 431–440, 2007.

[134] W. Van Winsum and A. Heino, "Choice of time-headway in car-following and the role of time-to-collision information in braking.," *Ergonomics*, vol. 39, no. 4, pp. 579–592, 1996.

[135] R. J. Hanowski, M. Blanco, A. Nakata, J. S. Hickman, W. a Schaudt, M. C. Fumero, R. L. Olson, J. Jermeland, M. Greening, G. T. Holbrook, R. R. Knipling, and P. Madison, "The Drowsy Driver Warning System Field Operational Test: Data Collection Methods," no. DOT HS 811 035. NHTSA, 2008.

[136] Technical Committee ISO/TC 204, *ISO 17361 - Intelligent transport systems — Lane departure warning systems — Performance requirements and test procedures*. International Organization for Standardization, 2007.

[137] K. D. Kusano, J. Montgomery, and H. C. Gabler, "Braking TTC of Drivers from the 100-Car Naturalistic Driving Study." Submitted to Toyota Collaborative Safety Research Center (CSRC), 2014.

[138] R. Fujishiro and H. Takahashi, "Research on Driver Acceptance of LDA (Lane Departure Alert) System," *Proc. 24th Enhanc. Saf. Veh. Conf.*, no. 15–0222, 2015.

[139] J. P. Stevens, *Applied Multivariate Statistics for the Social Sciences*, 5th ed. New York, NY: Taylor & Francis Group, 2009.

9 APPENDIX

9.1 APPENDIX A – DRIVER RANKING OF 10TH PERCENTILE TTC AT BRAKING AND LANE CHANGE

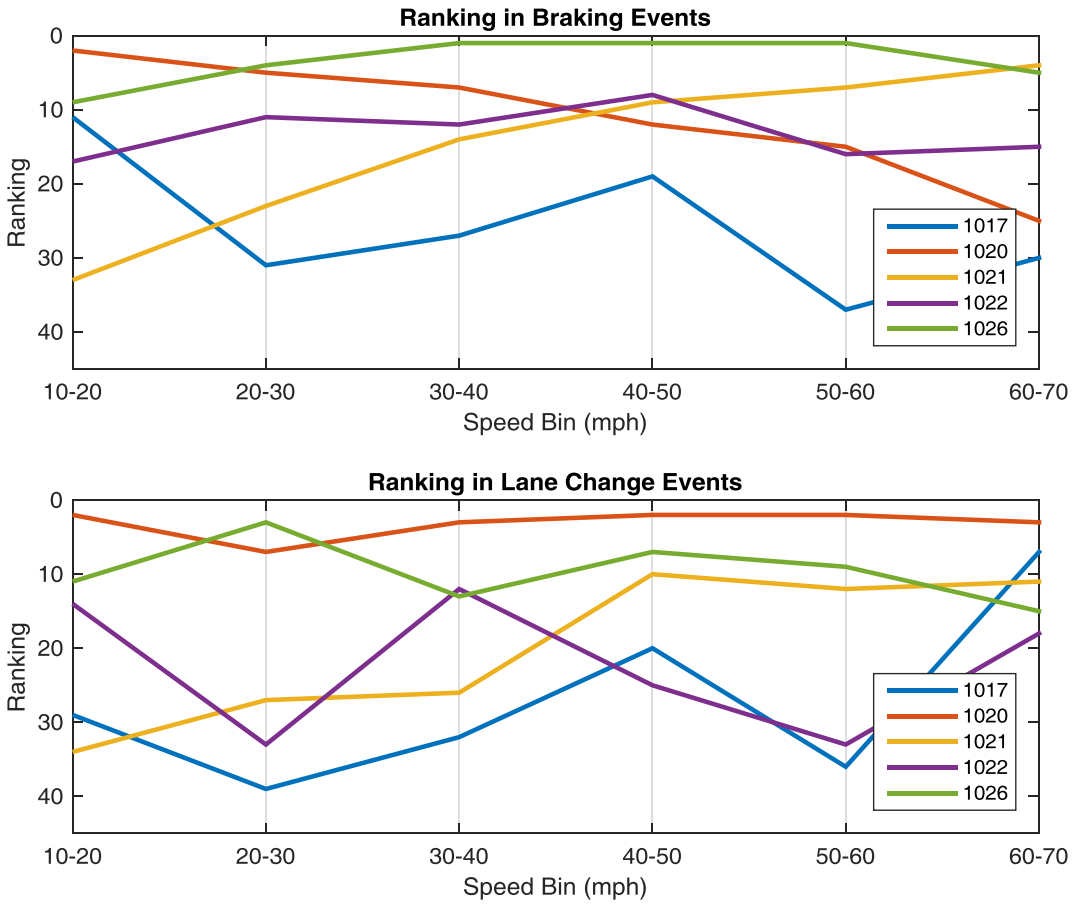

a) Driver Ranking of 10th Percentile TTC at Braking and Lane Change Events

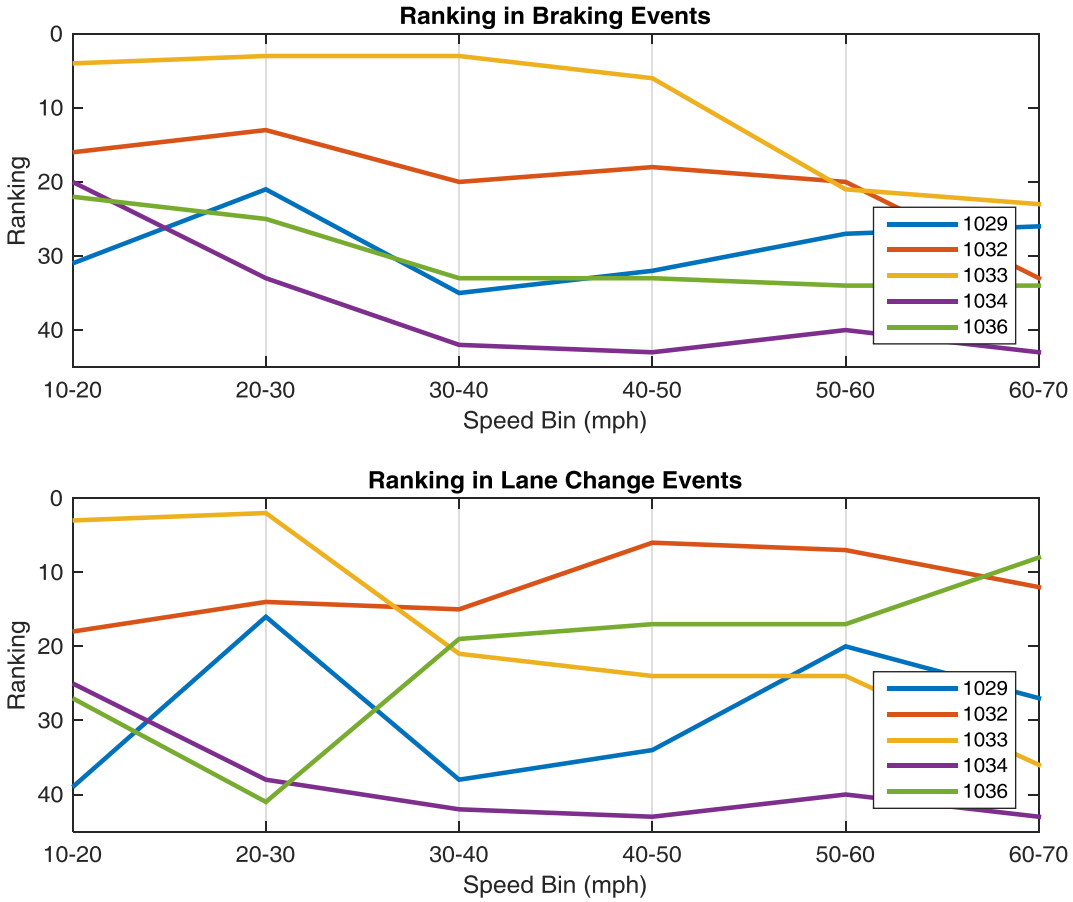

b) Driver Ranking of 10th Percentile TTC at Braking and Lane Change Events

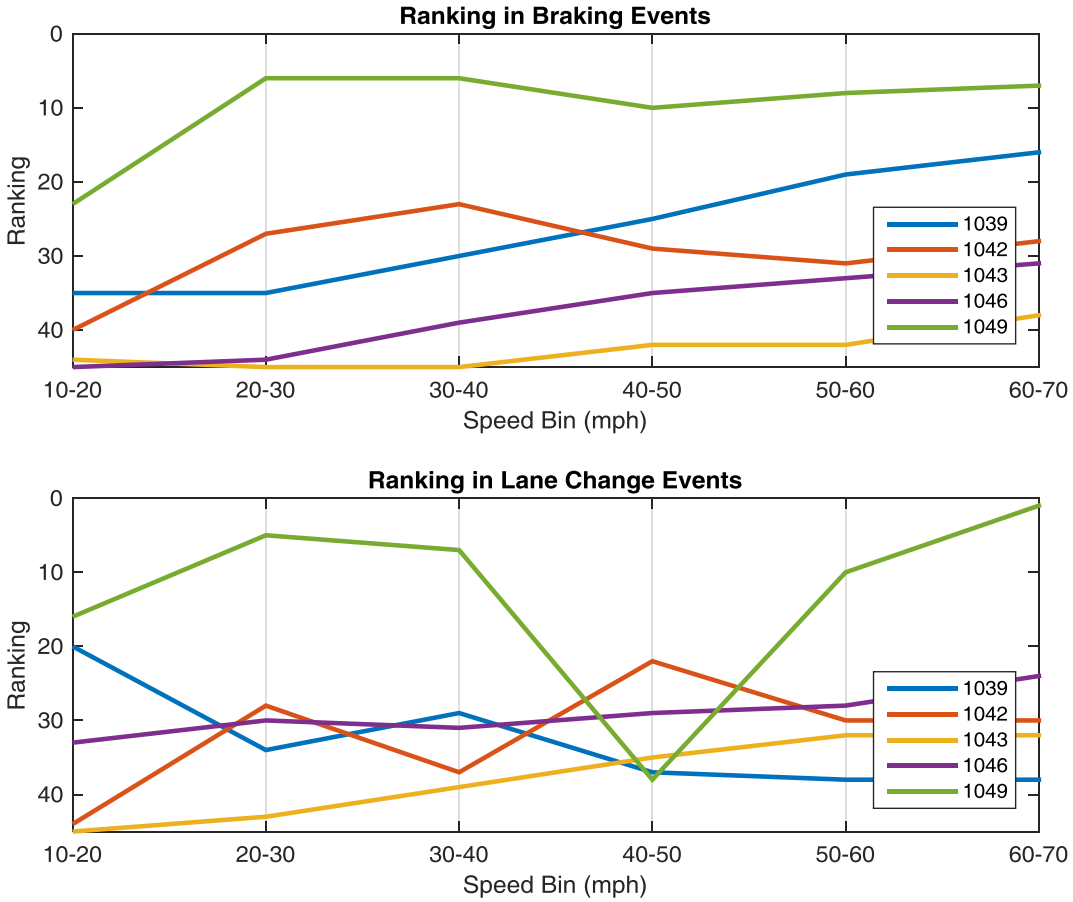

c) Driver Ranking of 10th Percentile TTC at Braking and Lane Change Events

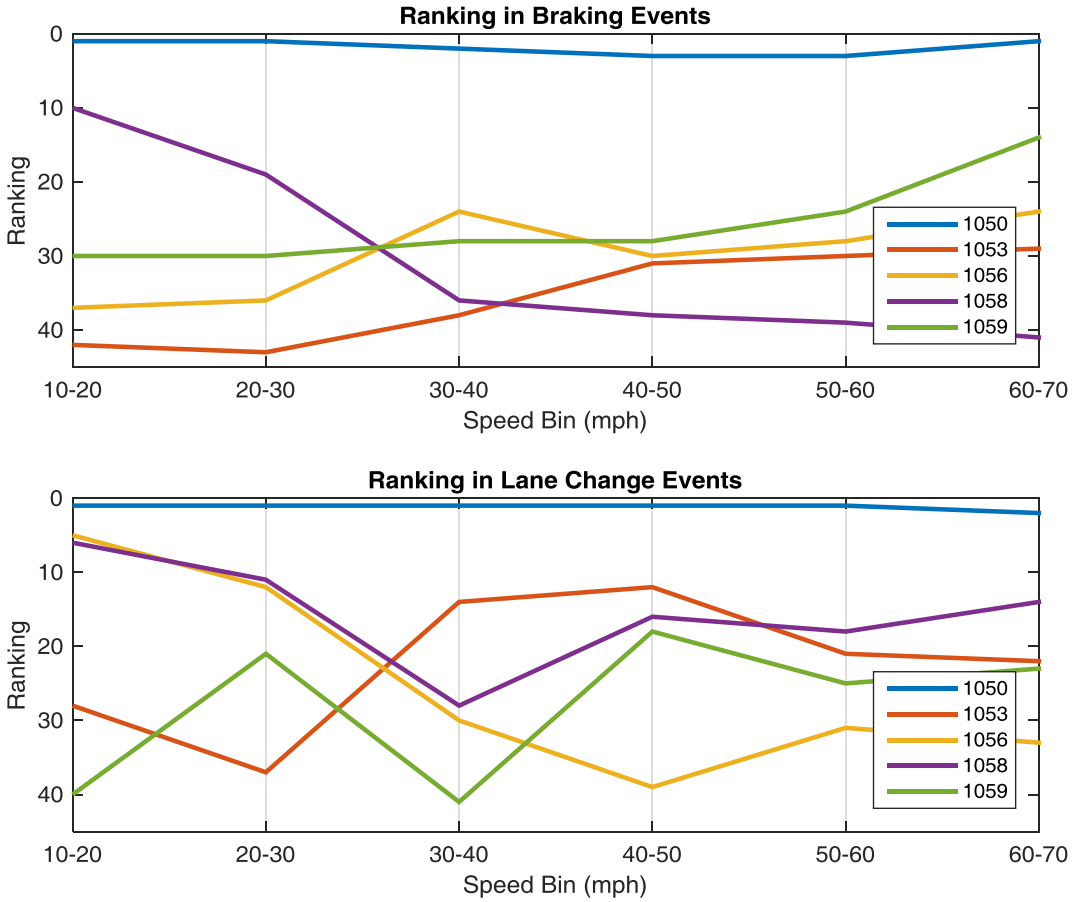

d) Driver Ranking of 10th Percentile TTC at Braking and Lane Change Events

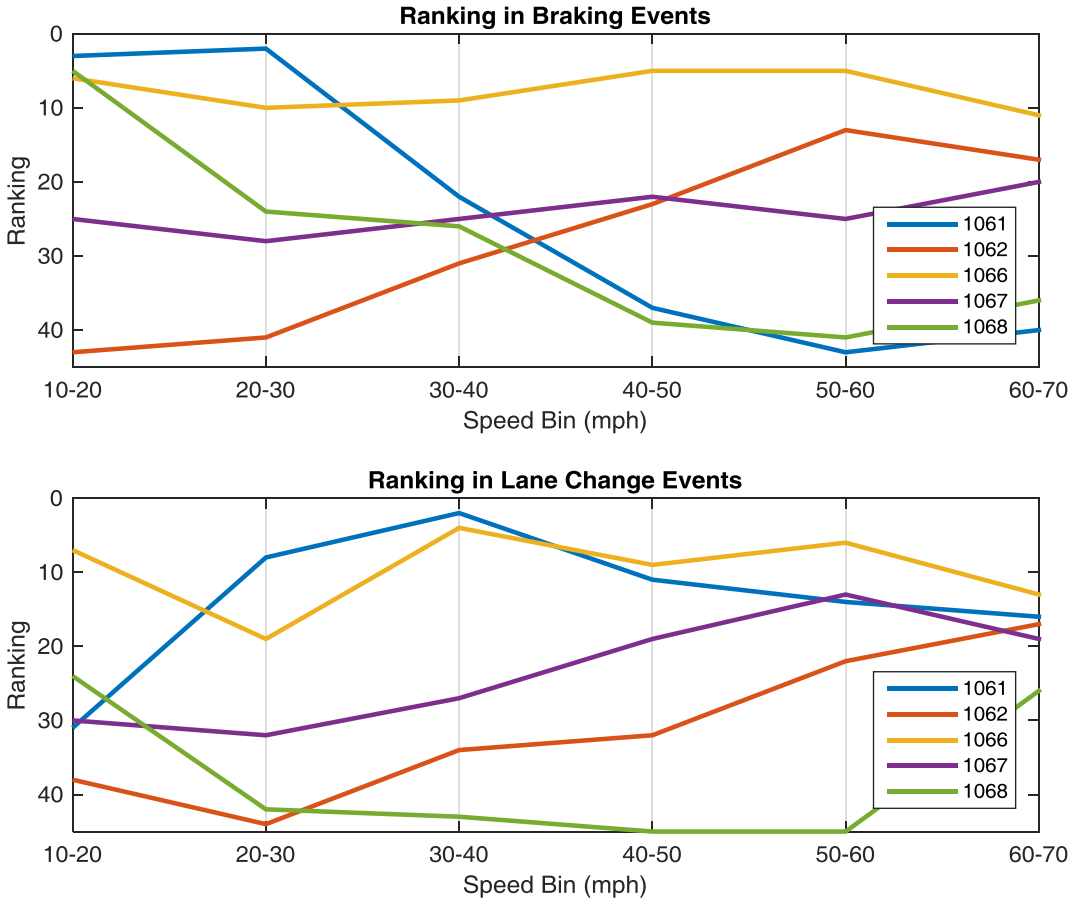

e) Driver Ranking of 10th Percentile TTC at Braking and Lane Change Events

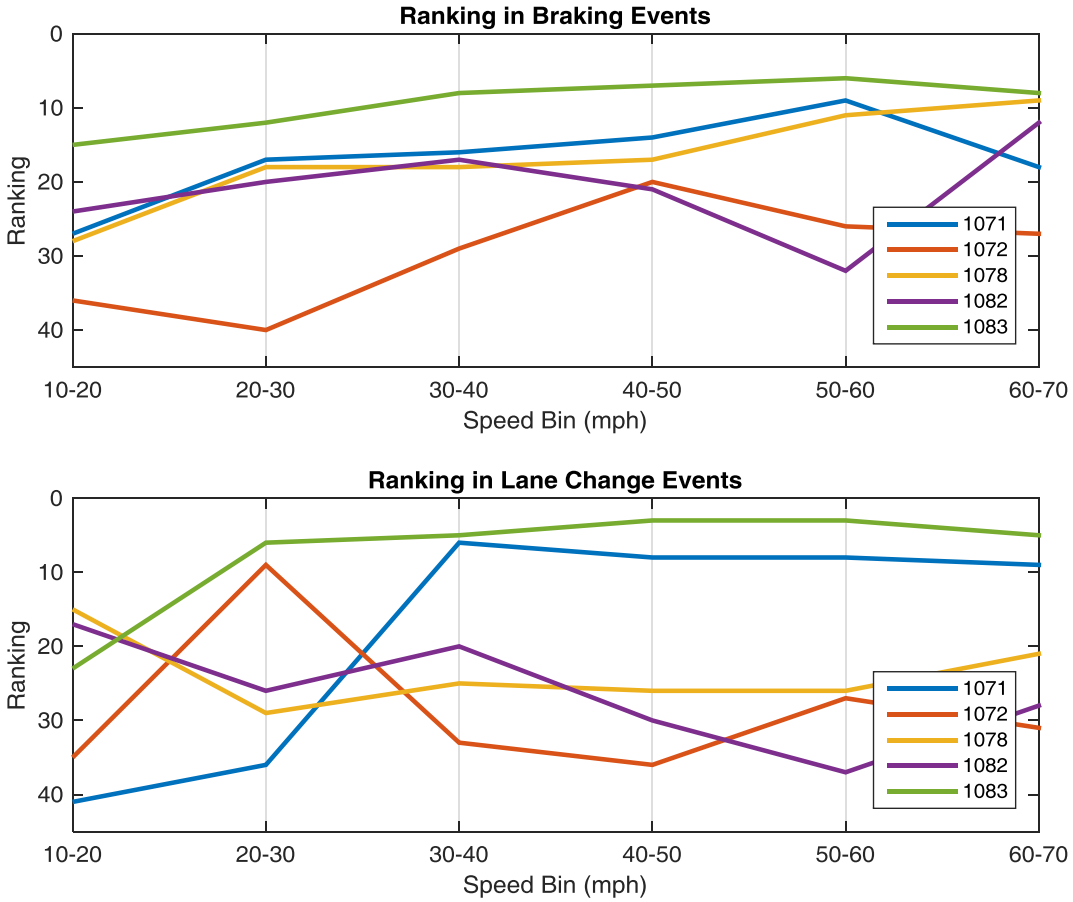

f) Driver Ranking of 10th Percentile TTC at Braking and Lane Change Events

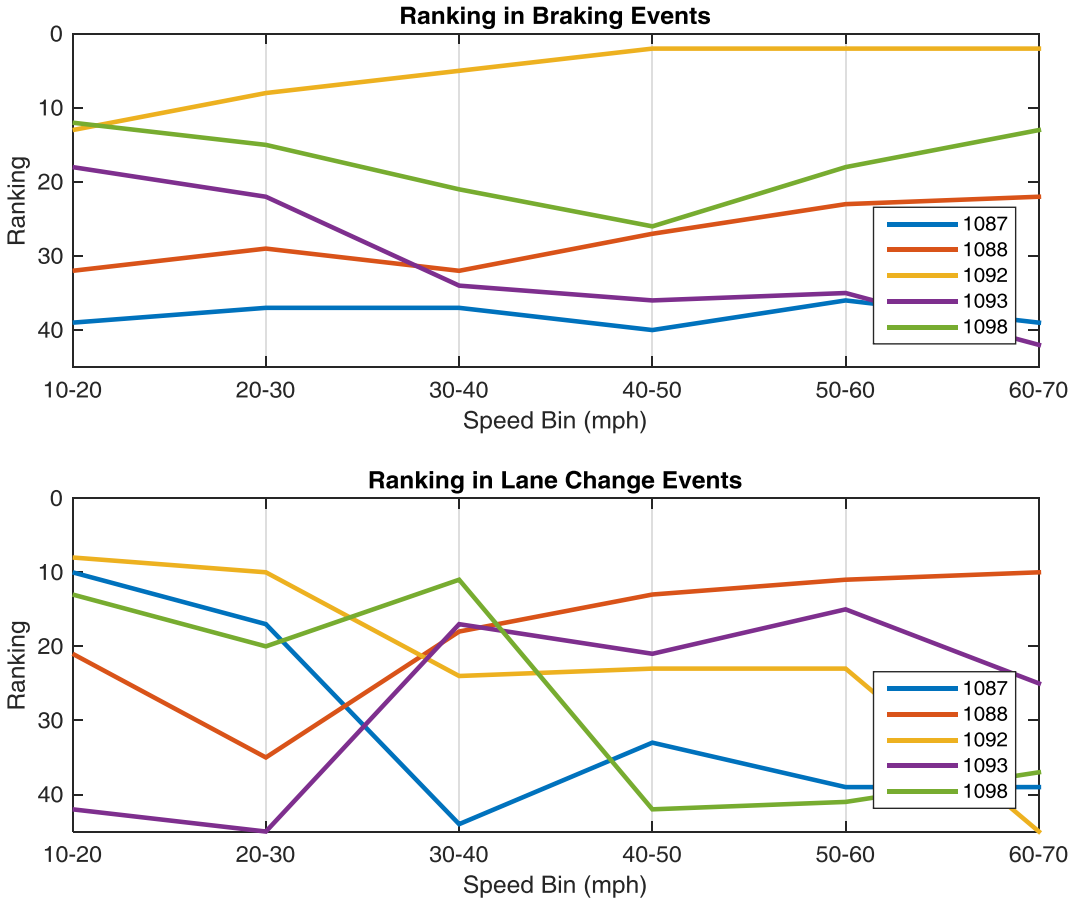

g) Driver Ranking of 10th Percentile TTC at Braking and Lane Change Events

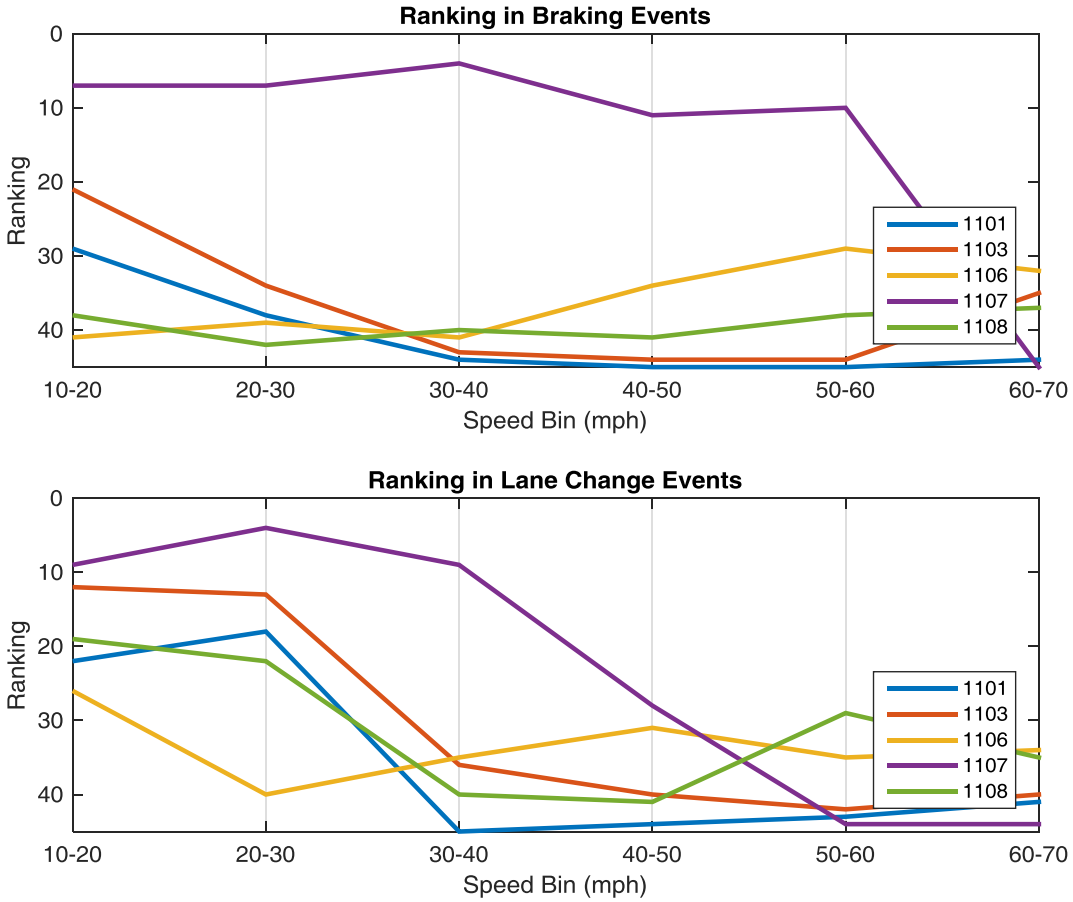

h) Driver Ranking of 10th Percentile TTC at Braking and Lane Change Events

9.2 Appendix B – Driver Max Probability TTC at Braking and Lane Change Events

Table 28. Driver Max Probability TTC at Braking Events

Driver ID	10-20 mph	20-30 mph	30-40 mph	40-50 mph	50-60 mph	60-70 mph
1002	3.80	4.60	7.01	7.81	8.01	8.21
1005	5.41	6.81	7.41	8.61	9.21	6.81
1009	4.40	5.41	6.41	6.81	7.21	6.61
1013	4.80	6.41	7.61	9.01	9.01	7.61
1014	4.20	6.01	6.81	7.61	8.01	7.41
1017	4.40	6.81	8.41	8.61	9.81	8.61
1020	3.00	4.00	6.21	7.81	8.21	9.41
1021	5.41	6.41	7.01	7.41	7.21	6.81
1022	4.20	5.01	6.61	6.81	7.61	7.41
1026	4.00	4.00	4.40	5.21	4.40	6.81
1029	5.41	6.81	8.81	10.01	9.21	8.61
1032	4.20	5.21	7.61	8.41	9.21	11.21
1033	3.60	3.80	5.61	7.21	8.61	7.61
1034	4.60	6.61	9.81	11.81	12.61	14.21
1036	5.01	6.41	8.81	10.01	12.01	11.41
1039	5.41	7.01	8.61	9.21	9.21	8.41
1042	5.41	6.41	8.01	9.41	9.61	9.01
1043	7.21	8.41	11.21	12.61	13.61	14.41
1046	7.41	8.41	9.61	10.21	9.81	9.41
1049	5.01	5.21	6.61	8.21	7.81	7.81
1050	3.00	2.80	5.41	7.01	5.81	5.01
1053	6.61	8.21	9.41	9.81	10.41	9.41
1056	6.21	8.01	9.61	10.81	11.41	10.21
1058	4.00	6.21	9.01	11.21	13.21	14.81
1059	5.41	6.81	8.41	9.21	9.81	7.61
1061	3.40	4.00	8.01	10.61	14.41	14.61
1062	6.81	7.61	8.41	8.61	8.01	7.41
1066	3.80	4.80	6.41	6.81	6.81	7.21
1067	4.80	6.61	8.01	8.61	8.81	7.61
1068	4.40	6.41	8.41	12.21	13.41	12.61
1071	5.01	5.61	7.21	7.81	7.41	7.81
1072	5.61	7.61	8.41	8.41	9.01	8.61
1078	5.01	6.01	7.41	7.81	7.81	7.01
1082	4.60	6.21	7.41	8.61	9.61	-
1083	4.20	5.01	6.41	7.01	6.81	7.01

1087	5.41	7.01	9.61	11.61	12.01	15.02
1088	5.21	6.61	8.41	9.21	9.21	8.01
1092	4.00	5.01	5.61	5.61	5.21	5.41
1093	4.20	6.21	8.61	11.01	13.21	15.62
1098	4.00	5.81	7.61	8.41	7.61	7.01
1101	5.21	7.21	10.61	12.81	15.22	16.42
1103	4.60	6.81	10.81	13.21	13.21	12.21
1106	6.21	7.81	9.41	10.21	9.81	9.41
1107	4.00	4.60	5.81	7.61	10.01	24.62
1108	6.01	7.81	9.61	11.01	12.01	11.01

Table 29. Driver Max Probability TTC at Lane Change Events

Driver ID	10-20 mph	20-30 mph	30-40 mph	40-50 mph	50-60 mph	60-70 mph
1002	3.60	4.60	6.81	7.41	7.21	6.81
1005	6.41	3.20	8.01	9.61	11.21	12.01
1009	5.21	4.20	6.21	7.01	7.21	6.81
1013	5.21	3.20	6.41	8.61	11.61	11.61
1014	4.20	3.80	7.41	10.81	12.01	18.62
1017	4.40	5.01	9.21	9.41	11.81	7.01
1020	4.20	2.40	5.01	6.01	6.01	5.41
1021	4.20	4.00	8.01	8.21	8.41	8.01
1022	3.80	4.40	6.21	10.01	12.21	10.41
1026	3.00	2.40	7.61	8.21	8.81	9.61
1029	4.80	3.60	10.21	11.21	11.21	10.61
1032	4.00	3.00	8.01	8.21	8.21	9.01
1033	2.20	1.80	8.81	9.41	11.61	13.01
1034	4.20	5.01	9.21	11.61	14.61	13.61
1036	4.20	4.60	7.81	9.01	10.01	8.21
1039	3.20	4.40	8.41	11.21	11.21	6.21
1042	4.60	3.60	9.21	10.61	13.41	11.01
1043	5.21	5.21	9.81	12.21	14.21	13.41
1046	4.00	5.41	9.21	10.41	11.81	10.21
1049	3.40	2.60	4.60	7.81	4.40	2.80
1050	-	2.00	4.60	3.60	2.80	5.41
1053	4.80	5.01	6.61	8.61	11.21	10.81
1056	3.80	3.40	10.61	14.21	14.21	14.21
1058	3.60	2.80	8.41	9.41	10.41	8.81
1059	5.21	3.80	10.81	10.61	11.41	11.01
1061	3.40	3.00	3.80	7.21	8.01	10.81
1062	5.01	6.01	10.41	11.01	11.01	9.81
1066	3.80	3.00	5.21	7.61	7.21	8.81
1067	4.60	3.60	9.21	10.01	10.41	9.01

1068	3.60	5.81	10.61	21.82	18.02	9.41
1071	5.01	5.01	5.81	8.21	7.81	7.81
1072	4.80	3.00	10.21	12.41	12.41	12.81
1078	4.00	4.20	9.01	10.41	12.81	10.61
1082	3.60	3.80	6.41	11.21	14.21	9.61
1083	4.20	2.60	6.61	6.61	6.61	6.81
1087	4.40	3.00	11.61	10.01	16.02	16.82
1088	3.80	5.21	8.41	9.41	8.21	8.21
1092	-	6.41	-	-	-	-
1093	5.61	7.41	6.61	10.41	11.01	10.81
1098	3.00	3.40	6.41	11.61	15.22	12.41
1101	3.80	3.60	10.41	12.21	18.42	20.42
1103	3.40	2.80	8.61	12.21	15.42	18.22
1106	4.60	4.60	7.81	10.21	13.41	12.41
1107	3.40	2.20	5.81	9.01	33.43	-
1108	3.60	4.40	8.01	13.41	13.21	13.41